Vol. 57 • No. 12

December 2014

Microwave® Journal .com

MVP
NI LabVIEW Comms Design

horizon house®

Founded in 1958

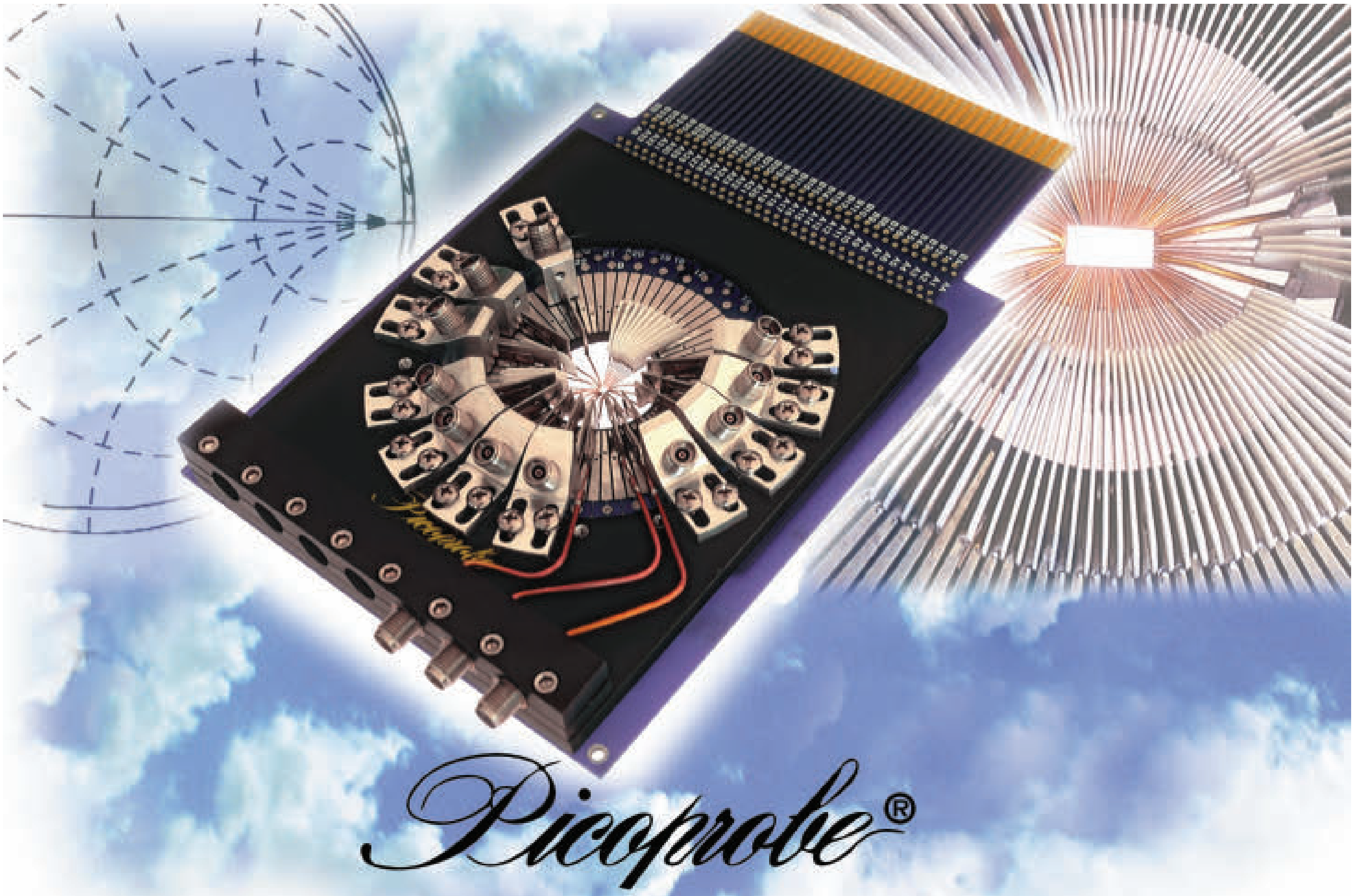

Picoprobe elevates probe cards to a higher level…

(…110 GHz to be exact.)

Since 1981, GGB Industries, Inc., has blazed the on-chip measurement trail with innovative designs, quality craftsmanship, and highly reliable products. Our line of custom microwave probe cards continues our tradition of manufacturing exceptional testing instruments.

Through unique modular design techniques, hundreds of low frequency probe needles and a variety of microwave probes with operating frequencies from DC to 40, 67, or even 110 GHz can be custom configured to your layout.

Our patented probe structures provide the precision and ruggedness you require for both production and characterization testing. And only Picoprobe® offers the lowest loss, best match, low inductance power supplies, and current sources on a single probe card.

Our proven probe card design technology allows full visibility with inking capability and ensures reliable contacts, even when probing non-planar structures.

Not only do you get all the attractive features mentioned, but you get personal, professional service, rapid response, and continuous product support--all at an affordable price so your project can be completed on time and within budget.

Typical Specs	10GHz	20GHz	40GHz
Insertion Loss	0.6 dB	0.8 dB	1.3 dB
Return Loss	22 dB	18 dB	15 dB

For technical assistance, custom product designs, or off-the-shelf delivery, call GGB Industries, Inc., at (239) 643-4400.

GGB INDUSTRIES, INC. • P.O. BOX 10958 • NAPLES, FL 34101

Telephone (239) 643-4400 • Fax (239) 643-4403 • E-mail email@ggb.com • www.picoprobe.com

MCL B 744
ADP-2-10
MCL B 744
ADP-2-10
MCL B 744
ADP-2-10
MCL
GBA-12

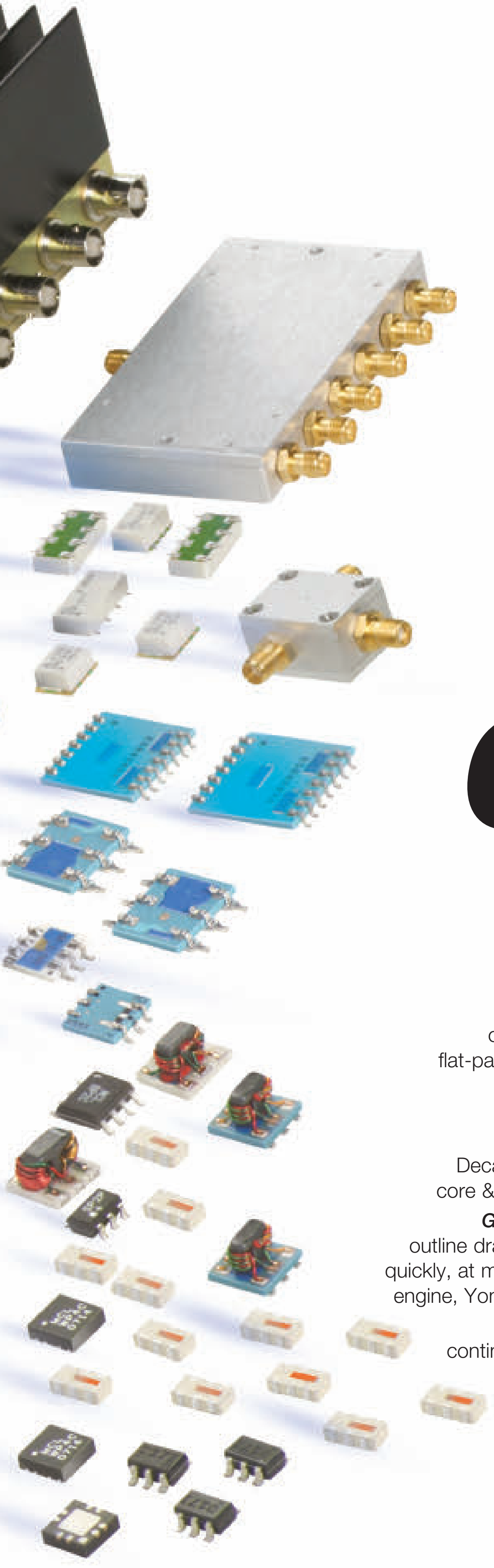


Does your RF test lab
need this....
K&L MICROWAVE
A DOVER COMPANY
105 Fixed Filters
6 foot rack
Switches
Control Circuitry
Greater Selectivity
Higher Power Handling
Better PIM Performance
or...
This?
1 Adjustable Bandwidth Tunable Filter
Smaller Size
Greater Flexibility
Lower Cost
The Choice is Yours
Choose K&L Microwave, your reliable source for both RF test lab solutions.
Microwave Products Group
A DOVER COMPANY
BSC FILTERS • DOW-KEY MICROWAVE • K&L MICROWAVE • POLE/ZERO
www.klmicrowave.com • www.klfilterwizard.com • 410-749-2424 • sales@klmicrowave.com

Solid State Power Amplifiers

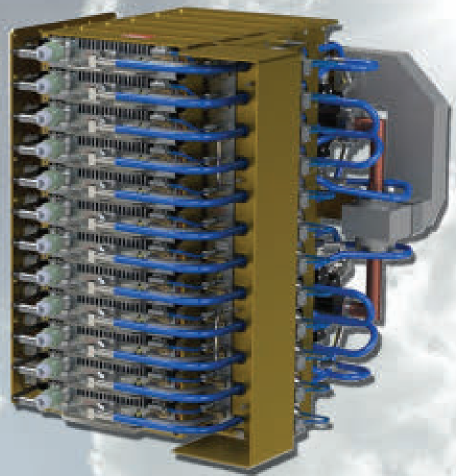

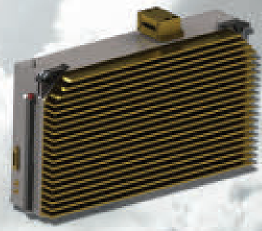

GaN Solid State Amplifiers

FEATURES

- High Efficiency Pulsed Modules (10% duty)
- BIT & Controls via - EIA 422
- Compact Light Weight
- High Reliability
- Field Replaceable Modules
- 9.0 - 9.2 GHz X-Band: 1 kW Modules
- 2.7 - 2.9 GHz S-Band: 1.3 kW Modules
- 1.2 - 1.4 GHz L-Band: 700 W Modules
- Power Combine Modules up to 25KW

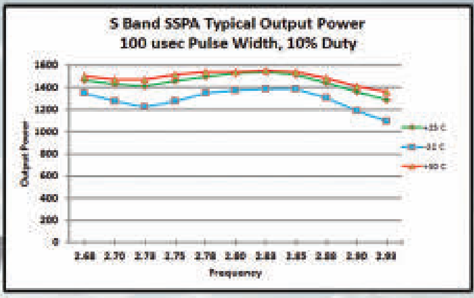

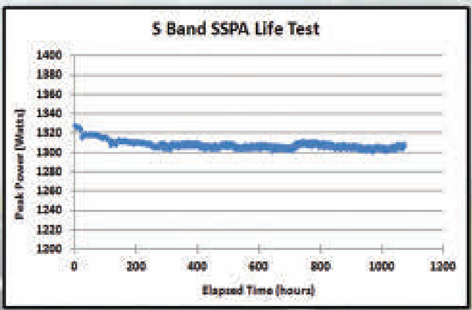

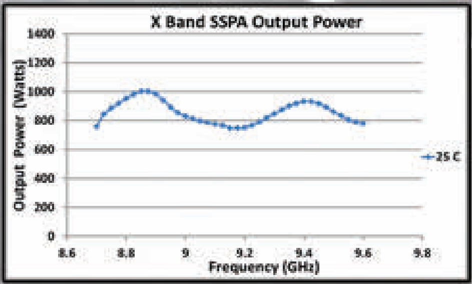

For more information contact

Communications & Power Industries
Beverly Microwave Division
150 Sohier Road Beverly, MA 01915
Phone:(978) 922-6000 Fax: (978) 922-2736
Email: bmdmarketing@cpii.com

Communications & Power Industries

www.cpii.com/bmd
Beverly Microwave Division

Microwave Journal
CONTENTS

December 2014
Vol. 57 • No. 12
Industrial, Scientific and Medical Applications
mwjournal.com

Dick Tracy © 2014 Tribune Content Agency, LLC

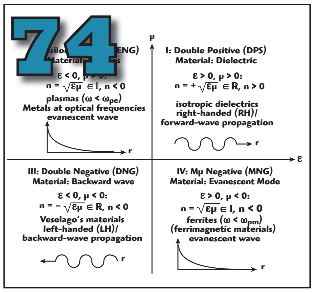

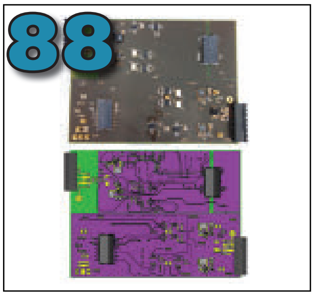

2014 Editorial Index

A complete listing of 2014 Microwave Journal articles organized by subject and indexed alphabetically by author can be found at mwjournal.com/edindex2014

AUGMENTED REALITY: HOW IT WORKS

STEP 1
Download the free Layar app from the iTunes (iOS) or Google Play (Android) store.

STEP 2
Launch the app to view enhanced content on any page with the layar logo.

STEP 3
Frame the entire page in the screen and tap to experience enhancements (tap screen again for full screen view).

Refer to page 120 for this month's participants

AR pages may expire after 60 days.

57 YEARS OF PUBLISHING EXCELLENCE

+50dBm OIP3 at 240MHz

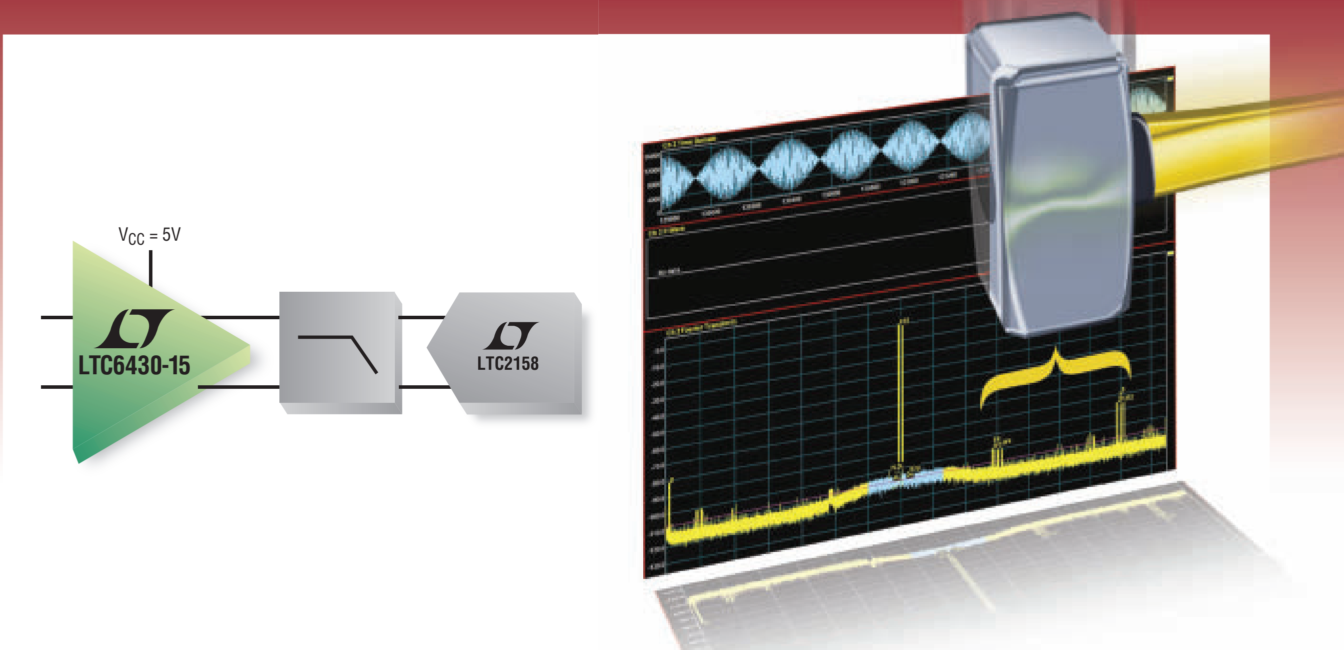

3.3dB Noise Figure Gain Block Hammers Distortion

Make your design choice easy with the LTC®6430-15's differential interface or the LTC6431-15's single-ended interface. Both offer extremely low distortion and unparalleled low noise performance. Whether you are driving an A/D converter, processing wideband signals, or designing broadband wireless infrastructure receivers, software-defined radios or RF test instrumentation, these amplifiers deliver 15dB of stable gain and consistent performance over a wide frequency range with excellent power savings. "A" grade versions offer guaranteed tested OIP3 performance.

▼ Fixed Gain Options

Configuration	15dB Gain	20dB Gain
Single-ended	LTC6431-15	LTC6431-20
Differential	LTC6430-15	LTC6430-20

▼ Info & Free Samples

www.linear.com/product/LTC6430

1-800-4-LINEAR

video.linear.com/132

LINEAR TECHNOLOGY

Microwave Journal CONTENTS

mwjournal.com

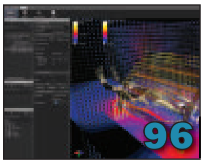

Product Features

Tech Briefs

Departments

Microwave Journal (USPS 396-250) (ISSN 0192-6225) is published monthly by Horizon House Publications Inc., 685 Canton St., Norwood, MA 02062. Periodicals postage paid at Norwood, MA 02062 and additional mailing offices.

POSTMASTER: Send address corrections to *Microwave Journal*, PO Box 3256, Northbrook, IL 60065-3256 or e-mail mwj@omeda.com. Subscription information: (847) 291-5216. This journal is issued without charge upon written request to qualified persons working in the RF & microwave industry. Other subscriptions are: domestic, $120.00 per year, two-year subscriptions, $185.00; foreign, $200.00 per year, two-year subscriptions, $370.00; back issues (if available) and single copies, $10.00 domestic and $20.00 foreign. Claims for missing issues must be filed within 90 days of date of issue for complimentary replacement.

STAFF

Publisher: Carl Sheffres
Editor: Patrick Hindle
Technical Editor: Gary Lerude
Managing Editor: Jennifer DiMarco
Associate Technical Editor: Cliff Drubin
Multimedia Staff Editors: Barbara Walsh and Leslie Nikou
Consulting Editor: Harlan Howe, Jr.
Consulting Editor: Frank Bashore
Consulting Editor: David Vye
Consulting Editor: Raymond Pengelly
Web Editor: Chris Stanfa
Client Services Manager: Kristen Anderson
Audience Development Manager: Carol Spach
Traffic Manager: Edward Kiessling
Director of Production & Distribution: Robert Bass
Art Director: Janice Levenson
Graphic Designer: Sachiko Stiglitz

EUROPE

International Editor: Richard Mumford
Office Manager: Nina Plesu

CORPORATE STAFF

CEO: William M. Bazzy
President: Ivar Bazzy
Vice President: Jared Bazzy

Executive Editorial Office
685 Canton Street, Norwood, MA 02062
Tel: (781) 769-9750
FAX: (781) 769-5037
e-mail: mwj@mwjournal.com

European Editorial Office
16 Sussex Street, London SW1V 4RW, England
Tel: Editorial: +44 207 596 8730 Sales: +44 207 596 8740
FAX: +44 207 596 8749

Subscription Services
Send subscription inquiries and address changes to:
Tel: (847) 291-5216
e-mail: mwj@omeda.com

BPA WORLDWIDE

www.mwjournal.com

Printed in the USA

Microwave Journal Online

Scan page using layar app

Visit us @ mwjournal.com

eLEARNING free webinars

RF PCB Design, Inclusive of EM Analysis
Sponsored by: National Instruments (formerly AWR Corp.) 12/3

RF System Design, Prototype & Production with X-Parameters in One Pass
Presented by: Keysight Technologies 12/4

Antennas for Automobile Applications
Presented by: CST 12/4

Design Challenges for Handset Power Amplifiers Due to LTE-Advanced
Presented by: Rohde & Schwarz 12/10

Non-Destructive Testing of Powders, Ceramic, Oils and Other Composite Materials
Sponsored by: Keysight Technologies
Presented by: MWI Laboratories 12/11

Simulation-Enabled 5G Antenna Design
Presented by: CST 12/11

Marchand Balun and Its Evolution Into Modern Microwave Systems
Sponsored by: National Instruments (formerly AWR Corp.) 12/17

Web Survey

Where will the Internet of Things see the most adoption over the next few years?

Look for our multiple choice survey online at mwjournal.com

October Survey
Will RF industry consolidation continue?

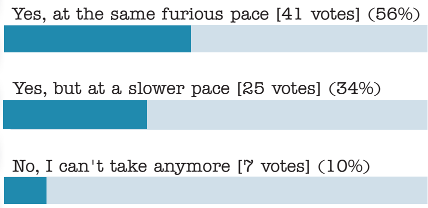

Executive Interview

Dr. Linda P.B. Katehi, Chancellor of the **University of California, Davis**, discusses her experience working in a predominantly male profession and suggests ways to encourage more women to pursue technical roles in the microwave industry.

WHITE PAPERS

Mercury Systems — OpenRFM™- A Better Alternative For An Open Architecture to Support EW, EA and SIGINT Applications

National Instruments (formerly AWR Corp.) — Design of a Class F Power Amplifier Using Cree GaN HEMTs and NI AWR Design Environment to Optimize Gain, Efficiency and Stability

Signal Hound — Cost-efficient and Extensible RF Spectrum Monitoring & Management

COM

SUPER ULTRA WIDEBAND

AMPLIFIERS

up to +27 dBm output... 0.1 to 21 GHz

from $845 ea.

Ultra wide coverage and super flat gain make our ZVA family ideal for ECM, instrumentation, and test systems. With an output power up to 0.5 Watts, they're simply some of the most usable amplifiers you'll find, for a wide range of applications and architectures!

All of our ZVA models are unconditionally stable, ruggedly constructed, and able to withstand open or short circuits at full output. For more details, from data sheets to environmental ratings, pricing, and real-time availability, just go to minicircuits.com!

All models IN STOCK!

RoHS compliant

Electrical Specifications (-55 to +85°C base plate temperature)

Model	Frequency (GHz)	Gain (dB)	P1dB (dBm)	IP3 (dBm)	NF (dB)	Price $ * (Qty. 1-9)
NEW ZVA-183WX+	0.1-18	28±3	27	35	4.0	1345.00
ZVA-183X+	0.7-18	26±1	24	33	3.0	845.00
ZVA-213X+	0.8-21	25±2	24	33	3.0	945.00

* Heat sink must be provided to limit base plate temperature. To order with heat sink, remove "X" from model number and add $50 to price.

Wideband Performance

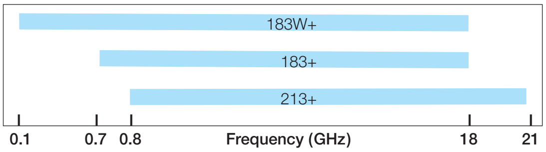

Mini-Circuits®

www.minicircuits.com P.O. Box 350166, Brooklyn, NY 11235-0003 (718) 934-4500 sales@minicircuits.com

440 rev R

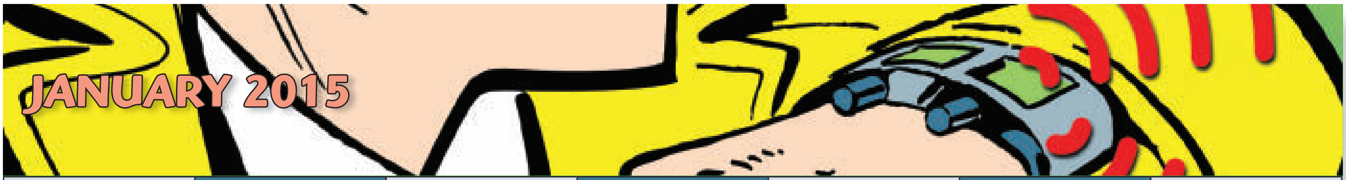

SUNDAY	MONDAY	TUESDAY	WEDNESDAY	THURSDAY	FRIDAY	SATURDAY
28	29	30	31	1	2	3
4	5	6	7	8 **Webinar:** **Nonlinear Effects in Active Phased Array Systems with Dr. Larry Williams** **Visit ANSYS.com/ events**	9	10
11	12	13	14	15	16	17
18	19	20	21	22 **Webinar:** **Aerospace & Defense** Sponsored by KEYSIGHT TECHNOLOGIES	23	24
25	26 RWW **Radio and Wireless Week** San Diego, Calif. **Webinar:** **LTE** Sponsored by KEYSIGHT TECHNOLOGIES	27	28 DESIGNCON 2015 Santa Clara, Calif.	29	30	31

Visit mwjournal.com/events

ComingEvents

CALL FOR PAPERS

WAMICON 2015
January 5, 2015

RFIC 2015
January 12, 2015

mwjournal.com

DECEMBER

IMaRC 2014
IEEE MTT-S International Microwave and RF Conference
December 15–17, 2014 • Bangalor, India
www.imarc-ieee.org

IEDM 2014
IEEE International Electron Devices Meeting
December 15–17, 2014 • San Francisco, Calif.
www.ieee-iedm.org

JANUARY 2015

RWW 2015
Radio and Wireless Week
January 25–28, 2015 • San Diego, Calif.
www.radiowirelessweek.org

DesignCon
January 27–30, 2015 • Santa Clara, Calif.
www.designcon.com

FEBRUARY

ISSCC 2015
International Solid-State Circuits Conference
February 22–26, 2015 • San Francisco, Calif.
www.isscc.org

IDGA 2015
Military Radar Summit
February 23–25, 2015 • Washington, DC
www.militaryradarsummit.com

MARCH

Mobile World Congress
March 2–5, 2015 • Barcelona, Spain
www.mobileworldcongress.com

CS International Conference 2015
March 11–12, 2015 • Frankfurt, Germany
www.cs-international.net

IEEE EMC & SI 2015
March 15–21, 2015 • Santa Clara, Calif.
www.emc2015usa.emcss.org

Satellite 2015
March 16–19, 2015 • Washington, DC
www.satshow.com

GOMACTech 2015
March 23–26, 2015 • St. Louis, Mo.
www.gomactech.net

APRIL

Microwave & RF 2015
April 1–2, 2015 • Paris, France
www.microwave-rf.com

WAMICON 2015
IEEE Wireless and Microwave Technology Conference
April 13–15, 2015 • Cocoa Beach, Fla.
www.wamicon.org

EDI CON 2015
Electronic Design Innovation Conference
April 14–16, 2015 • Beijing, China
www.ediconchina.com

SPACOMM 2015
7th International Conference on Advances in Satellite and Space Communications
April 19–24, 2015 • Barcelona, Spain
www.iaria.org/conferences2015

MAY

AUVSI's Unmanned Systems 2015
May 4–7, 2015 • Atlanta, Ga.
www.auvsi.org

RFIC 2015
IEEE Radio Frequency Circuits Symposium
May 17–19, 2015 • Phoenix, Ariz.
www.rfic-ieee.org

IMS 2015
IEEE MTT-S International Microwave Symposium
May 17–22, 2015 • Phoenix, Ariz.
www.ims2015.org

Space Tech Expo 2015
May 19–21, 2015 • Long Beach, Calif.
www.spacetechexpo.com

85th ARFTG Microwave Measurement Symposium
May 22, 2015 • Phoenix, Ariz.
www.arftg.org

EW Europe 2015
May 26–28, 2015 • Stockholm, Sweden
www.eweurope.com

Merger Movement in 2014

Pat Hindle
Microwave Journal *Editor*

It was a year of surprises – the RF and microwave industry was dominated by acquisitions and mergers as we experienced an unprecedented level of consolidation. While a couple of major mergers were expected, I was not prepared for the large number that actually occurred and the speed at which some took place. Some of the major company consolidations included the merger of RFMD and TriQuint (now Qorvo); the acquisition of several companies like Nitronex and Mindspeed by MACOM; the acquisition of Aeroflex by Cobham; Global Foundries' buyout of IBM's microelectronics business; the purchase of Peregrine by Murata and the acquisition of Hittite by Analog Devices (which took place in just over a month). Meanwhile, Skyworks hit the $2 billion mark in sales as probably the first RF/microwave semiconductor company to break that milestone (having completed its major merger quite a while back with Conexant).

Most of the consolidation was focused in the semiconductor industry, where volume is a major cost driver. It is a sign that RF and microwave applications are being used in mainstream consumer applications where the cost needs to be driven down to realize the needed volume. Even giants like Qualcomm and Intel are eyeing these markets as wireless has become an integral part of our everyday lives. I think the consolidation will taper off soon as the buying opportunities have mostly been realized, although I could see a similar scenario hitting some of the software and test & measurement companies. Leveraging software with testing hardware presents a strong value proposition to users, which could potentially drive consolidation in that area.

On the technology side, 5G research and prototyping took off this year as investments expanded quickly with support from industry and academia. Massive MIMO, software defined radio/cloud RAN, coordinated small cells/HetNets, mmWave transceivers and alternative modulation schemes are being analyzed for possible inclusion into the 5G standards. We highlighted 5G technologies several times this year including our November supplement cover story, which featured the latest mmWave propagation test results for 5G. This happened at the same time as the 4G rollout gathered steam, especially in the Chinese market where demand for components has been strong. CMOS continued to advance in the RF marketplace by showing off single chip RF fronts ends for 4G handsets and integrated mmWave AESA chips with up to 16 elements, discussed in our May cover story. Although CMOS has taken more market share in the RF marketplace along with GaN, GaAs still has a major presence in our industry due to its flexibility and already established manufacturing infrastructure. As the focus for more efficient amplifiers continued in 2014, envelope tracking entered the mainstream as a MIPI standard, eTrak. This topic was highlighted in our April cover feature, discussing various high efficiency amplifier design techniques, and again in September, more specifically about the standard.

On the aerospace and defense front, *Microwave Journal* covered the growing trend toward smaller satellites in our August issue, with antenna design techniques for nano satellites. As previously noted in our January cover feature, these small structures are challenging for traditional antenna designers and could require new technologies like metamaterials for realizing the required performance and features. In October, our cover

UNMATCHED TEST POWER AND SENSITIVITY. **UNMATCHED PERFORMANCE.**

BRIDGING THE THz GAP WITH VERSATILITY.

Virginia Diodes' AMC and MixAMC standardized product lines provide high performance frequency extension of microwave signal generators and analyzers into the mm-wave and THz frequency ranges (50GHz-1.1THz). These modules offer full waveguide band frequency coverage with market leading performance.

AMC's can be paired with common signal sources for CW power generation at high frequencies. Standard features include voltage controlled output attenuation, on-off modulation and switchable input frequency range.

MixAMC's can be used in a variety of different modes including frequency extension of spectrum analyzers and block up or down-conversion. These modules offer low-loss/low-noise performance with high instantaneous IF BW (up to 20GHz standard and 40GHz upon request).

Waveguide Band (GHz)	**WR15** 50-75	**WR12** 60-90	**WR10** 75-110	**WR8.0** 90-140	**WR6.5** 110-170	**WR5.1** 140-220	**WR4.3** 170-260	**WR3.4** 220-330	**WR2.8** 260-400	**WR2.2** 325-500	**WR1.5** 500-750	**WR1.0** 750-1100
AMC Performance												
Test Port Power - Typical (dBm)	20	18/15	14	9	8	4	2	-2	-6	-10	-21	-23
Test Port Power - Minimum (dBm)	17	12/11	10	3	2	0	-5	-8	-12	-18	-30	-33
MixAMC Performance												
SSB Intrinsic Mixer Conversion Loss (dB)	9	11	11	12	12	12	14	14	15	17	20	30
Displayed Average Noise Level (dBm/Hz)	-150	-150	-150	-150	-150	-150	-150	-150	-150	-150	-150	-135
Maximum IF Bandwidth (GHz)	8	9	11	14	17	20	20	20	20	20	20	20

VDI

Virginia Diodes, Inc.
979 2nd St. SE, Suite 309
Charlottesville, VA 22902
434.297.3257

vadiodes.com

Editor's Note

feature on the DARPA program for Mobile Hotspots focused on a gigabit E-Band UAV mobile network. The components designed for this program obtained 17 W at 74 GHz with a goal of 20 W, which is very impressive.

As Apple and Samsung released wearable technologies in the form of connected watches and other devices, and connected vehicles started to hit the market, the Internet of Things was revived as a fast growing (but often over-hyped) trend. There are a lot of forecasts circulating, but ABI Research believes the installed base of active wireless connected devices will exceed 16 billion in 2014 and is forecast to be 40.9 billion by 2020. On the vehicle side, IHS Automotive predicts the number of cars connected to the Internet worldwide will grow to 152 million in 2020 from 23 million in 2013.

The design of these devices presents many challenges, which is why we decided to include two articles in our December cover feature. The first takes a look at low power design techniques for wearable technologies, and the second talks about mesh networking for industrial applications. ABI Research expects the installed base for 802.15.4-enabled devices to increase almost fivefold over the next five years, rising from just under 425 million today to over 2.1 billion in 2019. ABI also expects IPv6-enabled alternative 802.15.4 technologies to take a significant market share of 35 percent by 2019. There is no doubt that 5G and IoT are two areas that will demand significant coverage in 2015.

Microwave Journal also continued coverage of these topics in its third year with *Microwave Journal China* and second successful year with EDI CON China, an industry driven conference and exhibition. We will continue to increase our offerings to clients and readers in 2015 by expanding our digital and print products along with our live events. The EDI CON industry driven event model, focused on the practicing engineer, has been well received and allows the practical conference to be integrated within the exhibition, including workshops and tutorials on the latest technology being offered by leaders in the industry. We look forward to any feedback you have as we strive to improve our coverage and technical content. Happy Holidays! ■

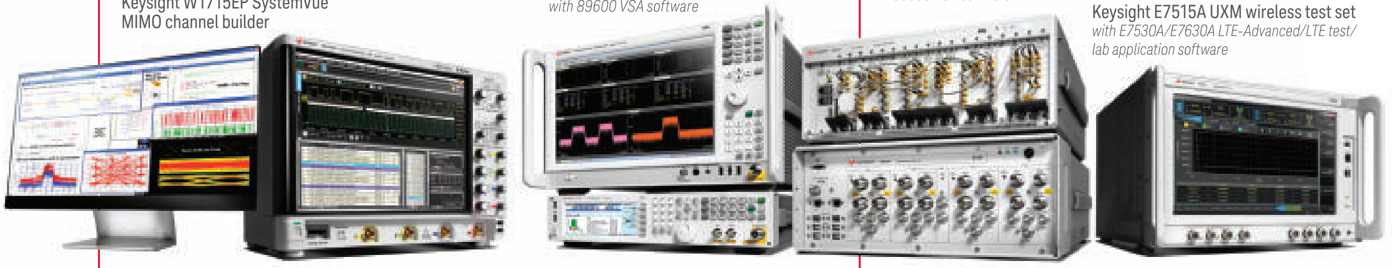

Keysight W1715EP SystemVue MIMO channel builder

Keysight N9040B UXA signal analyzer
with 89600 VSA software

Keysight MIMO PXI test solution
with N7624/25B Signal Studio software for LTE-Advanced/LTE FDD/TDD and 89600 VSA software

Keysight E7515A UXM wireless test set
with E7530A/E7630A LTE-Advanced/LTE test/lab application software

Keysight Infiniium S-Series high-definition oscilloscope
with N8807A MIPI DigRF v4 (M-PHY) protocol decode software

Keysight N5182B MXG X-Series RF vector signal generator
with N7624/25B Signal Studio software for LTE-Advanced/LTE FDD/TDD

Keysight E6640B EXM wireless test set
with V9080/82B LTE FDD/TDD measurement applications and N7624/25B Signal Studio software for LTE-Advanced/LTE FDD/TDD

HARDWARE + SOFTWARE

The more complex your LTE-A design, the more you need help from test and measurement experts. Keysight is the only company that offers benchtop, modular and software solutions for every step of the LTE-A design process. From R&D to manufacturing, we can give you the expertise, instruments and applications you need to succeed.

- *Complete LTE-Advanced design and test lifecycle*
- *Identical software algorithms across platforms*
- *300+ software applications for the entire wireless lifecycle*

PEOPLE

We know what it takes for your designs to meet LTE-A standards. After all, Keysight engineers have played major roles in LTE-A and other wireless standards bodies, including 3GPP. Our engineers even co-authored the first book about LTE-A design and test. We also have hundreds of applications engineers. You'll find them all over the world, and their expertise is yours for the asking.

- *Representation on every key wireless standards organization globally*
- *Hundreds of applications engineers in 100 countries around the world*
- *Thousands of patents issued in Keysight's history*

KEYSIGHT TECHNOLOGIES

Unlocking Measurement Insights

COVER FEATURE
INVITED PAPERS FROM
Silicon Labs
and
Linear Technology Corp.

Internet of Things Focus

Winning Design Strategies for Wireless Wearables

Mendy Ouzillou, Silicon Labs, Austin, Texas

Mesh Network Protocols for the Industrial Internet of Things

Ross Yu, Linear Technology Corp. (Dust Networks Group), Milpitas, Calif.

Editor's Note: The Internet of Things (IoT) has become a hot topic this year with the release of some major wireless wearable devices and increased use of wireless appliances and industrial controls. The following two articles cover the low power design of wearable devices by Silicon Labs and industrial mesh networking by Linear Technology.

WINNING DESIGN STRATEGIES FOR WIRELESS WEARABLES

Mendy Ouzillou, Silicon Labs, Austin, Texas

When Chester Gould drew that iconic watch on Dick Tracy's wrist, little did he realize that science fiction would become a reality some 70 years later. As a comic strip artist, Gould envisioned a futuristic device without worrying too much about the details. Today, these very real wrist-top devices and other wireless wearable devices (WWD) present engineers with a slew of challenging design details that they must address. Engineers must seamlessly integrate complex sensing, processing, display and wireless technologies into affordable, compelling, compact designs that can run for months or even years on a single, small and cost-effective battery. Here we examine the unique requirements of wearable devices and the technology and component choices that enable a combination of sophisticated functionality, long battery life and seamless wireless connectivity – all within extremely small form factors.

The three key factors an engineer must consider in a wearable design are power consumption (energy friendliness) across all modes of operation, proper RF design from the matching circuits to the antenna(s) and the integration level of the devices used in the design. We will explore the integration challenge in more detail as it is difficult to discuss this factor in isolation without taking into account energy efficiency and RF design.

Most wireless wearable devices share common components including a battery, an antenna, a microcontroller (MCU), a radio and a sensor. What is immediately obvious from this list is that the battery will in large part drive realizable functionality and operating life of the WWD. As the majority of WWDs are not meant to stream data continuously due to the severe drain on the battery, we can assume that communications are bursty and infrequent. Furthermore, since MCUs with integrated radios, often called wireless MCUs (WMCU), are readily available, save board space and reduce power consumption, we can also assume the use of WMCUs in the wearable design.

Selecting the right WMCU for the application can be a complex decision since the desire for high functionality in a feature-rich device must be constrained by the battery operating

life. If we look at just the peak power consumption of the WMCU and extrapolate battery life from that single metric, the results would be rather disappointing. However, WWDs typically operate in many different energy modes (EM) and rarely enter a high power state. By taking into account the amount of time spent in each of these energy modes, we can determine a device's realistic operating life.

For example, at Silicon Labs we have defined five energy modes for the ARM-based EFM32 MCUs: EM0 (active/run), EM1 (sleep), EM2 (deep sleep), EM3 (stop) and EM4 (shut-off). These five modes enable the designer to properly determine and optimize the system's overall power consumption. However, identifying these modes and attaching specs to them in a datasheet does not guarantee low power consumption across all modes or more succinctly, energy friendliness. What ensures energy friendliness, and by extension a positive end-customer experience, is the way the WMCU is architected to operate in these different modes. In fact, depending on the time between bursts, active mode EM0 might represent a small percentage of the overall power consumption, and the time spent in deep-sleep mode, EM2 may represent the largest percentage of the battery drain.

When selecting the best WMCU for their application, engineers should look for the following features of an ultra-low-power WMCU:

- Lowest active power consumption (EM0)
- Lowest standby currents (EM1 and EM2)
- Choice of microprocessor cores including 8 and 32-bit ARM Cortex (M0+ to M4)
- Range of radio configurations to choose from, including TX-only, RX-only, TX+RX and performance levels.

There are additional MCU features, both related to architecture and integration, which are equally important:

- Very fast wake-up times
- Autonomous peripheral operation
- Autonomous inter-peripheral operation (Peripheral Reflex System)
- Low energy sensor interface (LESENSE)
- Rich set of energy-efficient peripherals and interfaces
- RF integration

LOWEST STANDBY CURRENTS AND FAST WAKE-UP TIMES

When designing a wireless wearable device that is as energy friendly as possible, one must ferret out every possible optimization of power consumption. When a device wakes up, it must do so as quickly as possible, collect and process data as quickly as possible and go back to sleep as quickly as possible (see ***Figure 1***). Ensuring a fast transition from a sleep mode to active mode is a critical consideration. If one processor spends even 10 percent more time in active mode than another processor, the impact on battery life can be dramatic. For example, assume that processor 1 spends 99.9 percent of its time in deep sleep (1 μA) and 0.1 percent of its time in active mode (10 mA), while processor

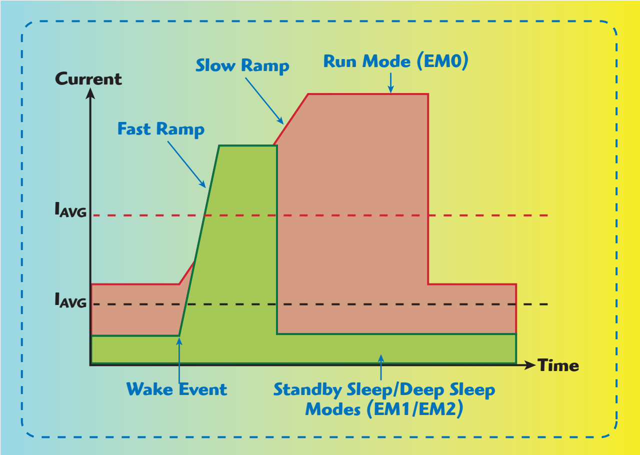

▲ *Fig. 1 Very fast wake-up time, low active current and very low sleep current are keys to minimizing energy consumption.*

2 spends 99.89 percent of its time in deep sleep and 0.11 percent of its time in active mode, then the overall current consumption of the second processor is increased by 9.1 percent. Interestingly, if processors 1 and 2 are now active for only 100 ms and 110 ms respectively out of every 6 hours, the results will highlight the importance of very low deep sleep current. In this case, the second processor will only consume 0.44 percent more current than the first. However, make the active mode time the same and increase the deep sleep current from 1 to 1.1 µA, then the current consumption goes up by 9.6 percent (see ***Table 1***).

AUTONOMOUS PERIPHERAL OPERATION

Wearables, depending on their function, may need to interact with or monitor on-chip peripherals frequently or even continuously. In either case, requiring the CPU to be active during those times represents a significant drain on the battery. Ensuring that the on-chip peripherals can operate autonomously without waking the CPU enables the system to operate in low energy modes while still performing very advanced tasks (see ***Figure 2***). These peripherals can include serial interfaces (e.g., low-energy UART, crystal-less USB), I/O ports (e.g., external interrupts, GPIO), timers and triggers (e.g., low-energy timer, low-energy sensor interface), analog modules (e.g., ADC, LCD controller) and security (e.g., AES accelerator).

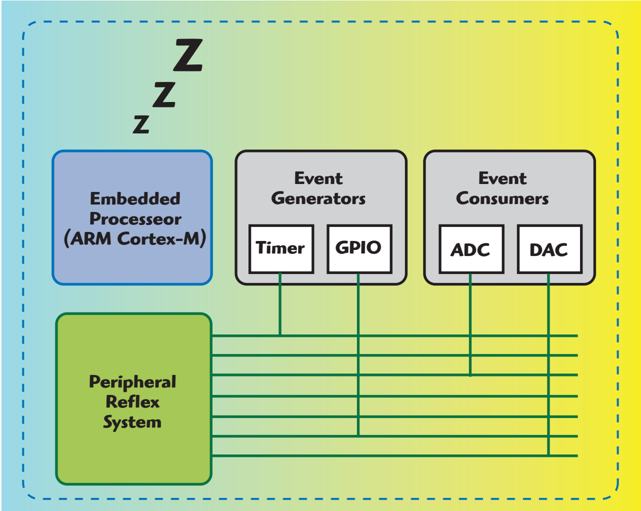

▲ *Fig. 2 Autonomous peripheral operation, autonomous inter-peripheral operation and configurable/energy efficient operation are keys to wearable design success.*

AUTONOMOUS INTER-PERIPHERAL OPERATION

There are also circumstances where peripherals may need to communicate with each other. In these cases, one peripheral can generate an event or events that can be instantaneously acted upon by another on-chip peripheral. For example, a timer may be set to create an event that then triggers an ADC to begin sampling. Enabling autonomous operation between these peripherals without waking the CPU ensures the lowest system power consumption (see Figure 2). As an example, this capability is a key aspect of Silicon Labs' EFM32 MCU architecture and is known as the Peripheral Reflex System.

LOW ENERGY SENSOR INTERFACE

Eventually, the CPU will need to be awakened to perform a specific task. Most MCUs will be set to awaken on a set schedule and monitor its interfaces, and if no action is required, it will go back to sleep. These periodic

TABLE I

ENERGY CONSUMPTION COMPARISON

Case 1: Wake-up time increased by 10% (system active for 86.4 seconds per day)						
	Processor 1			Processor 2		
	% of time	Current (mA)	Time-Weighted (mA)	% of time	Current (mA)	Time-Weighted (mA)
Sleep	99.9%	0.001	0.0000999	99.89%	0.001	0.0009989
Active	0.1%	10	0.01	0.11%	10	0.011
		Aggregate Current	0.010999		Aggregate Current	0.0119989
				9.09% increase in current consumption		
Case 2: Sleep current increased by 10% (system active for 100 ms seconds per 6 hours)						
Sleep	99.999537%	0.001	0.0009910	99.999537%	0.0011	0.001099995
Active	0.000463%	10	0.0000463	0.000463%	10	0.0000463
		Aggregate Current	0.0010463		Aggregate Current	0.001146295
				9.56% increase in current consumption		

wake cycles unfortunately drain unnecessary power from the battery. The LESENSE architecture used in EFM32 MCUs allows autonomous monitoring of analog sensors (resistive, capacitive and inductive) and only awakens the CPU on a relevant event or even conditionally, like every other event. For example, LESENSE can be set up to autonomously monitor a temperature sensor and take the action via the Peripheral Reflex System to wake up the CPU only if the programmed threshold of 99°F is exceeded. Using LESENSE minimizes the amount of time the CPU is enabled and consuming the greatest amount of power.

RICH SET OF ENERGY-EFFICIENT PERIPHERALS

Developing a wearable device that consumes as little power as possible in all modes of operation requires an MCU architecture in which every aspect of operation is scrutinized. Although autonomous operation of the peripherals has been discussed, it is helpful to take a closer look at the low power requirements of the peripherals themselves. Autonomous operation achieves very little if the peripherals are power hungry or if clocks are enabled unnecessarily.

As a peripheral itself, the clock management unit plays a significant role in determining the MCU's or WMCU's overall power consumption. The clock management unit enables individual control of the various clocks and oscillators and optimizes clock selection based on the energy mode of operation and the peripherals enabled. Using low-power oscillators combined with a flexible clock control scheme, it is therefore possible to minimize the energy consumption in any given application. Aspects of an energy-efficient clock management unit include current starved oscillators, low start-up times, dynamic system clock division, clock pre-scalers for 32 kHz peripheral modules and clock gating.

Availability of a low-energy autonomous universal asynchronous receiver/transmitter (UART) is also important to achieve low system power consumption especially during deep sleep (EM2) where most other peripherals and the CPU are turned off. This UART should include the necessary hardware support to make asynchronous serial communication possible with minimal software intervention. By using a 32.768 kHz clock source, the low-energy UART can support up to 9600 baud, and when a complete UART frame is received, the CPU can be quickly awakened.

A low-energy timer can be used for timing and output generation when most of the device is powered down, thus allowing simple tasks to be performed while the power consumption of the system is kept at an absolute minimum. When properly configured, such a timer can provide glitch-free waveforms at frequencies up to 16 kHz (half the frequency of a 32 kHz oscillator).

Analog resources such as an ADC, DAC, LCD controller, analog comparators and other peripherals commonly found in MCUs and WMCUs should be carefully analyzed for their power

consumption as well as their flexibility. For example, a 12-bit 1 Msps ADC may consume 350 µA at full rate, but not all applications may require operation at that level. The application may only require 6-bits and 1 ksps, in which case the ADC would consume only 0.5 µA – a significant reduction. An LCD controller should be able to run custom animations without any CPU intervention and only wake the CPU when data needs to be updated.

Encryption can be very resource intensive and a noticeable drain on the battery. The lowest cost 8-bit MCUs will require the security algorithms to be performed as run-time code while 32-bit MCUs will most likely include an AES accelerator. When a hardware AES accelerator is available, it should be capable of running autonomously without involving the CPU and include DMA support for autonomous cipher modes to minimize the battery drain.

RF INTEGRATION

The previous discussion centered largely on the MCU architecture. However, there are additional features related to the radio transceiver. Wireless wearable devices may never need to receive information based on the application requirement, but most will need to transmit data at some point. Poor power amplifier efficiency in battery-operated devices can dramatically increase the system power consumption and require an application to increase the size and cost of a battery to meet the system operating life requirement. For example, long-range devices may require RF output power levels of +13, +16 or even +20 dBm. Though integration of +10 dBm RF power amplifiers (PA) in WMCUs is widely available, if the application requires any more output power, an external transistor or amplifier will be needed. These external amplifiers are not economically viable because they are very difficult to make efficient and cost-effective. Therefore, in long-range applications and/or applications that require frequent communication, efficiency and battery life are typically sacrificed to achieve aggressive cost targets. One way to address this issue is to ensure that the WMCU integrates the appropriately sized power amplifier, even up to +20 dBm. By integrating the PA into the WMCU, the PA's current consumption can be minimized more effectively. There are no losses due to poor matching between the PA output and the booster amplifier and no overdesigning of the transmit chain to compensate for temperature and voltage variations. A completely integrated PA enables full control of the PA's operation and ensures the lowest power consumption.

There are many applications that operate at 2.4 GHz, and in these cases IC vendors have an opportunity to simplify the system design by integrating matching circuits and providing a single-ended RF input and output. Sub-GHz applications tend to span a very wide frequency range, from hundreds of MHz up to 1 GHz. In these cases, it is not feasible to integrate matching components. However, integrated passive devices used externally with the WMCU, and comparable in cost with discrete implementations, will become available for use in the most popular frequency bands.

It's Not Bragging When You Can Back It Up.

Lots of suppliers claim to have "The Best Products", but do they have any proof to back it up? AR has been proving it for over 43 years. We've built a reputation for reliable products that go the distance… and then some. Products that are more powerful, faster, smaller, and more efficient. Products that outlast, outperform, and outrun any of our competitors. And if that wasn't enough, every one of our products is backed by our comprehensive worldwide support and no nonsense warranty.

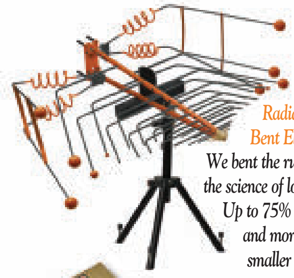

Radiant Arrow® Bent Element Antennas

We bent the rules and advanced the science of log periodic antennas. Up to 75% smaller, lighter, and more compact to fit in smaller chambers.

New Hybrid Power Modules

We've complemented our previous line of 4-18 GHz HPM's to cover the entire 1-6 GHz frequency range in one amplifier module. High gain 50 ohm modules provide 15 watts of Class A or 25 watts of Class AB output power in a convenient, small connectorized housing.

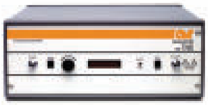

0.7 to 2.5 GHz Solid State Amplifiers

The solid state alternative to TWTA's. Improved harmonics, lower noise, superior linearity and reliability and now featuring 1,000 watts CW.

Integrated Test Systems

All-in-one test systems for any EMC application, DC to 50 GHz. Our systems make testing more efficient, accurate, and affordable.

RF Conducted Immunity Test Systems

These self contained systems driven by our proprietary software; simplify calibration, testing, troubleshooting and reporting. They allow accurate, sensitive and repeatable measurement in one unit. And did we mention incredible speed with outputs up to 150 watts and 400 MHz.

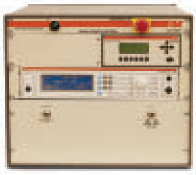

Dual Band Amplifiers

For the first time you can go from 0.7 to 18 GHz with the reliability of solid state in a single housing. Numerous models with various output powers help you reduce the footprint and cost of separate instruments.

"S" Series Amplifiers

Lighter, more portable, and up to 50% smaller. Available with all the power you need up to 1200 watts.

A Special Family of Antennas for High Intensity Radiated Field (HIRF) Testing

These are all high-gain,high-power microwave horn antennas that provide typical 20 dBi over isotropic. They supply high intensity fields for DO 160 HIRF testing.

multi star Field Analyzer

The new series of laser-powered electric field analyzers have an extremely high sample rate and can precisely measure pulsed electric fields in the microsecond range. They represent a whole new way to more accurately measure modulated and CW electric fields in both conventional and reverberation chambers and allow the user to see the modulation envelope.

multi star Multi-Tone Tester

This incredible system cuts RF Radiated Immunity testing from days down to hours by testing multiple frequencies simultaneously, reducing product development cost and time to market.

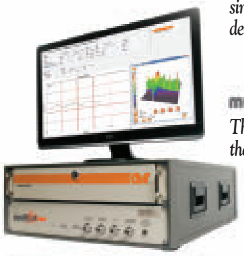

multi star Precision DSP Receiver

This 18 GHz EMI receiver changes the way you think about emissions testing. Data is more accurate and test time is reduced. Testers have a suite of new mitigation tools.

16,000 Watts of Pure Power

The new 16000A225 amp. It covers 10 kHz to 225 MHz and delivers 16,000 watts of power and we're not stopping there.

www.arworld.us/notBragging

ISO 9001:2008 Certified

rf/microwave instrumentation

Other ar divisions: modular rf • receiver systems • ar europe

www.arworld.us

USA 215-723-8181. For an applications engineer, call 800-933-8181.

In Europe, call ar United Kingdom +44 1908 282766 • ar France +33147917530 • ar Deutschland +49 6101 80270 0 • ar Benelux +31 172 423000

ANTENNNAS

No discussion of wireless wearable devices is complete without considering the antenna's transmit and receive characteristics. Due to size and cost constraints, most antennas for wireless wearable devices tend to have poor transmit characteristics, as they are often simply printed on the PCB material like FR4. The simplest way to compensate for a lossy/low gain antenna is to increase the RF output power. Unfortunately, this can consume far more power than where the antenna has been optimized. Better designed and lower loss matching circuits will ensure optimized operation, but the antenna design remains the big challenge, considering the varied RF environment of a wearable device. Mismatch fluctuations due to proximity to the user's body, such as a hand covering the device, can cause many problems. Some WMCU devices have integrated antenna tuning circuits that actively compensate the antenna during these times. Such circuits play an important role in controlling power consumption and ensuring that radiated emissions stay within regulatory limits.

One method to compensate for poor antenna reception is to design the system with antenna diversity (i.e., with multiple antennas). Though many applications will benefit from antenna diversity, there are some factors to consider. First, antenna diversity tends to help most when the distance between the transmitter and receiver is such that the received signal level is near the background noise level (i.e., near the end of link range) or in fading environments created by multipath propagation or obstacle shadowing of the signal.

To reduce power consumption and die cost, wireless MCU ICs integrate only one receive path. So antenna diversity must be performed through an external switch that alternately selects between the two antennas. However, sharing of one receive path by two antennas may consume more power than one might expect. In this case, the transmit preamble length has to be extended to provide enough time for both antennas to be sequentially evaluated. There is also the added computational cost and current consumption to analyze and select the best antenna.

SEPARATION ANXIETY

Finally, there is the issue of space. The minimum spacing between antennas recommended in wireless communication systems is ¼ λ. At 2.4 GHz, the wavelength is 125 mm, so separating the antenna by the minimum of ¼ λ or 31.25 mm is feasible with some wireless wearable devices. However, for WWDs operating in sub-GHz frequencies, the challenge becomes far more difficult. At 868 MHz, the antennas should be separated by a minimum of 86 mm, which may preclude the use of antenna diversity in many applications. An engineer must therefore trade off improved range and reception for added complexity and size, computation cost and current consumption. Assuming that antenna separation is not an issue, the increased computation cost and associated current consumption can be addressed. In a variable or unsynchronized environment, periodic toggling between antennas is required because the radio has no prior knowledge of which antenna will prove to be the "better" antenna when the packet arrives. Some transceivers use an integrated preamble quality detector to determine signal quality based on RSSI values and to confirm arrival of a valid packet on both antennas. The benefit of an integrated detector is that it will select the best antenna and, by offloading the MCU, will also decrease overall power consumption during the selection process.

CONCLUSION

If Chester Gould were alive today, he would certainly be impressed by how his vision has been realized. Companies have already delivered devices far beyond Dick Tracy's walkie-talkie enabled wrist-watch and are developing a wide range of advanced wearable devices. As designers try to pack more and more features and functionality into their wireless wearable devices, the underlying concerns will remain the same – how will they achieve low power consumption, fit the design into a small form factor and ensure reliable wireless communication with the device? The final concern is how to achieve these product design goals for as low a price point as possible, but that is a topic for another day. "Six-two and even, over and out."

MESH NETWORK PROTOCOLS FOR THE INDUSTRIAL INTERNET OF THINGS

Ross Yu, Linear Technology Corp. (Dust Networks Group), Milpitas, Calif.

One of the biggest promises of the Industrial Internet of Things is to leverage real-world data gathered through wireless sensor networks (WSN) to drive higher efficiencies and streamline business practices. The demands on WSNs are diverse, with sensors placed throughout buildings, city streets, industrial plants, tunnels and bridges, moving vehicles or in remote locations such as along pipelines and weather stations. A common requirement across such applications for the Industrial Internet of Things is for WSNs to deliver both low power and wire-like reliability and to do so across a broad spectrum of network shapes, sizes and data rates.

Wireless mesh networks have become increasingly well accepted due to their ability to cover large areas using relatively low power radios that relay messages from node to node and to maintain high reliability by using alternate pathways and channels to overcome interference. One technique in particular, Time Synchronized Channel Hopping (TSCH) mesh networking, pioneered by Linear Technology's Dust Networks and incorporated into the WirelessHART industrial standard, is field proven to deliver the performance needed by the Industrial Internet of Things. TSCH networks typically experiencing >99.999 percent data reliability and all wireless nodes, even routing ones, have multi-year battery life on small lithium batteries. However, a variety of mesh networks use similar sounding networking techniques (e.g., "frequency agility" vs. "channel hopping," "sleepy" vs. "time synchronized"), yet yield drastically different performance levels. These wireless networking details determine how such protocol level choices greatly impact a WSN's performance and the network's overall suitability for an application.

WIRELESS SENSOR NETWORK CHALLENGES

Since wireless networks can be unreliable, it is important to understand the sources of unreliability and account for them in a communications system. Unlike wired communications, where the signal is shielded from the outside world by cabling, RF propagates in the open air and interacts with the surrounding environment. There is the possibility other RF transmission sources will cause active interference.

However, much more common is the effect of multipath fading, where the RF message may be attenuated by its own signal reflected off surrounding surfaces and arriving out of phase (see ***Figure 3***). Mobile phone users

SIDEBAR

The Effects of Multipath Fading on Wireless Communications

Multipath fading depends on the position and nature of every object in the environment and is unpredictable in any practical setup. One good property is that the topography depicted in ***Sidebar 1*** changes with the frequency. If a packet is not received because of multipath fading, retransmitting on a different frequency has a high probability of succeeding.

Because objects in the environment are not static, the effect of multipath changes over time. For example, cars drive by and doors are opened and closed, ***Sidebar 2*** shows the packet delivery ratio on a single wireless path between two industrial sensors over the course of 26 days and for each of the 16 channels used by the system. There are weekly cycles where workdays and weekends are clearly visible. At any given time, some channels are good (high delivery), others poor, and still others highly varying. Channel 17, while generally good, has at least one period of zero delivery. Each path in the network shows qualitatively similar behavior but unique channel performance. There is never any one channel that is viable everywhere in the network. The key to building a reliable wireless system is to exploit channel and path diversity to mitigate interference and multipath fading.

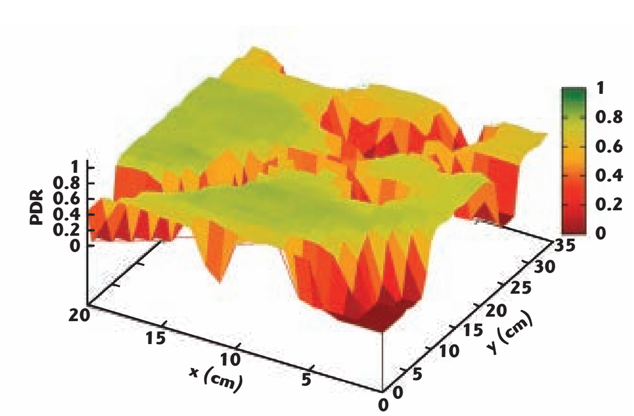

▲ *Sidebar 1 Multipath fading causes the quality of a link to vary dramatically, even when moving the receiver by only a couple of centimeters.*

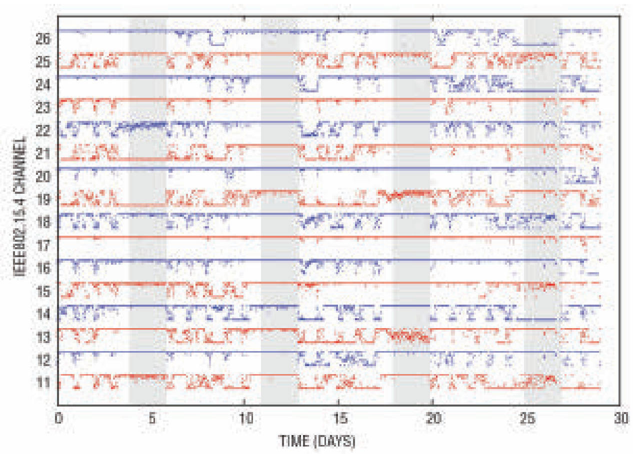

▲ *Sidebar 2 The packet delivery ratio of a wireless link varies over time.*

experience multipath fading every day when their phones seemingly have poor signal strength in one spot, but it improves by moving just a few centimeters. The effects of multipath change over time, as nearby reflective surfaces (e.g., people, cars, doors) typically move. The net result is that any one RF channel will experience significant variation in signal quality over time.

Further adding to the challenge is that multipath fading is unpredictable. By definition, a network must be actively transmitting on a channel to experience (and therefore measure) the channel's performance in the face of multipath fading. Therefore, while the notion of using a simple passive signal strength measurement (RSSI) of an unused channel may be helpful to detect active interferers, it cannot predict that channel's suitability in the face of multipath fading. Fortunately, since multipath fading affects each RF channel differently and changes over time, using channel hopping for frequency diversity minimizes the negative effects of multipath fading. The challenge for WSN protocols is the ability to use channel hopping over large networks with multiple hops.

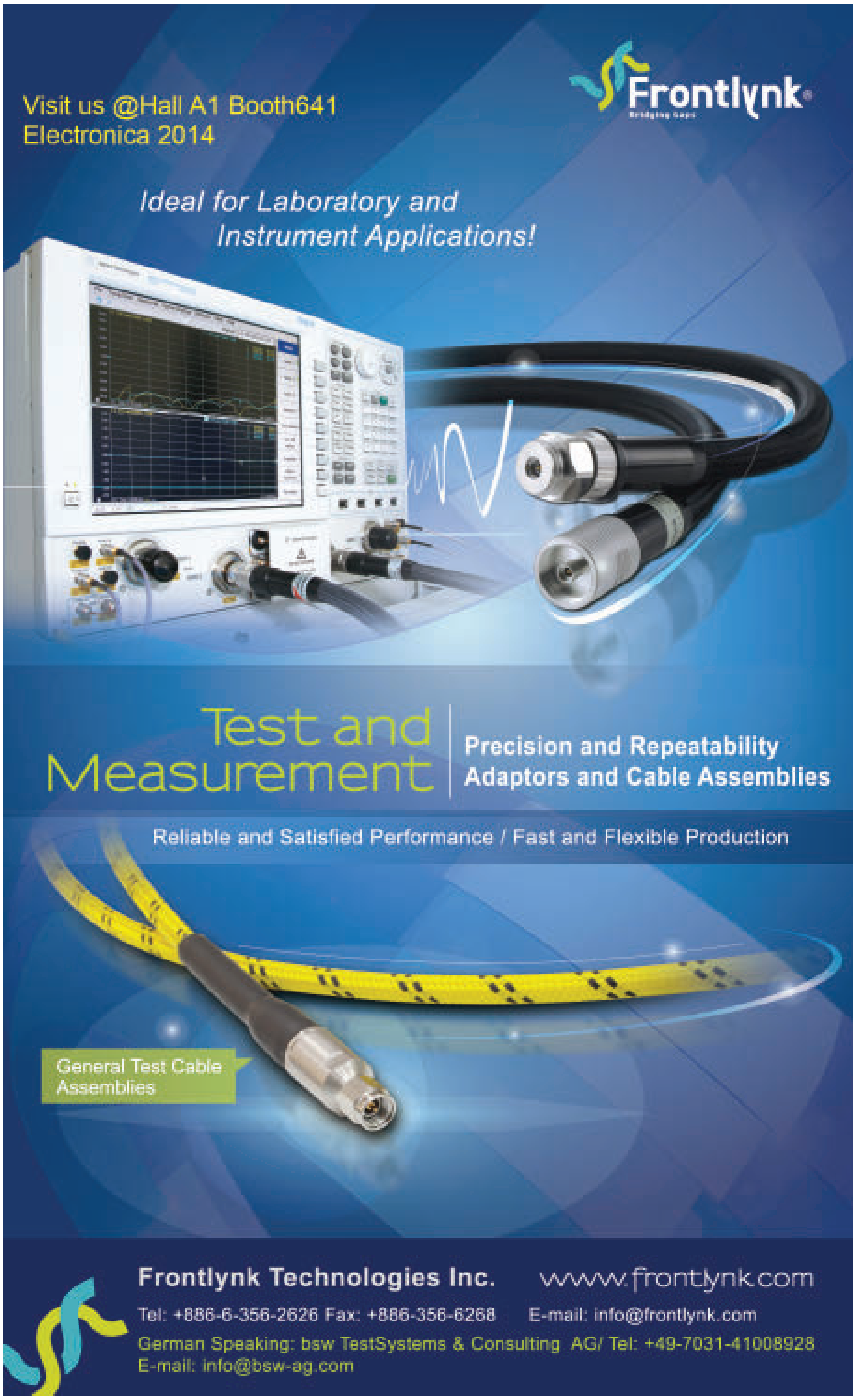

COMMON APPROACHES

To understand how different WSNs perform in the face of these constraints, let us examine techniques often used in some wireless mesh networks to address frequency diversity and to deliver low power.

Single Channel WSNs and Channel Agility – A common approach in simple implementations of wireless mesh networks is to have all nodes operate on a single channel. Since only one RF channel is used, only one device can be transmitting at a time. Network stack developers often still choose single channel operation due to the relative simplicity of implementation, and in doing so provide a WSN with virtually no frequency diversity.

In order to respond to the presence of active RF interference in channel, some single channel WSNs have a mechanism called channel agility, where a network can broadcast a message to all nodes to change the operating channel. But even in channel agile networks, at any point in time the network is still operating on a single channel. The use of channel agility assumes that there is a single channel that is good for the entire network. However, with the effects of multipath fading, real world data shows that any RF channel will experience severe path degradation during the lifetime of the network, causing nodes to drop out for periods spanning minutes or hours. (See ***sidebar:*** "The Effects of Multipath Fading on Wireless Communications.") While a network with channel agility can change the chan-

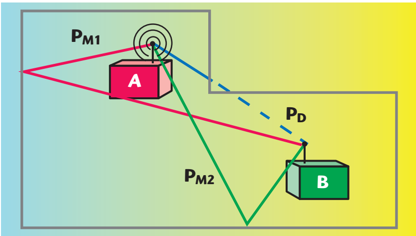

▲ *Fig. 3 A radio signal's strength at the receiver (B) is affected not only by the direct path (P_D), but also by reflections (P_{M1} & P_{M2}), which may arrive out of phase and cause significant fading.*

nel away from an active interferer, the network is still susceptible to the devastating effects of multipath fading.

Duty Cycling by Network-Wide Sleeping - For low power operation, wireless sensor networks perform some form of duty cycling to minimize the percentage of time spent in active operation (e.g., transmit or receive, which typically draws milliamps of power) and maximize the percentage of time spent in a low power sleep mode (typically 1 mA or lower). Some wireless sensor networks incorporate a network-wide sleeping scheme (sometimes called a "sleepy" mesh), in which all the nodes in the network are put into a low power sleep state for an extended period and wake up at approximately the same time to send/receive/forward network traffic. In such sleep schemes, the network is completely unavailable for communications during the inactive period. For example, if a WSN only wakes once an hour for communications, then the network is unable to send an alarm message during that hour, nor can it receive a message from a controller to light up an attached warning indicator. It is also important to consider how the use of network-wide sleeping affects the WSN's ability to cope with real-world operating conditions. During the extended sleep periods, the surrounding RF environment remains dynamic and changing. Any signal pathway that became unusable during network sleep can only be repaired when the network awakens. Even more troublesome is the fact that sleepy networks tend to be single channel networks, placing further stress on the network during its active period and adding to the risk of communication instability.

Another repercussion of using network-wide sleep is that a network-wide sleeping approach forces a user to settle for a slower data rate (and therefore less data) than could be called for by the application. This is an unfortunate trade-off, since the main purpose of a WSN is data reliability and to use that information to enable deeper insight into the user's systems, showing operational trends and inefficiencies such as degrading performance in aging motors, or increased cyclic power draw of old refrigeration equipment in a retail store. When the data delivered by the WSN is sparse due to network limitations, the utility and insight derived from the WSN becomes limited and runs the risk of reducing the overall value proposition of the monitoring/control system.

TIME SYNCHRONIZED CHANNEL HOPPING MESH NETWORKS

Time Synchronized Channel Hopping (TSCH) mesh networks use tight time synchronization across a multi-hop network to closely coordinate communications and frequency channel usage. In a TSCH network, each node shares a common sense of time that is accurate across the network to within a few tens of microseconds. The nodes exchange timing offset information with neighboring nodes to maintain time synchronization. Network communication is organized into time slots, in which individual packet transmit/receive opportunities are scheduled. Each time slot is long enough (e.g., 7.5 ms) for a transmitting node to wake up, transmit a packet, and receive

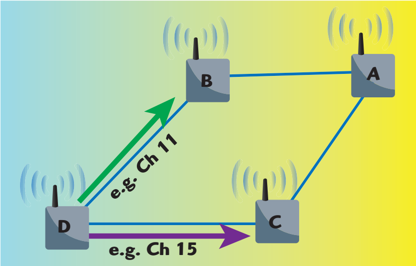

Fig. 4 If communication fails on the "green" arrow, node D retries on the "purple" arrow using another channel and pathway.

its link-layer acknowledgment from the receiving node. Data traffic in a TSCH network can be dynamically scheduled, which enables pair-wise channel hopping, full path and frequency diversity, low power packet exchange and high-availability duty cycling.

Pair-Wise Channel Hopping - Time synchronization enables channel hopping on every transmitter-receiver pair for frequency diversity. In a TSCH network, every packet exchange channel hops to avoid RF interference and fading. In addition, multiple transmissions between different device pairs can occur simultaneously on different channels, increasing network bandwidth. For example, there are fifteen usable channels available in the IEEE 802.15.4 2.4 GHz radio specification, which is a popular choice for WSN implementations due to the global availability of this ISM band. This represents up to 15 times the available bandwidth for a TSCH network, compared to that of a single-channel 802.15.4 WSN.

Full Path and Frequency Diversity - Each device has redundant paths to overcome communications interruptions due to interference, physical obstruction or multipath fading. If a packet transmission fails on one path, a mote will automatically retry on the next available path and a different RF channel (see ***Figure 4***). By exercising path diversity and frequency diversity on each retry (time diversity), the probability of success on each retry is higher compared to a single-channel system.

Low-Power Packet Exchange - The use of TSCH allows nodes to sleep at ultralow power between scheduled communications. Each device is only active if it is sending a packet or listening for a potential packet from a neighbor device. More importantly, since each node knows when it is scheduled to wake up, each node is always available to relay information from its neighbors. Therefore, TSCH networks often reach duty cycles of <1% while keeping the network completely available. Furthermore, since each packet transaction is scheduled, there are no in-network packet collisions in a TSCH network. Networks may be dense and scale without creating debilitating RF self-interference.

High Availability Duty Cycling – Unlike in a network-wide duty cycled network, in a TSCH network individual nodes wake up their transceivers only when they need to transmit a packet or listen for a packet to be received. By scheduling network traffic to the granularity of individual transmitter-receiver exchanges, a TSCH network can easily accommodate heterogeneous data traffic across the network. For example, if there is a tank level sensor that only needs to transmit once an hour, and elsewhere, pressure/flow sensors that report every few seconds, then a TSCH network will wake up nodes (and their parents) only as frequently as needed to reliably support its level of data traffic.

THE POWER OF COMBINING TSCH WITH LOW POWER HARDWARE

The operating currents for 802.15.4 transceivers for general operations, such as transmit, receive and sleep, have steadily reduced over the past decade. For example, the LTC5800-IPM from Linear Technology draws 9.5 mA for a +8 dBm transmit power and 4.5 mA for receive, which is three to five times lower than prior generation 802.15.4 transceivers. Reducing peak current is a good start, but the energy required to send a packet is a function of the amount of charge drawn over a period of time. If current is measured on an oscilloscope and plotted over time (see ***Figure 5***), then the energy required to send a packet is shown as the area under the curve and affected not only by peak currents, but also by how long each operation is active. Products such as this deliver precisely optimized pack-

Leading Global Communications

PP10-10/-11 0.1μm Power pHEMT

- 0.1μm high performance power / low noise process
- 50μm and 100μm thickness are standard
- Useable gain to 110GHz
- 4V operation - Psat > 800mW/mm, > 50% PAE, and 13dB Gain at 29GHz

PP10 Transfer Curve

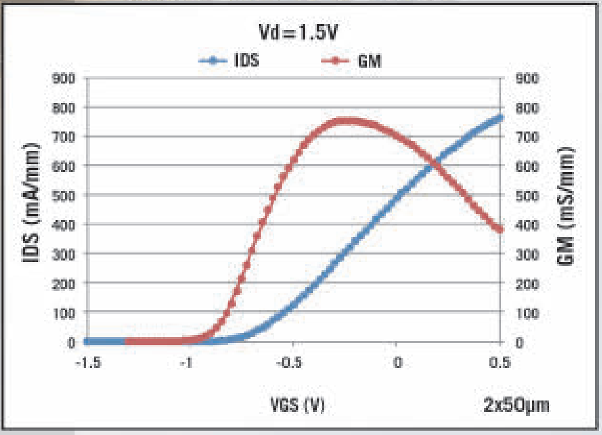

PP10 I-V Curves

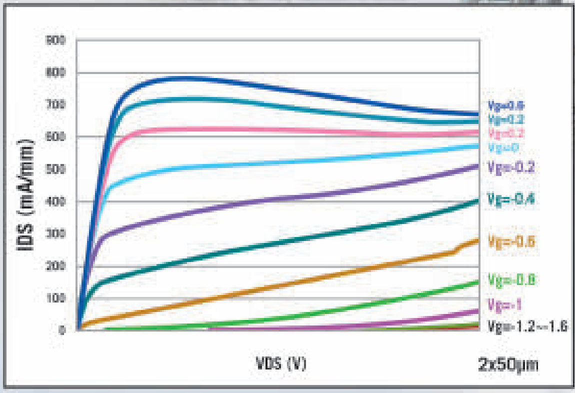

PP10 Load Pull Data

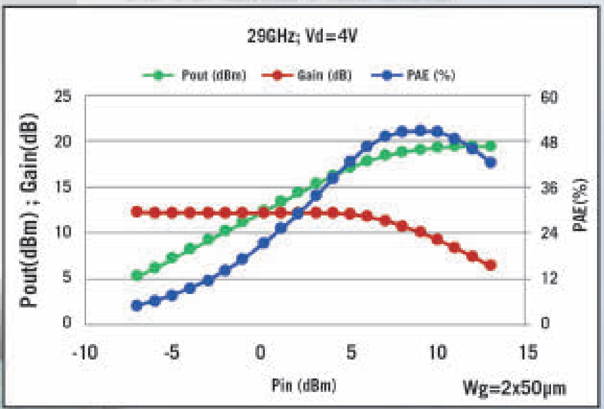

PP10 Max Gain

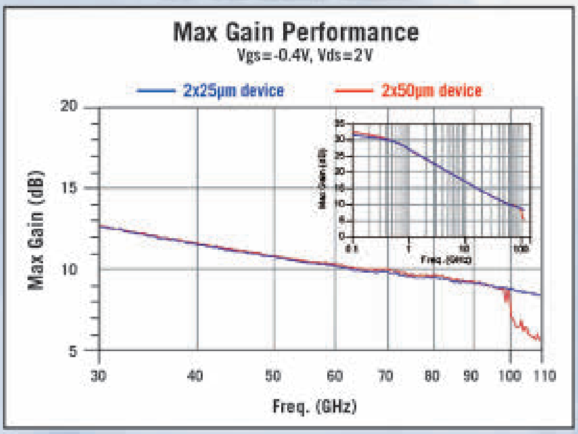

WIN SEMICONDUCTORS CORP. Tel:+886-3-397-5999 Fax:+886-3-397-5069 http://www.winfoundry.com

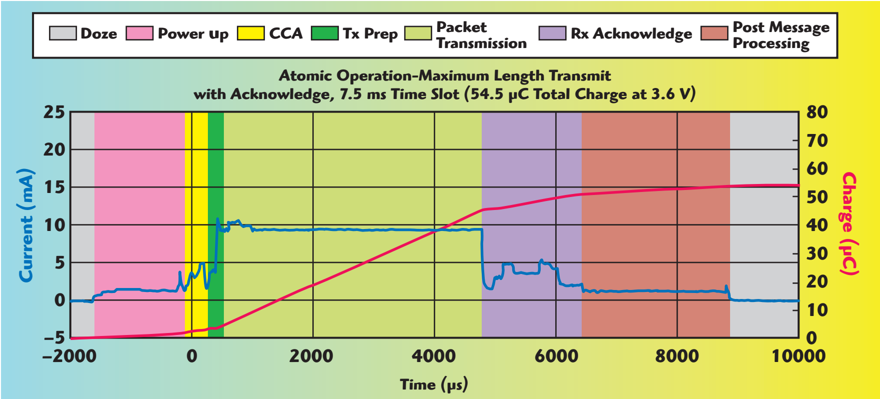

▲ *Fig. 5 The current during packet transmission and receipt of the link-layer acknowledgement. With TSCH-optimized hardware, individual transactions can reach as low as 54.5 μC.*

et exchanges with a successful packet transmission/acknowledgment for a mere 54.5 μC charge at 3.6 V supply voltage (or 196.2 μJ of energy).

A SYSTEM APPROACH TO LOW POWER

By taking a more holistic view of how energy is spent in a wireless sensor network, low power consumption can be thought of as a function of data traffic as well as the energy required to send a packet and the number of retries needed to successfully send a packet from one node to the other:

$$\text{Average Energy} = f\left(\left(\frac{\text{Num Packets}}{\text{Period of Time}}\right) \times \left(\text{Energy per Packet}\right) \times \left(\text{Num Retries to Successfully Send A Packet}\right)\right)$$

By focusing on energy per packet and using a networking protocol that exercises time, path, and frequency diversity on every retry (thereby reducing the average number of retries required to send a packet), low current consumption can be attained by improving efficiency throughout the system rather than making sacrifices on the application layer. The communication schedules in a TSCH network are highly configurable, with communications timeslots automatically allocated based on application needs. A TSCH network can be configured for slow data rates to minimize power and potentially enable the use of energy harvesting. That same TSCH network can be configured to support heterogeneous report rates, as is commonly done in industrial plants that have slow-changing variables (e.g., tank level) and faster changing variables (e.g., flow in a pipe). A TSCH network will automatically allocate the required timeslots to the portions of a network that need it. Instead of forcing users to tailor their applications to meet the needs of the network, a TSCH network can be tailored to meet the needs of a wide variety of applications.

ENABLING THE INDUSTRIAL INTERNET OF THINGS

TSCH is already a foundational building block of existing industrial wireless standards, such as WirelessHART (IEC62591), and is an enabling piece of emerging Internet Protocol-based WSN standards, including IEEE802.15.4e.[1] Work is underway to standardize a TSCH link layer within the IETF 6TiSCH group as well.[2] The adoption of TSCH into relevant standards will continue to encourage far-reaching adoption. TSCH networks have already proven to deliver multiyear battery life and >99.999 percent data reliability in such diverse and demanding applications as industrial process monitoring,[3] fence line perimeter security,[4] data center energy efficiency,[5] and metropolitan-scale smart-parking solutions.[6] By delivering highly reliable, low-power wireless networks that are highly configurable, TSCH networks are ideally suited for the Industrial Internet of Things. ■

References

1. Reliable, Low Power WSNs for the Internet of Things, www.linear.com/docs/44202.
2. https://datatracker.ietf.org/wg/6tisch/charter/.
3. Emerson Process, www.linear.com/docs/41383.
4. Integrated Security Corp., www.isc-hydra.com.
5. Vigilent, www.linear.com/docs/41384.
6. Streetline, www.linear.com/docs/41387.

CEL
INTRODUCING
TOKYO KEIKI
CUSTOM RF PRODUCTS
Delivering High Quality & Performance
5 CLEANROOMS
JIS-Q9100 CERTIFIED FACTORY
AS9100 U.S. EQUIVALENT
Bring us your challenging specs
X-Band
100 W
GaN Power AMP
Best in Class
High Power Amplifier
Lumped Element Filter
Directional Coupler
Monitor
Broadband Amplifier
PIN Diode Switch
VCO/Synthesizer
Power Divider
Cavity Filter/Duplexer
Low Noise Amplifier
Balanced Mixer
Filter
Amp
Mixer
HPA
Divider
CEL
TOKYO KEIKI
Scan code to learn more or visit:
www.cel.com/TK-MJ

Most Valuable Product

Scan page using layar app

Design Flow That Revolutionizes SDR

National Instruments
Austin, Texas

As society connects and shares more devices and data across networks, there is unprecedented demand for technology that will help today's system designers. While signal processing and communications designers work to define algorithms that overcome pressing challenges regarding bandwidth, security, power efficiency and coexistence, there is a void in prototyping solutions with real-world signals.

While those in industry, academia and government laboratories have turned to software defined radio (SDR) to evaluate new designs with real-world signals and conditions, the prototyping process is far from efficient. Unfortunately, existing software tools are often a bottleneck to innovation; they typically offer a disjointed, indirect design flow. In large part, the challenge emerges from the discontinuity between tools well suited for algorithm design and those required to program the hardware components of an SDR. It is precisely this discontinuity that the LabVIEW Communications System Design Suite bridges, providing a unified design flow from algorithm to hardware.

Designers today choose SDRs because their flexibility promises rapid prototyping. This flexibility stems primarily from computing elements that dictate the behavior of the generic, wide bandwidth RF front end multicore processors and large, user-programmable FPGAs. Unfortunately, today's tools for programming the processors and FPGAs found on SDRs typically eradicate any hope for truly rapid prototyping. Transitioning from algorithm to implementation on a processor and an FPGA demands different specializations and tools. Design teams on the bleeding edge of various technology vectors are forcibly larger than ideal and engage in design cycles that are long and costly. The result is not a smooth, iterative prototyping process that contributes to innovation; rather, the process hinders efficiency and thwarts innovation (see ***Figure 1***).

LabVIEW Communications offers a unified design flow for communications system prototyping. It is a single, cohesive design environment that can target both the processor and FPGA. This hardware-aware design environment includes SystemDesigner, which allows designers to validate system setup, access system documentation, describe the system architecture, configure system components, and partition and deploy algorithms to hardware. This hardware-software integration also provides access to I/O and resources, eliminating the need for middleware and driver development (see ***Figure 2***).

The advanced compiler technology found in LabVIEW Communications enables considerable flexibility and eases algorithm descriptions dictating how they will map and perform on SDR

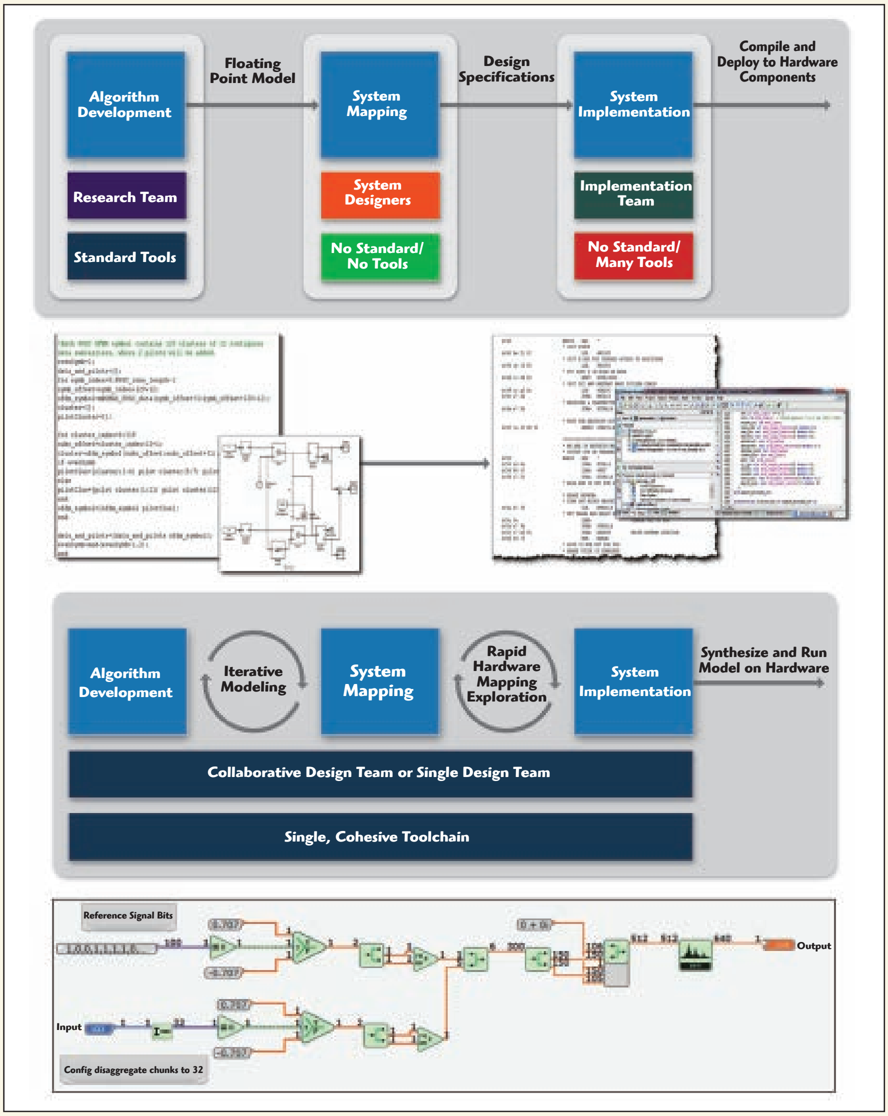

▲ *Fig. 1 The traditional design process necessitates numerous tools and re-writes of an algorithm to realize a hardware prototype. This inefficient flow hinders innovation.*

hardware. As an example for developing signal processing algorithms, the new multirate diagram (MRD) included in LabVIEW Communications makes it possible for designers to connect processes that run at different rates without the encumbrance of handshaking, buffering and queuing data between processes. Once researchers design a signal chain in a multirate diagram, they can rely on a built-in, interactive, data-driven tool for converting the design to a fixed point and can then explore how the design performs given different requirements. Simply defining a clock rate and a throughput for the algorithm allows the underlying compiler to analyze the implementation and provide designers with timing and resource estimates specific to the SDR hardware they wish to use.

Designers are liberated from having to contend with the underlying hardware architecture they deploy to. They no longer need to manu-

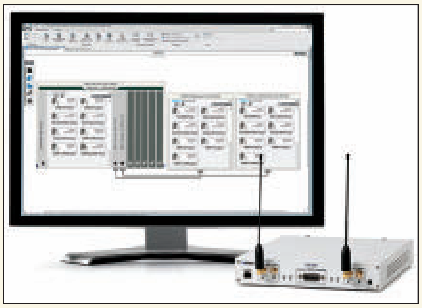

▲ *Fig. 2 LabVIEW Communications offers a hardware-aware design environment complete with tools that validate system setup and deploy algorithms to hardware.*

ally dissect a design to understand the tradeoffs between different implementations. The compiler in LabVIEW Communications does the often complex job of exploring the impact of unrolling loops, partitioning memory, modifying memory access schemes and selecting different FPGA resources/components. The designer can move forward with an implementation that best suits the design requirements based on the feedback from the compiler. As an added benefit, researchers can achieve considerable reuse as the core algorithms are defined in higher level languages, and the implementation is derived from the design requirements that are imposed upon the algorithm.

Users can rely on new Application Frameworks available with LabVIEW Communications to further expedite their design cycle. Application Frameworks provide documented, modifiable, standards-based source code for LTE and 802.11 PHYs. Designers can focus their efforts on the specific components to improve over existing LTE and 802.11 designs, instead of spending time building the requisite infrastructure needed to properly test the novel algorithms (see ***Figure 3***).

Today's system designers require a design flow that realizes the true potential of SDRs for rapid prototyping. LabVIEW Communications provides a seamless path from algorithm to prototype, helping designers innovate faster. Researchers have access to intuitive, high-level languages that enable efficient algorithm design and system abstraction. The hardware-aware nature of the software with SDR hardware allows for accurate, real-world I/O integration. LabVIEW Communications will help designers outpace competitors in the race to define standards for 5G and other future communications systems.

VENDORVIEW

National Instruments
Austin, Texas
www.ni.com/labview

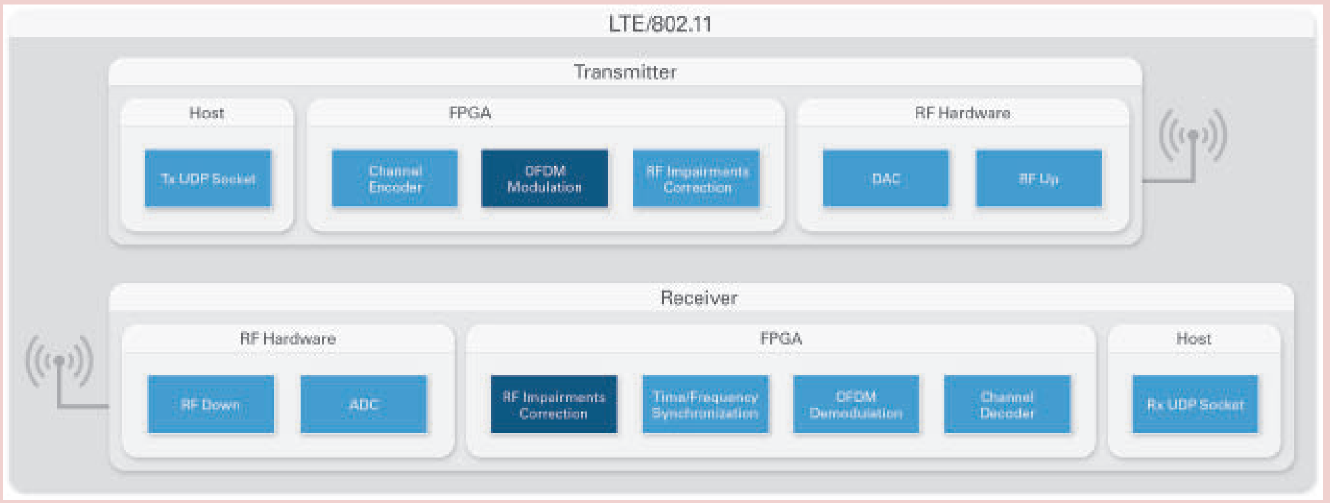

▲ *Fig. 3 Application Frameworks included with LabVIEW Communications provide standards-based source code implementations for LTE and 802.11 to further accelerate designs.*

50 MHz to 26.5 GHz

THREE AMPLIFIERS COVER IT ALL !

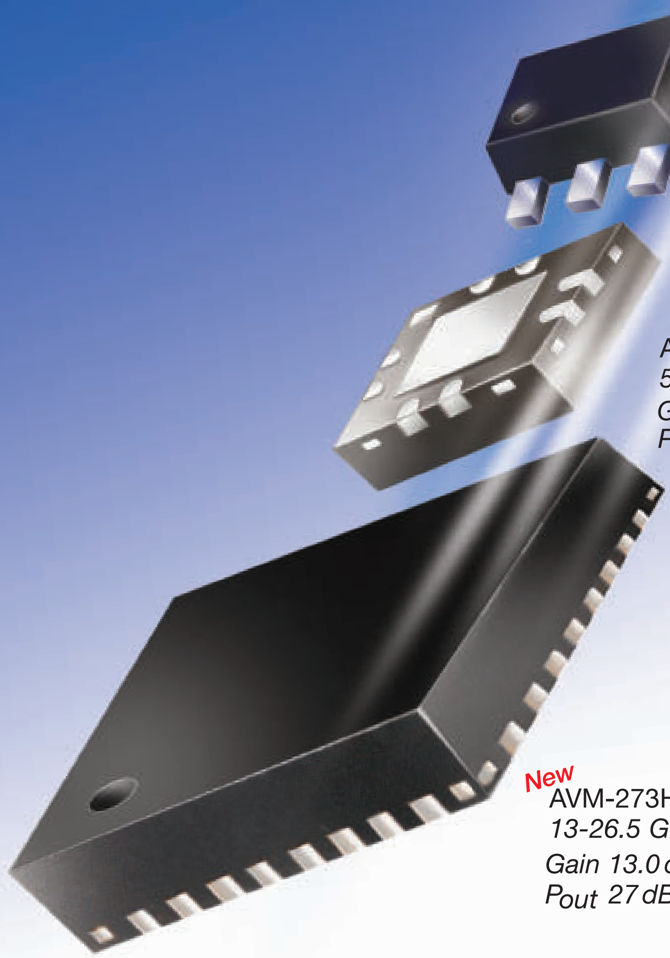

PHA-1+
0.05-6 GHz
$1.99 ea. (qty. 20)
Gain 13.5 dB
Pout 22 dBm

AVA-183A+
5-18 GHz
$6.95 ea. (qty. 10)
Gain 14.0 dB
Pout 19 dBm

New
AVM-273HP+
13-26.5 GHz
$27.95 ea. (qty. 10)
Gain 13.0 dB
Pout 27 dBm

Mini-Circuits' New AVM-273HP+ wideband, 13 dB gain, unconditionally stable microwave amplifier supports applications from 13 to 26.5 GHz with 0.5W power handling! Gain flatness of ±1.0 dB and 58 dB isolation make this tiny unit an outstanding buffer amplifier in P2P radios, military EW and radar, DBS, VSAT, and more! Its integrated application circuit provides reverse voltage protection, voltage sequencing, and current stabilization, all in one tiny package!

The AVA-183A+ delivers excellent gain flatness (±1.0 dB) from 5 to 18 GHz with 38 dB isolation, and 19 dBm power handling. It is unconditionally stable and an ideal LO driver amplifier. Internal DC blocks, bias tee, and microwave coupling capacitor simplify external circuits, minimizing your design time.

The PHA-1+ + uses E-PHEMT technology to offer ultra-high dynamic range, low noise, and excellent IP3 performance, making it ideal for LTE and TD-SCDMA. Good input and output return loss across almost 7 octaves extend its use to CATV, wireless LANs, and base station infrastructure.

We've got you covered! Visit minicircuits.com for full specs, performance curves, and free data! These models are in stock and ready to ship today!

RoHS compliant

FREE X-Parameters-Based
Non-Linear Simulation Models for ADS
Modelithics®

http://www.modelithics.com/mvp/Mini-Circuits.asp

Mini-Circuits®

www.minicircuits.com P.O. Box 350166, Brooklyn, NY 11235-0003 (718) 934-4500 sales@minicircuits.com

478 rev N

Global Spending on Defense to Increase at a CAGR of 2.25 Percent

Global spending on defense will grow to over $2.1 trillion by 2023 with the Asia-Pacific region showing the fastest growth. The Strategy Analytics Advanced Defense Systems (ADS) service report, "Opposing Trends in North America and Asia-Pac will Dictate Defense Spending Outlook," predicts that while budgetary challenges remain at the forefront of global defense spending, regional geopolitical factors will translate to increases across all regions.

Strategy Analytics' projections for global defense spending are derived from analyzing and assessing 84 countries collectively accounting for around 98 percent of total global defense expenditure. Spending in Europe will remain flat as an overall proportion of global expenditure reflecting a mix of priorities. While budgets in Western Europe are expected to remain flat to stable, this will be offset by increased spending by Nordic and Eastern European countries. Both the Central America - Latin America and Middle East - Africa regions will also see growth, collectively accounting for 16 percent of global defense spending in 2023.

> While budgetary challenges remain at the forefront of global defense spending, regional geopolitical factors will translate to increases across all regions.

"North American spending will be dictated by U.S. budgets and the impact of sequestration. We expect supplementary add-ons to U.S. spending to smooth out the overall impact of sequestration reducing the net cuts through 2019 before flattening out and showing a moderate increase over 2022 to 2023," observed Eric Higham, North American director for ADS. "This will translate to North America spend dropping to just over 31 percent of global spend in 2023, versus 37 percent in 2013."

"China will both underpin and spur spending in the Asia-Pacific region, leading to the Asia-Pacific regional spend approaching 30 percent in 2023, up from 25 percent in 2013," noted Asif Anwar, director of the ADS service. "The continued growth in the Chinese military budget will lead to other countries such as Japan, South Korea, Taiwan and others maintaining strong momentum behind their budgets."

Regional Shifts in Global Defense Spending

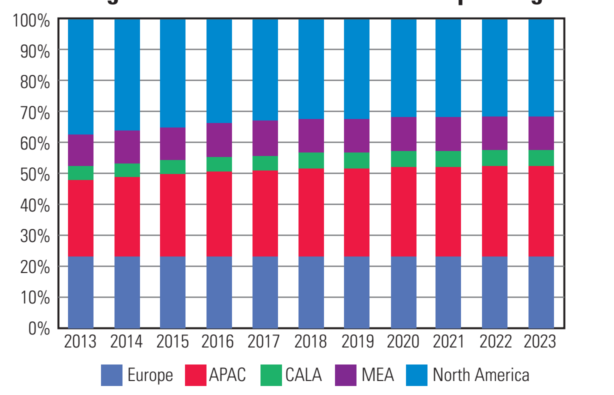

Source: Strategy Analytics

Global Airborne ISR Market to Grow at CAGR of Over Three Percent Through 2023

Amid a tight budgetary environment, global militaries are faced with the challenge of reducing costs while maintaining and even enhancing defense capability in critical areas such as airborne intelligence, surveillance and reconnaissance (ISR). The Strategy Analytics Advanced Defense Systems (ADS) service series of reports forecast that the global airborne ISR market will grow at a compound annual growth rate (CAGR) of 3.2 percent to approach $28 billion in 2023.

- The Airborne Early Warning and Control segment is forecast to have the fastest growth in spending, largely driven by anticipated new spending by emerging countries as well as some renewed market demand from a few mature market countries.
- Spending for airborne ISR platforms dedicated to electronic warfare (EW) missions will center on advanced countries including the U.S., China, Russia and India.
- Demand for maritime patrol aircraft will come from countries with large maritime boundaries.
- Growth in the airborne ground surveillance and reconnaissance market will be driven by emerging regions with procurements of both manned and unmanned systems, as well as a continued focus on using unmanned surveillance systems in the West.

> Despite budgetary challenges, airborne ISR asset investment will remain a critical priority.

"Airborne ISR assets will be critical to countering both asymmetric and conventional warfare threat environments as global militaries adjust to the shifting battle-space paradigms of net-centricity, cyber-warfare and electronic warfare," noted Asif Anwar, director of the ADS service. "This will include the use of unmanned platforms to both complement and in some cases substitute for manned platforms, while the need to balance affordability will see military customers look towards platforms that can embody multiple mission capabilities and offer flexibility, agility, efficiency and interoperability."

For More Information

Visit mwjournal.com for more defense news

U.S. Army's Missile-Fighting Radar-blimp Achieves Critical Milestone

VIEW VIDEO

The East Coast is one step closer to being better defended against cruise missiles and drones. Raytheon Co. completed a series of laboratory tests that demonstrated the Joint Land Attack Elevated Netted Sensor (JLENS) radar can be integrated into the North American Aerospace Defense Command (NORAD).

JLENS is a system of two aerostats, or tethered blimps, that float 10,000 feet in the air. The helium filled aerostats, each nearly as long as a football field, carry powerful radars that can protect a territory roughly the size of Texas from airborne threats. JLENS provides 360 degrees of defensive radar coverage and can detect and track moving objects like cruise missiles, drones and airplanes from up to 340 miles away.

"The lab tests proved that information from JLENS can be converted into a format that can be used by NORAD's command and control system," said Raytheon's Dave Gulla, vice president of Integrated Defense Systems' Global Integrated Sensors business area. "With JLENS providing data to NORAD, our military will have a more accurate picture of what is flying in the National Capital Region's airspace, and be able to identify slow-and-low flying threats such as cruise missiles and drones."

"With JLENS providing data to NORAD, our military will have a more accurate picture of what is flying in the National Capital Region's airspace, and be able to identify slow-and-low flying threats such as cruise missiles and drones."

One JLENS system is scheduled to be strategically emplaced at Aberdeen Proving Grounds, Md. later this year to help defend the National Capital Region from airborne threats. It will be under the control of NORAD-U.S. Northern Command, and operated by soldiers of the U.S. Army's A Battery, 3rd Air Defense Artillery. A second JLENS system is in strategic reserve, ready to be deployed anywhere in the world at the request of combatant commanders, should they require comprehensive cruise missile defense.

Scan page using layar app

Reactel, Incorporated

Reacting First to All Your Filter Needs.

When Being the First to React Makes all the Difference in the World

- **RF & Microwave Filters**

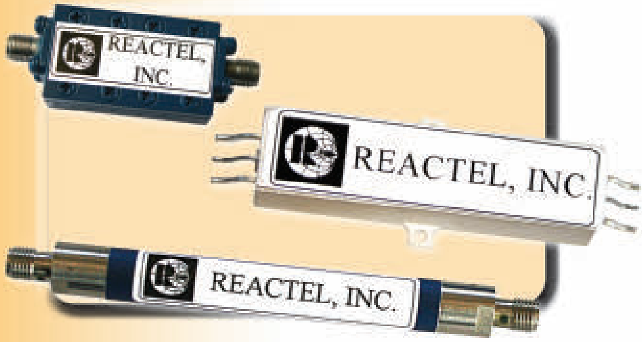

- **Diplexers & Multiplexers**

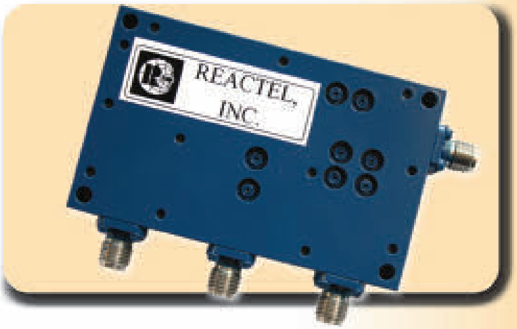

- **Multifunction Assemblies**

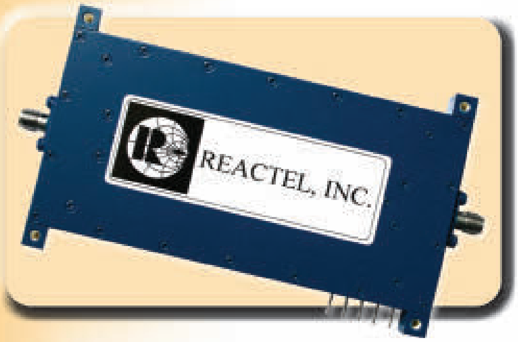

- **Ceramic Filters**

Reactel, Incorporated is your source for RF & Microwave Filters, Multiplexers and Multifunction Assemblies covering DC - 50 GHz.
Trust in Reactel's highly skilled engineers and technicians to quickly develop and produce the most reliable products for your filter requirements.

- Submitting a request for immediate attention will never be easier.
- Full featured App contains expanded RFQ capability, catalog, data sheets and more.
- Available for iPad, iPod and Android devices via the App Store and Google Play.

Available on the App Store

Google play

8031 Cessna Avenue • Gaithersburg, Maryland 20879 • Phone: (301) 519-3660
For general inquiries, please email reactel@reactel.com • http://twitter.com/reacteljim
Go online to www.reactel.com to download your Reactel catalog today.

RoHS Compliant

@reacteljim

BAE Systems and Dassault Aviation Define Franco-British FCAS Requirement

BAE Systems and Dassault Aviation, along with industrial partners, have been awarded a £120 million, two-year contract by the UK and French governments to help define the Franco-British requirement for a Future Combat Air System (FCAS) programme.

Co-operation between the UK and France is seen as the optimum way to progress an Unmanned Combat Air System (UCAS) solution, while supporting both governments' intentions for closer defence ties. The joint study contract of £120 million will be supplemented with additional UK and French national funding to the combined value of £80 million in the same period.

The two-year study will build the foundations on which a long-term joint programme will be based by focusing on the development of concepts for an operational system and the maturation of key technologies that will be required for a future operational UCAS.

Ian King, BAE Systems CEO, commented, "This contract award is a key step in the partnership between our two nations, governments and industries. The Feasibility Phase will allow UK and French industry to work closely together and provide a strong foundation for a potential follow-on Future Combat Air System Demonstration programme as well as supporting a number of highly skilled jobs."

"This contract award is a key step in the partnership between our two nations, governments and industries."

Following the completion of the study at the end of 2016, work could then commence on a UCAS demonstration development programme that addresses both nations' future military requirements.

The Feasibility Phase will sustain hundreds of highly skilled jobs at Dassault Aviation and BAE Systems with more jobs sustained by Rolls-Royce, Selex ES, Snecma (Safran), Thales and SME's involved in the programme. In addition, the contract supports the strategically important Military Aerospace Industries in both nations and is testament to the importance that the UK and French governments place in maintaining a cutting edge, sovereign military air capability.

Graphene Flagship Welcomes First Associated Members

The Graphene Flagship, which brings together scientists, engineers and commercial companies looking to turn graphene and related materials from academic research into real-world products, welcomes its first four associated members: Netzsch (Germany), NetComposites (UK), ABB and Imerys (Switzerland).

As part of its mission to strengthen Europe's graphene research and development community, the Graphene Flagship has built a pan-European structure based on partner organizations. The original 76 partners in 17 countries have grown to 142 in 23 countries.

This radical increase in the number of partners effectively doubles the size of the Graphene Flagship, but it is not stopping there. The concept of associated membership has been introduced to facilitate the alignment and information flow between the flagship and related national and international activities.

"This is a must for moving basic research advances into concrete innovation opportunities."

Graphene Flagship director Professor Jari Kinaret said, "We are very happy to welcome our first four associated members. The flagship is much more than just the EU-financed part and we are keen to form partnerships with groups that help the flagship reach its overriding goal, taking graphene and related materials from academic laboratories into society."

Associate membership of the Graphene Flagship will help it achieve its science and technology targets by creating a greater synergy with other graphene-related organizations: bodies funded by member states and various EU projects, organizations part of the FLAG-ERA network, and coordinating regional and national funding agencies within Europe.

Speaking for the European Commission, Thierry Van der Pyl, director of 'Excellence Science' within the Directorate General for Communications Networks, Content and Technology, said, "We are very pleased to see the Graphene Flagship consortium associating with leading European industry, paving the way of graphene from lab to market. This is a must for moving basic research advances into concrete innovation opportunities."

DOCOMO Achieves World's First Transmission Exceeding 1.2 Gbps

NTT DOCOMO Inc. claims to have achieved the world's first transmission exceeding 1.2 Gbps in a field test using a single-size antenna incorporating a new transmission technology – Smart Vertical MIMO for LTE-Advanced systems.

The new Smart Vertical MIMO transmission technology, which uses adaptive grouping of vertical antenna components according to the reception

Space reduction is particularly beneficial for deployments in congested urban areas.

For More Information Visit mwjournal.com for more international news quality for mobile devices in the transmission area, enables a single-size antenna to achieve throughput equivalent to that of a four-antenna system.

Smart Vertical MIMO, a key technological development for the planned deployment of DOCOMO's LTE-Advanced network by the fiscal year ending March 31, 2016, reduces the cost and space of installing antenna equipment and improves spectrum utilization efficiency. Space reduction is particularly beneficial for deployments in congested urban areas.

The company will continue to enhance its Smart Vertical MIMO transmission technology, aiming to provide maximum-quality network services with its coming commercial LTE-Advanced network.

ThalesRaytheonSystems ACCS Ready to Provide NATO Interoperability

ThalesRaytheonSystems has completed system testing for NATO's Air Command and Control System (ACCS) program. The tests demonstrated the system's ability to operate in a network configuration linking the pilot sites at Lyon Mont Verdun in France, Glons in Belgium, Uedem in Germany and Poggio Renatico in Italy.

During the tests, the system handled a daily number of military air movements several times higher than for any operations conducted up to now, proving its high level of performance and its ability to interconnect NATO and National Air Command and Control (AirC2) units across four European nations into a single integrated AirC2 system.

"This success marks a key milestone in the adoption of the ACCS system by NATO member nations. It will be phased in alongside existing national systems and then replaced progressively, ultimately enabling member nations to plan and conduct air operations together in a full automated manner," said Enzo Montalti, director AirC2 Programme Office and Services, at NATO Communications and Information Agency.

"This is the last milestone before full deployment of ACCS in all European NATO nations. Once fully deployed, the system will protect 10 million square kilometres of European airspace against a range of threats by coordinating systems in member nations," said Philippe Duhamel, CEO of ThalesRaytheonSystems.

"...the system will protect 10 million square kilometres of European airspace against a range of threats..."

CommercialMarket

Cliff Drubin, Associate Technical Editor

Internet of Things, Smart Home and Wearables Will Drive Next Growth Wave

Nearly 12 billion Internet-connected devices will be in use worldwide by the end of 2014, according to the latest research from Strategy Analytics. That is equivalent to 1.7 devices for every person on the planet, a ratio which will rise to 4.3 by 2020, when 33 billion devices will be in use. The report, "Connected World: The Internet of Things and Connected Devices in 2020," quantifies the scale of the connected device opportunity across the Internet of Things (IoT), smart homes, smartphones, PCs, tablets, smart TVs, internet media devices and wearable devices.

- Traditional connected devices like PCs, smartphones and tablets now account for less than a third of all connected devices in use.
- Emerging categories alone will connect an additional 17.6 billion devices to the Internet by 2020.
- The IoT is leading to rapid growth in new categories like machine-to-machine (M2M), smart objects, smart grid and smart cities.

"Back in 2007, PCs accounted for two thirds of internet devices – now it is only 10 percent," notes David Mercer, principal analyst and the report's joint author. "The impact of the Internet on daily lives has increased rapidly in recent years. Huge growth potential still lies ahead, in terms of both the number of devices relying on Internet connectivity and its geographic reach."

> "The Internet of Things has already connected five billion devices and we are only at the beginning of this revolution..."

"The Internet of Things has already connected five billion devices and we are only at the beginning of this revolution", says Andrew Brown, executive director and the report's joint author. "Smart cities and smart grid are just two of the ways in which the Internet of things will touch everyone's lives over the coming years and decades."

Global Internet Device Installed Base Forecast

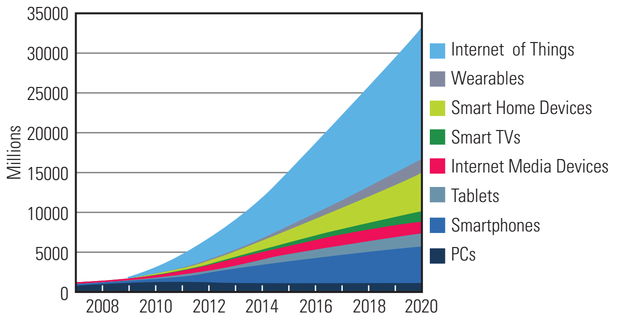

Source: Strategy Analytics, Oct. 2014

mHealth Elderly Home Monitoring Growth Drawing New Players to the Market

Over the next five years, a new generation of elderly home care services will drive wearable device shipments to more than 44 million in 2019, up from just 6 million in 2013. In 2014 alone, shipments of wearable devices linked to elderly care systems will more than double over those in 2013, finds the latest ABI Research analysis of the mHealth market.

Growing adoption comes as tech savvy families increasingly turn to home monitoring offerings for assurance their aging parents and family members are safe and well. In addition, new offerings are boosting and extending a market that has long been the territory of dedicated, "Help! I've fallen and I can't get up" personal emergency response systems. A host of niche players including BeClose, GrandCare Systems, Independa and others have all emerged to capitalize on a combination of market demand and the potential to leverage connected devices and systems.

> In 2014 alone, shipments of wearable devices linked to elderly care systems will more than double over those in 2013.

In the past few months alone, one start-up, Live!y, has revamped and re-launched its offerings to include a watch that offers activity tracking alongside personal emergency response services, while AT&T has added elderly care monitoring to its Digital Life smart home package. These players reflect how device manufacturers and service providers alike are increasingly targeting the elder care market and doing so with more feature rich offerings.

Home Monitoring Wearable Wireless mHealth Device Shipments by Device Type
Worldwide Forecast: 2013 to 2019

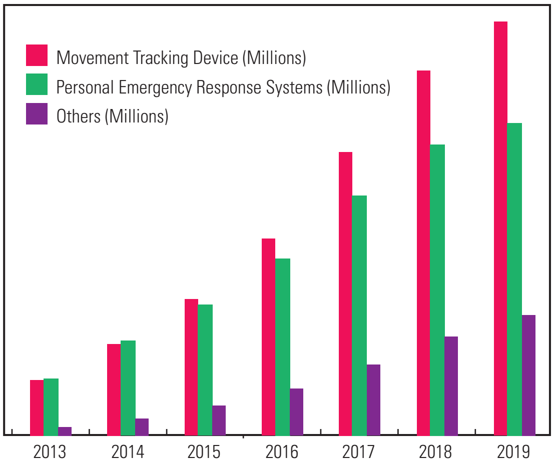

Source: ABI Research

For More Information Visit mwjournal.com for more commercial market news

OEMs Solve Deployment Challenges with Small Cells as a Service Rejuvenating Growth for 2015

ABI Research's latest forecast for outdoor small cells includes new market research and revises expectations for 2014 and the forecast period to a 48 percent CAGR through 2019. "We expect operators like AT&T, Verizon, Vodafone, Telefnica, Softbank, SK Telecom and Sprint to drive the growth by deploying both outdoor small cell and metrocell networks," says Nick Marshall, mobile networks research director at ABI Research. "These changes to ABI Research's small cell forecasts reflect real deployment scenarios from discussions with vendors and MNOs which now report that 2015 will witness meaningful small cell deployments."

> **In 2015, 4G small cells will be the fastest growing small cell type in the market driven by venue and dense urban deployments.**

The challenges of backhaul, power, permitting and siting have all served to throttle back small cell rollout. This has driven the rise of Small Cells as a Service (SCaaS) from OEMs such as Alcatel-Lucent, Nokia Networks and Ericsson, and infrastructure owners such as Towerstream, Crown Castle, Cloudberry Mobile and Virgin Media Business. These services all solve small cell deployment challenges for the mobile operator, removing fear, uncertainty and doubt.

In 2015, 4G small cells will be the fastest growing small cell in the market, driven by venue and dense urban deployments. ABI Research forecasts the number of LTE small cells to double in 2015 and by a similar factor each year through 2019 where the value of LTE small cells will represent almost 70 percent of the small cell equipment market.

Outdoor Small Cell Shipments by Technology
Worldwide Forecast: 2013 to 2019

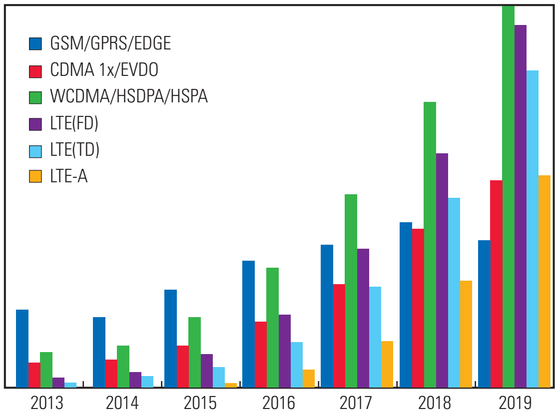

Source: ABI Research

Around the **Circuit**

Barbara Walsh, Multimedia Staff Editor

MERGERS & ACQUISITIONS

Raytheon Co. announced that it has acquired **Blackbird Technologies**. The purchase price is approximately $420 million, subject to post-closing adjustments. The transaction will not materially impact Raytheon sales or earnings per share for the fourth quarter of 2014. Located in Herndon, Va., Blackbird will become part of Raytheon Co.'s Intelligence, Information and Services (IIS) business. With customers in the Special Operations Command (SOCOM), the intelligence community and organizations supporting the Department of Defense, Blackbird Technologies expands Raytheon's special operations capabilities in tactical intelligence, surveillance and reconnaissance, secure tactical communications and cybersecurity across a broad spectrum of globally dispersed platforms and communications networks.

IBM and **GLOBALFOUNDRIES** announced that they have signed a definitive agreement under which GLOBALFOUNDRIES plans to acquire IBM's global commercial semiconductor technology business, including intellectual property, world-class technologists and technologies related to IBM Microelectronics, subject to completion of applicable regulatory reviews. GLOBALFOUNDRIES will also become IBM's exclusive server processor semiconductor technology provider for 22, 14 and 10 nm semiconductors for the next 10 years. The agreement, once closed, enables IBM to further focus on fundamental semiconductor research and the development of future cloud, mobile, big data analytics and secure transaction-optimized systems.

RF Micro Devices Inc. and **TriQuint Semiconductor Inc.** announced the two companies have received all necessary shareholder and regulatory approvals to move forward with their previously announced merger of equals and have set Wednesday, December 31, 2014, as the anticipated closing date for the transaction. Trading in the common stock of the new combined company, **Qorvo Inc.**, is expected to commence on the NASDAQ Global Select Market on January 2, 2015, under the stock ticker symbol "QRVO."

Qualcomm Inc. announced that it has reached an agreement with **CSR plc** regarding the terms of a recommended cash acquisition. The entire issued and to be issued ordinary share capital of CSR will be acquired by Qualcomm Global Trading Pte. Ltd., an indirect wholly owned subsidiary of Qualcomm Inc. The acquisition complements Qualcomm's current offerings by adding products, channels and customers in the important growth categories of Internet of Everything (IoE) and automotive infotainment, accelerating Qualcomm's presence and path to leadership.

Altair acquired 100 percent of **EM Software & Systems – S.A. (Pty) Ltd.** and its international distributor offices in the United States, Germany, and China in June 2014. This development adds the FEKO® solver to the HyperWorks® suite and strengthens the Altair simulation offerings in the aerospace, automotive and shipbuilding industries in particular, reflecting the commitment of the company to provide comprehensive, best-of-breed solutions to its customers.

MaxLinear Inc. announced that it has completed the acquisition of **Physpeed Co. Ltd.** MaxLinear will pay approximately $11 million in cash in exchange for all outstanding shares of capital stock and equity of Physpeed. A portion of the consideration payable to the former shareholders of Physpeed will be placed into escrow, pursuant to the terms of the definitive merger agreement.

COLLABORATIONS

Huawei plans to invest £5 million (€6.3 million/$7.9 million) in the **University of Surrey's 5G Innovation Centre** (5GIC), which is currently one of the leading 5G research initiatives in the world alongside other government, industry, and university-led programmes in the European Union, China, Japan, South Korea and the U.S. The China-based equipment manufacturer said the £5 million forms part of a $600 million investment the company is committing to 5G research and innovation globally by 2018. Huawei is one of the founding members of the 5GIC.

AR (Amplifier Research) and **MVG (Microwave Vision Group)** have signed a memorandum of agreement under which they plan to provide customers turn-key solutions. AR's brand name, experience and extensive line of EMC and RF/microwave products will complement MVG's installation expertise and diverse product range of MVG-EMC shielded anechoic chambers, shielded rooms and absorbers. Together they aim to deliver quality, high performance turnkey products for EMC and other markets.

Exelis signed a teaming agreement with **Airbus Group** to provide advanced missile warning capabilities for U.S. and international F-16 Fighting Falcon aircraft. Capabilities include lightweight protection against short-range air defense missiles and man-portable air defense systems. Under the agreement, Exelis is the lead U.S. contractor for the AAR-60(V)2 Missile Launch Detection System for Fighters (MILDS F). The agreement ensures customers will have access to the best system affordability, availability and supportability for U.S. F-16 missile warning requirements. MILDS F, an Airbus Defense and Space system, is optimized for installation on Terma's PIDS+ (Pylon Integrated Dispenser System Plus).

NEW STARTS

Harris Corp. announced the opening of a new facility in Sunrise, Fla., highlighting its commitment to developing advanced software for tactical radios used by the U.S. military as well as militaries and public safety officials around the world. The 19,000 square foot facility will support engineering activities and will serve as the Caribbean and Latin

For More Information For up-to-date news briefs, visit mwjournal.com

American sales hub for Harris RF Communications products and services.

Keysight Technologies Inc. announced that its separation from **Agilent Technologies Inc**. has been completed. The newly independent company will begin "regular-way" trading on the New York Stock Exchange under the ticker symbol KEYS. Keysight's separation from Agilent occurred on November 1, 2014 through a distribution of 100 percent of the outstanding common stock of Keysight to Agilent shareholders of record as of the close of business on October 22, 2014. Agilent shareholders of record received one share of Keysight common stock for every two shares of Agilent common stock held. Approximately 167.5 million shares of Keysight common stock were distributed on November 1, 2014 to Agilent shareholders.

Freescale Semiconductor announced the expansion of its system power management portfolio to support key members of its industry-leading embedded networking products. Available now, the highly efficient VR500 regulator is specifically designed to enable comprehensive system solutions leveraging Freescale's QorIQ Layerscape LS1 processors for a variety of applications including secure infrastructure equipment for the Internet of Things. The VR500 adds to Freescale's growing system power management portfolio, which already features solutions complementing popular Freescale microprocessors and microcontrollers.

ACHIEVEMENTS

Anritsu Co. announced that its ME7873L RF Conformance Test System has achieved GCF-approved test case validation for LTE evolved Multimedia Broadcast Multicast Services (eMBMS) Band 4 and Band 13 RF conformance test cases. With this new release approved by GCF in October 2014, Anritsu is the first company to earn GCF validation for WI-164 E-UTRA MBMS Rel-9 FDD conformance test cases that support the frequency bands expected to enter commercial service in North America.

RFMD announced that it has earned Huawei's Supplier of the Year Award at a ceremony recently held at Huawei's headquarters in Shenzhen, China. The award recognizes RFMD as Huawei's best supplier of RF components, which are used in Huawei's mobile phones and infrastructure products. RFMD is a key RF component supplier to Huawei. RFMD provides Huawei a growing suite of RF solutions including antenna switches and switch modules, power amplifiers, power management ICs, and Wi-Fi amplifiers for mobile devices as well as key components that support Huawei's wireless infrastructure and cellular backhaul business.

Isola Group S.à r.l. announced that its European subsidiary, **Isola GmbH**, complies with the European Space Agency's (ESA) specification for a cleaner class of base materials. Isola worked in collaboration with the ESA and its suppliers to reach this milestone. The enhanced standard, known as Appendix A, defines the supplemental requirements to the Institute for Interconnecting and Packaging Electronic Circuits' standard IPC-4101-D: Specification for base materials for rigid and multilayer printed boards.

Narda Microwave is celebrating its 60th year in business. Narda started in 1954 in a small storefront in Mineola, N.Y., offering innovative solutions for microwave applications. Sixty years later, Narda is recognized worldwide for highly reliable RF and microwave components, complex integrated microwave assemblies, and compact RF subsystems serving commercial and military markets. Today, Narda offers one of the largest selections of off-the-shelf RF and microwave components in the industry. Narda's 2014 catalog, the most comprehensive reference in the company's 60-year history, features more than 700 models and 125 new products.

Guinness World Records has recognized **DARPA's** Terahertz Electronics program for creating the fastest solid-state amplifier integrated circuit ever measured. The 10-stage common-source MMIC achieves 9 dB gain at 1.03 THz. Noise figure and output power have not yet been measured. The MMIC was designed and fabricated by Northrop Grumman Corp. using 25 nm InP HEMTs as the active devices. Researchers used E-beam lithography to define the gates on the MMIC, which was 18 µm thick and no bigger than a grain of kosher salt, according to Bill Deal, manager of the Terahertz Electronics program at Northrop Grumman.

Ineda Systems, a developer of low-power SoCs (system on a chip) for use in the fast-growing wearables and Internet of Things (IoT) market announced additional funding from Cisco Investments to bring the round of Series B funding to $19M. Cisco Investments joins existing investors Samsung Catalyst Fund, Qualcomm Ventures, and Imagination Technologies, among others. The funding will be used by Ineda to further develop its Dhanush family of Wearable Processor Units (WPU™).

CONTRACTS

Laurent Collet-Billon, head of the French defence procurement agency (DGA), and Bernard Gray, the UK Ministry of Defence's (MoD) Chief of Defence Materiel, launched the feasibility phase of the FCAS (Future Combat Air System) programme to carry out the system definition of an Anglo-French remotely-piloted combat aircraft. The total value of the feasibility phase contract led by BAE Systems and Dassault is €150M (£120M). As part of the feasibility phase, **Thales** and **Finmeccanica – Selex ES** have been awarded contracts to lead, specify and define the FCAS's multifunction sensor suite and communications sub-systems.

Harris Corp. has received an $18 million order from a nation in Central Asia for Falcon III® wideband tactical radios. The radios will provide advanced voice and data capabilities for the country's armed forces on the frontline. The nation is acquiring the RF-7800H high-frequency manpack and the RF-7850M multiband handheld radios. The RF-7800H is the first HF manpack radio with high-speed wideband data capabilities, allowing users to efficiently transmit large data files over beyond line-of-sight links. The RF-7850M multiband radio supports the latest wide-

band and narrowband networking waveforms and provides forward-deployed teams with capabilities to communicate with greater speed and detail.

The Malibu division of **Communications & Power Industries LLC (CPI)** has been awarded a follow-on order of more than $5 million for the continued production of tactical common data link (TCDL) antenna ground terminals operating in Ku-Band. CPI Malibu Division has received multi-year orders totaling more than $30 million for advanced ground data terminals in a two-year period. These ground data terminals are used by the U.S. military in intelligence, surveillance and reconnaissance (ISR) applications to communicate information, including video and radar, between ground control stations and unmanned aerial vehicle (UAV) platforms. CPI Malibu Division's Ku-Band advanced ground data terminals feature unique auto-tracking capabilities, which facilitate continuous contact between ground personnel and the UAV.

API Technologies Corp., a leading provider of high performance RF/microwave, power and security solutions for high-reliability applications, announced that it has received a follow-on order for $1.3 million to provide microwave modules for the latest generation radar. The customer program, anticipated to continue through 2025, is expected to add an additional $20 million in revenue. The product features the use of a proprietary Glass Microwave Integrated Circuit (GMIC) fabrication process, that offers shorter cycle time and affordability compared to traditional MMIC-based solutions.

Comtech Telecommunications Corp. announced that its New York-based subsidiary, **Comtech PST Corp.**, received a $1.1 million order for solid-state, high-power RF switches from a major domestic prime contractor. These switches provide very broad frequency coverage and are key components in an integrated electronic countermeasures system used by the U.S. military. Comtech PST Corp. is a leading independent supplier of broadband, high-power, high performance RF/microwave amplifiers used in a broad spectrum of applications including defense, medical, satellite communications systems and instrumentation.

The **U.S. Navy** and **Lockheed Martin** have delivered the third Mobile User Objective System (MUOS) spacecraft to Cape Canaveral Air Force Station, Fla., where it will be prepared for a January 2015 liftoff aboard a United Launch Alliance Atlas V rocket. MUOS operates like a smart phone cell tower in the sky, vastly improving current secure mobile satellite communications for warfighters on the move. For the first time, MUOS Wideband Code Division Multiple Access technology users will have beyond-line-of-sight capability to transmit and receive voice and data using an Internet Protocol-based system.

Crane Aerospace & Electronics Power Solutions has been selected by **BAE Systems** to provide ELDEC®Power Conditioning Modules (PCMs) and batteries on the Boeing 777X. BAE Systems is the prime supplier of the Integrated Flight Control Electronics (IFCE) fly-by-wire system, which delivers high integrity computing functionality for the 777X's all new composite wing with load alleviation, as well as its advanced high lift and folding wingtips; a first for commercial aircraft. The 777X is the newest family of twin-aisle airplanes, with production beginning in 2017 and first delivery scheduled for 2020. Also, Crane will deploy its A3000 A-SMGCS, multilateration and SR-3 Surface Movement Radars (SMR) to Ahmedabad, Amritsar, Guwahati, Jaipur and Lucknow Airports.

Saab has been selected by the **Airports Authority of India (AAI)** to deploy Advanced – Surface Movement Guidance & Control Systems (A-SMGCS) at five airports in India. The systems will enhance situational awareness and runway safety at these growing airports. Previously, Saab had deployed A-SMGCS to airports in Chennai, Kolkata and Mumbai and an A-SMGCS, multilateration and SMR to New Delhi's Indira Gandhi International Airport.

PEOPLE


▲ *Michael Ruppert*

Mercury Systems Inc. announced that, effective November 17, 2014, **Michael Ruppert** joined the company as senior vice president, Strategy and Corporate Development, reporting to Mercury's president and chief executive officer, Mark Aslett. Ruppert will be responsible for Mercury's corporate development activities, including strategy, planning, and mergers and acquisitions.

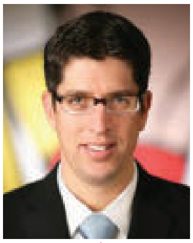
▲ *Haviv Ilan*

Texas Instruments Inc. announced the election of **Haviv Ilan** to senior vice president of High Performance Analog (HPA), succeeding Steve Anderson, who will now lead overall TI Analog. Ilan is responsible for managing an extensive portfolio of amplifiers, data converters, interface, medical and high-reliability products. Ilan joined TI in 1999 as system team leader and has since held a number of positions within the company including research and development manager responsible for TI's BlueLink Bluetooth technology, general manager and director of engineering for TI Ra'anana in Israel and general manager for TI's mobile connectivity solutions business.

Custom MMIC, a developer of performance driven monolithic microwave integrated circuits announced the appointment of **Cornes Technologies** as its new technical sales representative in Japan. Cornes Technologies is a specialist importer and distributor of electronic devices, systems and equipment, scientific equipment, and industrial machinery, with extensive experience in the promotion, marketing and selling of new products and technology sourced from overseas to a broad range of customers in Japan.

Vectron International, a Knowles company, and designer and manufacturer of precision oscillators and timing solutions for communication, industrial, military and space applications, announced they have entered into an agreement with **AccuBeat** to be their exclusive partner in North America.

Editor's Note: This is the second article addressing the theory, application and future possibilities of Möbius metamaterials and strip resonators. The first article was published in the November 2014 issue, and the next installment will be published next month, January 2015.

Metamaterial Resonators: Theory and Applications

Ulrich L. Rohde
Brandenburgische Technische Universitat, Cottbus, Germany
Ajay K. Poddar
Synergy Microwave, Paterson, N.J.

Metamaterials (MTM) are artificial composite materials engineered to possess extraordinary electromagnetic properties, such as negative index characteristics ($\varepsilon < 0$ and $\mu < 0$). The characteristics of MTMs depend on the properties of the host materials, embedded material, volume of the fraction, operating frequency and the morphology of the composite material such as the dimensions and shapes of the host structure. The array of MTM unit cells provides the effect of new medium when the sizes of unit cells are sub-wavelength, features that are actually smaller than the wavelength of the waves they affect. As depicted in ***Figure 1***, MTMs accommodate the missing quadrant III of the $\varepsilon - \mu$ domain.

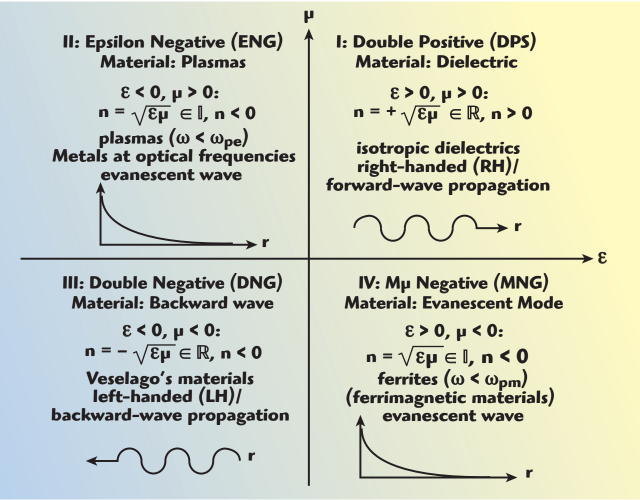

▲ *Fig. 1 Permittivity – permeability, where ℝ and 𝕀 represent real and imaginary terms and ω_{pe} and ω_{pm} are the electric and magnetic plasma frequencies, respectively.*[1]

The trend of nature is to favor conventional materials, illustrated in quadrant I of Figure 1, and, to a lesser degree, single negative materials (quadrants II and IV). The sign (+ or -) of permittivity/permeability are not restricted by physical law so long as generalized entropy conditions for dispersive media are satisfied.[1] This can be mathematically verified by inserting a plane wave into Maxwell's curl equations with $\varepsilon < 0$ and $\mu < 0$.

The negative index material n' ($n = \sqrt{\mu\varepsilon}$, $\varepsilon < 0$ and $\mu < 0$), also referred to as left-handed (LH) material, exhibits anti-parallelism between phase and group velocity (v_p-||v_g). This causes strong localization and enhancement of fields, thereby enhancement in effective group velocity of resonators realized from MMT structures. Increased group velocity yields improvement in the slew rate and quality factor of the resonator, which is advantageous for lower phase noise oscillator circuits. Additionally, several important phenomena of classical physics reverse in negative index or LH media, as illustrated in ***Figure 2***[1].


Master Your Power
Source Module with
Electronic Attenuation
90.000 000 000 000
10.00
S12MS-AG-EA2
60 to 90 GHz
Millimeter Wave Source Module
THROUGH ELECTRONIC CONTROL:
POWER FLATNESS AND POWER LEVELING ARE ONLY A CLICK AWAY
Innovation in Millimeter Wave Solutions
www.omlinc.com
(408) 779-2698
OML

Figure 2 depicts the following: (a) Doppler effect ($\Delta\omega > 0$ for an observer seeing a retreating source), (b) Vavilov – Cerenkov radiation (backward radiation of a fast-wave particle in motion), (c) Snell's law, (d) Goos – Hänchen effect (lateral shift in total internal reflection), (e) lensing effect (convex/concave LH lenses are diverging/converging) and (f) sub-wavelength focusing of an image by a flat slab (low spatial frequency features are focused by reversed Snell's law while high spatial frequency feature are enhanced, due to a reverse transfer function associated with surface wave or surface Plasmon excitation[2-8]).

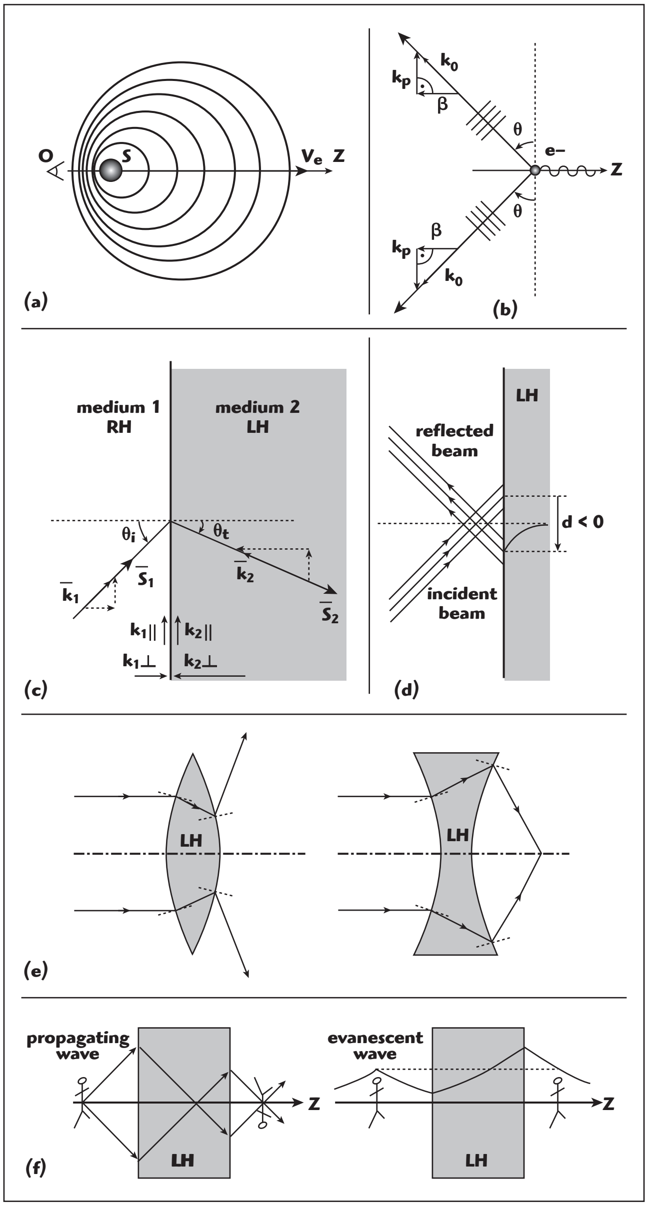

▲ *Fig. 2 Reversed phenomena in negative index material ($\varepsilon < 0$ and $\mu < 0$): Doppler shift (a) Vavilov-Cerenkov radiation (b) Snell's law (c) Goss-Hänchen effect (d) lens properties (e) and sub-wavelength focusing (f)*[1].

METAMATERIAL CHARACTERIZATION

MMTs characterized by double ($\varepsilon < 0$ and $\mu < 0$) or single negative ($\varepsilon < 0$ and $\mu > 0$ or $\varepsilon > 0$ and $\mu < 0$) structure can exhibit independent electric (E) and magnetic (H) responses described by ε and μ.

The E field causes magnetic polarization while the H field induces electrical polarization, known as magne-to-electric coupling. Such media are called bi-isotropic. Media that exhibit magneto-electric coupling and are also anisotropic are called bi-anisotropic.

Four material parameters are intrinsic to magneto-electric coupling of bi-isotropic media. These are: ε, μ, κ and χ, or permittivity, permeability, strength of chirality and the Tellegen parameter, respectively. In this type of media, the material parameters do not vary with changes along a rotated coordinate system of measurements. They are invariant or scalar.

The intrinsic magneto-electric parameters κ and χ affect the phase of the wave. The effect of the chirality parameter is to split the refractive index. In isotropic media, this results in wave propagation only if ε and μ have the same sign. In bi-isotropic media with χ assumed zero and κ a non-zero value, different results appear. Both a backward wave and a forward wave can occur. Alternatively, two forward waves or two backward waves can occur, depending on the strength of the chirality parameter.

The realization of negative index material for broadband operation from a set of arbitrary passive structure unit cells arranged in predefined order is challenging.[9] On the other hand, it is important to understand the limits imposed to negative index material ($\varepsilon < 0$, $\mu < 0$) by phase reversal between phase and group velocity and losses, as required by causality.

The estimation of refractive index calculated by[1]

$$n = \frac{1}{kd}\cos^{-1}\left[\frac{1 - S_{11}^2 + S_{21}^2}{2S_{21}}\right] \quad (1)$$

$$z = \sqrt{\frac{(1+S_{11})^2 - S_{21}^2}{(1-S_{11})^2 - S_{21}^2}} \quad (2)$$

$$\varepsilon = \frac{n}{z} \quad \mu = n \times z \quad (3)$$

where n is the refractive index, z is the wave impedance, k is wave factor, and d is the physical length.

In isotropic media, the group velocity is v_g

$$v_g(\omega_0) = \frac{d\omega}{dk} = \left(\frac{dk}{d\omega}\right)^{-1} \quad (4)$$

$$\frac{\partial k^2}{\partial \omega} = 2k\left(\frac{\partial(k)}{\partial \omega}\right) = 2\left(\frac{\omega}{v_p v_g}\right),$$

$$\text{where } v_p = \frac{\omega}{k}, k^2 = \omega^2\mu\varepsilon \quad (5)$$

v_g is the group velocity, v_p is the phase velocity, ω is angular frequency, k is the wave number. From equations 4 and 5,

$$\frac{\partial k^2}{\partial \omega} = \omega\varepsilon\frac{\partial(\omega\mu)}{\partial\omega} + \omega\mu\frac{\partial(\omega\varepsilon)}{\partial\omega} < 0 \quad (6)$$

$$\Rightarrow v_p v_g < 0$$

From equation 6, group velocity is anti-parallel to the phase velocity in MMT media. For MMT media, the group index n_g given by

$$n_g = n + \omega\left(\frac{dn}{d\omega}\right) =$$

$$\frac{1}{2}\left(\sqrt{\frac{|\varepsilon|}{|\mu|}}\frac{d(\mu\omega)}{d\omega} + \sqrt{\frac{|\mu|}{|\varepsilon|}}\frac{d(\varepsilon\omega)}{d\omega}\right) > 0 \quad (7)$$

where $n = (\mu\varepsilon)^{0.5}$

From equations 6 and 7, group and phase velocity of negative refractive index material manipulated for ampli-

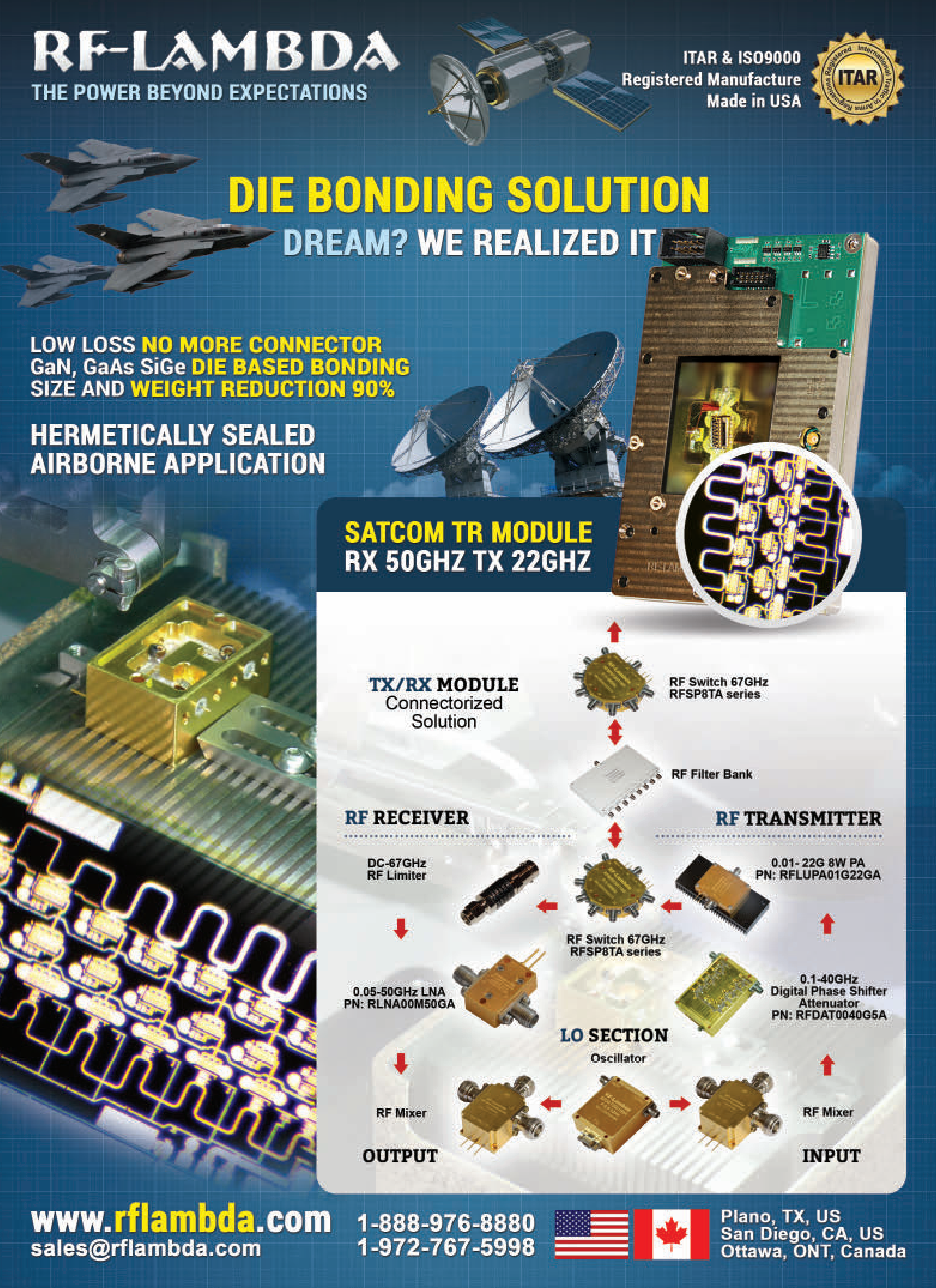
RF-LAMBDA
THE POWER BEYOND EXPECTATIONS
ITAR & ISO9000
Registered Manufacture
Made in USA
ITAR
DIE BONDING SOLUTION
DREAM? WE REALIZED IT
LOW LOSS NO MORE CONNECTOR
GaN, GaAs SiGe DIE BASED BONDING
SIZE AND WEIGHT REDUCTION 90%
HERMETICALLY SEALED
AIRBORNE APPLICATION
SATCOM TR MODULE
RX 50GHZ TX 22GHZ
TX/RX MODULE
Connectorized
Solution
RF Switch 67GHz
RFSP8TA series
RF Filter Bank
RF RECEIVER
RF TRANSMITTER
DC-67GHz
RF Limiter
0.01- 22G 8W PA
PN: RFLUPA01G22GA
RF Switch 67GHz
RFSP8TA series
0.05-50GHz LNA
PN: RLNA00M50GA
0.1-40GHz
Digital Phase Shifter
Attenuator
PN: RFDAT0040G5A
LO SECTION
Oscillator
RF Mixer
RF Mixer
OUTPUT
INPUT
www.rflambda.com
sales@rflambda.com
1-888-976-8880
1-972-767-5998
Plano, TX, US
San Diego, CA, US
Ottawa, ONT, Canada

fication of the evanescent mode waves in a resonator cavity improve resonator quality factor.[4] The determination of n, ε and μ can be evaluated from S-parameters.[10]

METAMATERIAL RESONATOR

Figure 3 shows the typical arrangement of planar split ring resonator (SRR) and complementary split ring resonator (CSRR) structures that exhibit negative permeability and negative permittivity.[11] They can be characterized as a magnetic and electric dipole excited by the magnetic (H) and electric (E) fields along the ring axis.[12]

Interestingly, single negative property (–ε or –μ) supported by a SRR or CSRR structure can offer a sharp stopband at the vicinity of resonant frequency. This enables storage of EM energy into the SRR or CSRR structure through an evanescent-mode coupling mechanism, resulting in a high quality factor.

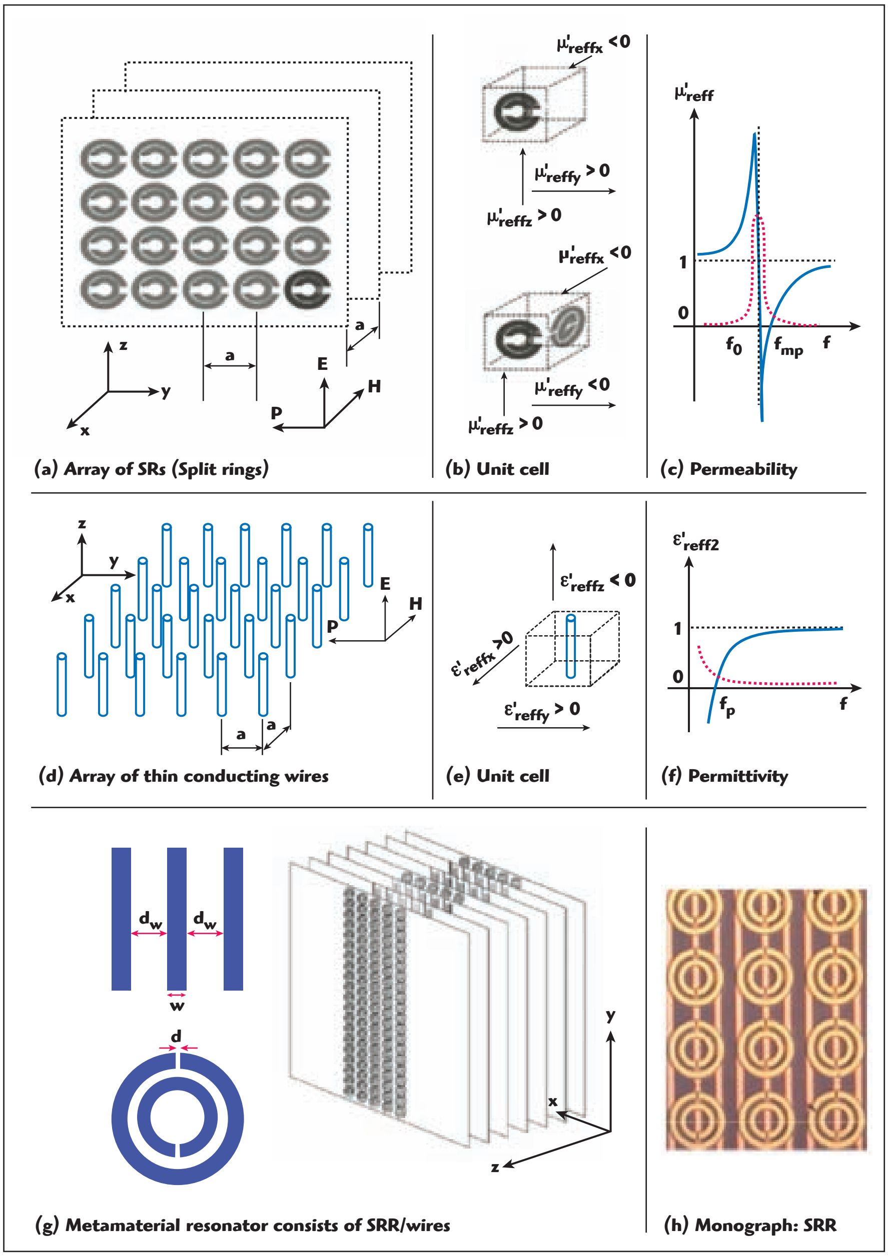

▲ *Fig. 3 Typical array of split ring (SR) and thin conducting wires for realizing negative values of magnetic permeability ($\mu_{eff} < 0$) and electric permittivity ($\varepsilon_{eff} < 0$): array of SRs (a) one dimensional (upper) and two dimensional (lower) unit cells (b) effective permeability showing real (solid line) and imaginary (dashed line) parts (c) array of thin conducting wires (d) thin wire unit cell (e) effective permittivity showing the real (solid line) and imaginary (dashed line) parts (f) metamaterial resonator comprised of SRR unit cells and micro wire patterns (g) and photomicrograph of SRR layer with wire layer stacked on top (h)*[12,20].

As shown in ***Figure 4***, SRR and CSRR structures act as an LC resonator driven by an external electromotive force. The value of inductance and capacitance of the SRR is described by[14-16]

$$L = \frac{\mu_o \pi^2}{I^2} \int_0^\infty \left[\tilde{I}(k)\right]^2 k^2 dk \qquad (8)$$

$$C_c = \frac{\varepsilon_o \pi^3}{c^2} \cdot \int_0^\infty \left[\frac{1}{2} + \frac{\varepsilon}{2\varepsilon_o}\left(\frac{\varepsilon_o + \varepsilon\,\mathrm{tgh}(kh)}{\varepsilon + \varepsilon_o\,\mathrm{tgh}(kh)}\right)\right] \cdot \left[\frac{\left[b\beta(kb) - a\beta(ka)\right]^2}{k^2}\right] dk \qquad (9)$$

where $\tilde{I}(k)$ is the Fourier–Bessel transform of the current function on the ring, $I(r)=\int_0^\infty J_{s,\varnothing}(r')dr'$, $J_{s,\varnothing}(r')$ is the azimuthal surface current density on the ring, c is the slot width, r_0 is the average radius of the ring of the SRR, a and b are the geometrical parameters shown in Figure 4b, and $\beta(x) = S_0(x)J_1(x)\text{-}S_1(x)J_0(x)$ with S_n and J_n being nth-order Struve and Bessel functions.[16]

The behavior of SRRs and CSRRs, and their derived geometries, are strictly dual for perfectly conducting and infinitely thin metallic screens placed in a vacuum. In reality, this is not the case and a shift in resonance frequency occurs from losses, the finite width of the metallization and the presence of a dielectric substrate.

The realization of MTM media using SRRs, as shown in Figure 4, is based on its unit cell size being much smaller than the wavelength of the incident wave. The SRR behaves as a quasi-static LC resonant circuit fed by the external magnetic flux linked by the SRR unit cell. The SRR unit cell, realized by two coupled conducting rings printed on a dielectric slab, requires precise placement of metal patterns at two sides of a dielectric substrate. A recent publication reports the use of spiral resonators (SR), which provide a potential reduction in the electrical size of the MTM unit cell. Moreover, the SR is not bi-anisotropic and uniplanar, making for an easier fabrication process compared to SRR unit cells, if the metamaterial is viewed as a continuous medium for superlens and cloaking purposes.[17]

Figure 5 shows the typical config-

Innovation Thats Open.

Introducing *Open**RFM***™

Meeting new government interoperability and affordability requirements in Electronic Warfare and Signals Intelligence, requires innovative approaches in advanced RF/Microwave and digital signal processing. OpenRFM is the first RF/Microwave open system approach that leverages best available commercial-item technology to deliver sophisticated, interoperable sensor processing subsystems to dominate the electromagnetic spectrum. OpenRFM is the better alternative for affordable RF subsystems for our war fighters and allies alike.

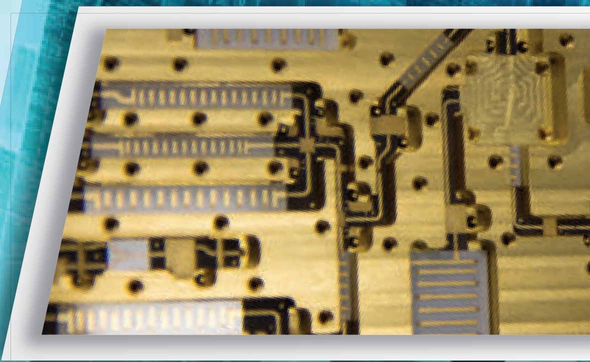

MERCURY SYSTEMS™

INNOVATION THAT MATTERS™

MADE IN AMERICA

Visit mrcy.com/OpenRFM and download our position paper: OpenRFM™ - A Better Alternative For An Open Architecture to Support EW, EA and SIGINT Applications uration of the SRR and SR. The SRR is shaped by two coupled conducting rings fabricated on a dielectric slab, whereas spiral resonators SR2 (two turns) and SR3 (three turns) are made by a single strip rolled up to form a spiral. Baena[17] describes the topology of the SRR and SR and their equivalent circuits, where C_0 is defined as the edge capacitance between the two rings over the whole circumference, L_s is the inductance of a single ring and r_0 the average radius.

As shown in Figure 5, the total current in the unit cell is the sum of the currents on each ring. For a given value of the angular polar coordinate (ϕ), the current lines go from one ring to another across the slot between the rings, in the form of field displacement current lines.[17] The normalized quasi-static voltage V (ϕ) and the electric current intensity I (ϕ) along the strips, as a function of the angular polar coordinate (ϕ), illustrate the size reduction advantages of SRs as a metamaterial medium. From the equivalent circuits depicted in Figure 5b, there is a reduction of the SR's resonance frequency with respect to the SRR. The capacitance value for a SRR is $C_0/4$, whereas for an SR it is C_0 and for an SR3 it is $2C_0$. Therefore, the resonance frequency ratios are $f_{SRR}=2f_{SR2}=2\sqrt{2}f_{SR2}$.

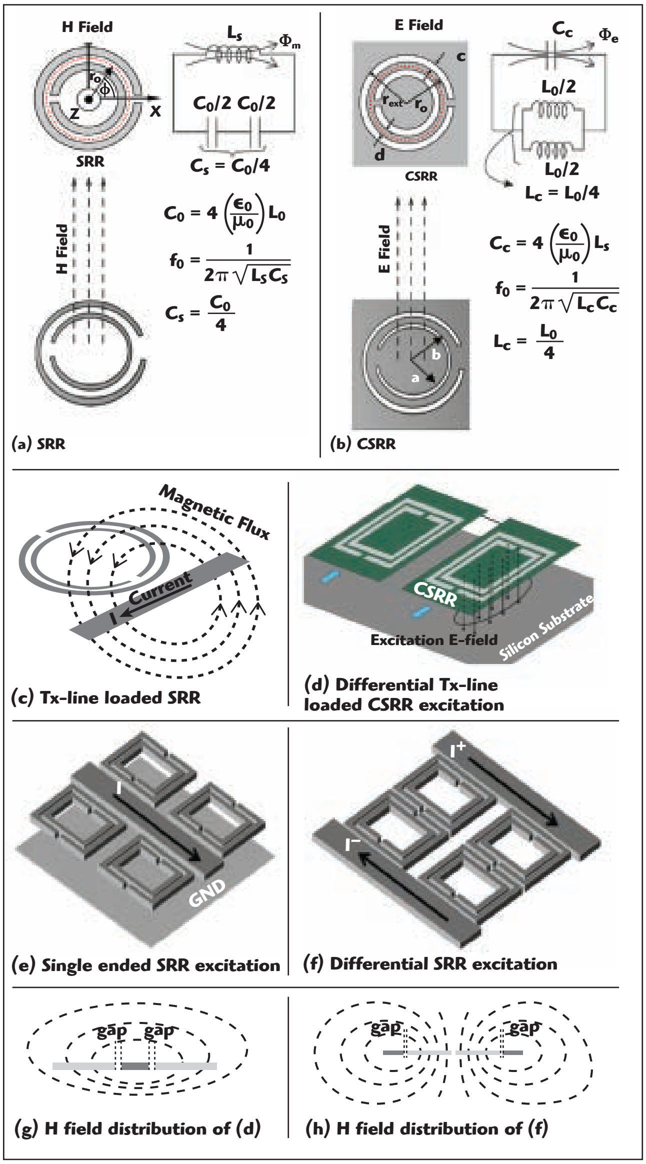

▲ *Fig. 4 Typical planar SRR and CSRR structure showing SRR excitation by H field (a) CSRR excitation by E field (b) transmission-line loaded SRR and H field excitation (c) on-chip differential transmission-line loaded CSRR (d) transmission-line single-ended SRR excitation (e) transmission-line differential SRR excitation (f) H field distribution of the single-ended SRR excitation (g) and H field distribution of the differential SRR excitation (h)*[13].

Figure 6 shows the comparative size reduction of the SR2 and SR3 with the identical resonant frequency. The size reduction is about 50 percent for the SR2 and 65 percent for the SR3 as compared to the SRR unit cell.[18] The SR structures shown in Figures 5 and 6 are also amenable for Möbius "TWIST" (discussed in the first part of this series, published in the November 2014 issue), resulting in high Q-factor Möbius metamaterial strips resonators [18-19].

METAMATERIAL RESONATOR DYNAMICS

Figure 7 shows the electromagnetic (EM) wave propagation dynamics.[1] The direction of the Poynting vector $\vec{S}$ is parallel with the direction of phase velocity or wave vector $\vec{k}$ in right-handed (RH) material, but these two directions are anti-parallel in left-handed (LH) material. CAD simulation exhibits a backward wave into the host transmission line, establishing a standing wave when coupled in-phase with the forward EM wave. The standing wave supports strong EM coupling between the host transmission line and the negative index resonator (MTM resonator), causing strong localization and enhancement of evanescent mode-coupled energy. The manipulation of MMT properties of evanescent mode-coupled resonators for tunable oscillator circuit applications has been reported.[21]

The propagation constant k_z for the electromagnetic wave propagation in + ve z-axis is given by[9]

$$k_z = \sqrt{\frac{\omega^2}{c^2} - \left(k_x^2 + k_y^2\right)} \qquad (10)$$

If $\frac{\omega^2}{c^2} < \left(k_x^2 + k_y^2\right)$ then

$$\left[k_z\right]_{\frac{\omega^2}{c^2} < \left(k_x^2 + k_y^2\right)} = j\sqrt{-\left[\frac{\omega^2}{c^2} - \left(k_x^2 + k_y^2\right)\right]} \qquad (11)$$

which describes the evanescent mode propagation waves ($\varepsilon > 0$, $\mu < 0$), and

$$\left[k_z\right]_{\frac{\omega^2}{c^2} > \left(k_x^2 + k_y^2\right)} = +\sqrt{\left[\frac{\omega^2}{c^2} - \left(k_x^2 + k_y^2\right)\right]} \qquad (12)$$

which describes the forward mode propagation waves ($\varepsilon > 0$, $\mu > 0$).

From equation 11, the evanescent mode propagation waves will have exponential decay along the z-axis.

The transmission and reflection coefficients, T and R, can be derived by matching the EM fields at the interface of medium 1 and medium 2:

$$T = \frac{2\mu k_z}{\mu k_z + k_z'} \qquad (13)$$

$$R = \frac{\mu k_z - k_z'}{\mu k_z + k_z'} \qquad (14)$$

The transmission and reflection coefficients T' and R' of the transition from inside medium 2 to medium 1 are given by[9]

$$T' = \frac{2k'_z}{\mu k_z + k'_z} \quad (15)$$

$$R' = \frac{k'_z - \mu k_z}{k'_z + \mu k_z} \quad (16)$$

The expression of the wave transmission coefficient (T) through both interfaces is derived by adding the multiple scattering dynamics, described by[9]

$$T_e = TT'e^{j(k'_z d)} + TT'R'^2 e^{j(3k'_z d)} + TT'R'^3 e^{j5(5k'_z d)} + TT'R'^4 e^{j(7k'_z d)} + (\ldots) \quad (17)$$

$$T_e = \frac{TT'e^{j(k'_z d)}}{1 - R'^2 e^{j(2k'_z d)}} \quad (18)$$

For metamaterial ($\varepsilon < 0$ and $\mu < 0$), ε = -1 and μ = -1

$$[T_e]_{\varepsilon\to -1,\mu\to -1} = \frac{\left[\left(\frac{-2k_z}{-k_z + k'_z}\right)\left(\frac{2k'_z}{-k_z + k'_z}\right) e^{j(k'_z d)}\right]}{\left[1 - \left(\frac{k'_z + k_z}{k'_z - k_z}\right)^2 e^{j(2k'_z d)}\right]} = e^{-j(k'_z d)} \quad (19)$$

where

$$[k'_z] = j\left(\sqrt{\left(k_x^2 + k_y^2\right) - \varepsilon_2\mu_2 \frac{\omega^2}{c^2}}\right) \quad (20)$$

$$[k'_z]_{\varepsilon\to -1,\mu\to -1} = \left(\sqrt{-\left(k_x^2 + k_y^2\right) + \frac{\omega^2}{c^2}}\right) = k_z \quad (21)$$

$$[T_e]_{\varepsilon\to -1,\mu\to -1} = \left[\frac{TT'e^{j(k'_z d)}}{1 - R'^2 e^{j(2k'_z d)}}\right] = e^{-j(k'_z d)} = e^{-j(k_z d)} \quad (22)$$

The overall reflection coefficient can be given by (R_r)[9]

$$[R_r] = R\left[1 + \frac{TT'e^{j(k'_z d)}}{1 - R'^2 e^{j(2k'_z d)}}\right] \to$$

$$[R_r]_{\varepsilon\to -1,\mu\to -1} \to 0 \quad (23)$$

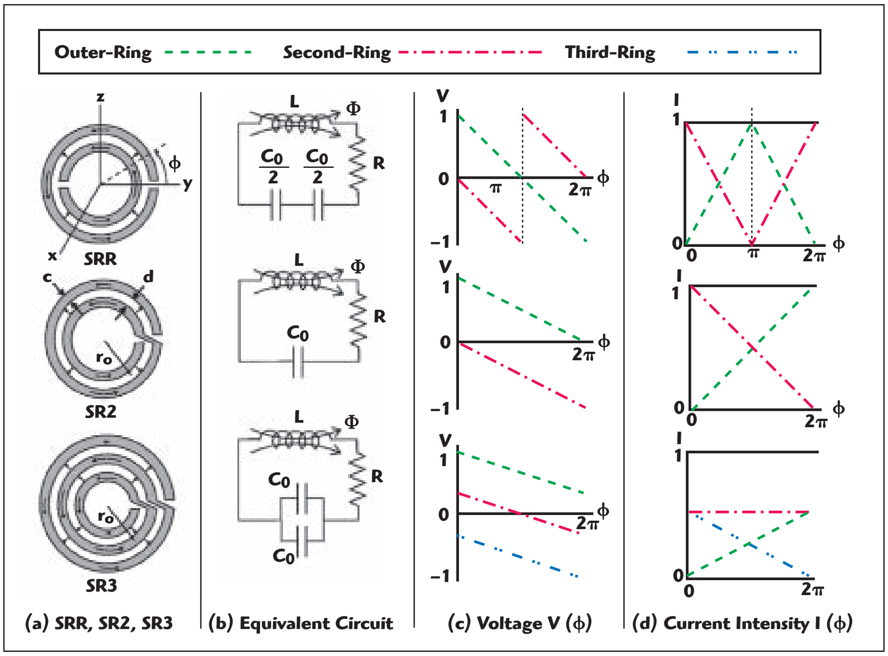

▲ *Fig. 5 Typical layout of SRR, SR2 and SR3 (a) equivalent circuits (b) normalized quasi-static voltage V (ϕ) as a function of the angular polar coordinate (ϕ) (c) and normalized electric current intensity I (ϕ) as a function of ϕ along the strips (d).*[17]

From equation 23, the reflection coefficient R_r is zero for double-negative MTM. The transmission coefficient can be represented by $e^{(jkzd)}$ at the interface, provided both permittivity and permeability are equal to –1. From equations 11 and 17, the transmission coefficient will increase exponentially with increasing distance traveled inside the MTM slab. Hence, MTM exhibits amplification of the evanescent wave, opening new degrees of freedom in designing high Q-factor resonators for compact, high frequency oscillators. The Q multiplier effect does not violate energy conservation because the evanescent mode only stores the energy and does not transport the energy.

The evanescent mode-coupled MTM based resonator has the potential to make a dramatic impact on the design of compact, tunable oscillators that otherwise cannot be achieved with conventional printed transmission-line resonators. MTM resonators present several advantages compared with conventional planar resonators, such as high Q-factor, improved selectivity, easy integration in MMICs, multi-band multi-mode characteristics and insensitivity to EMI/EMC.

Figure 8 shows the simulated S_{21} of MTM split ring, Möbius strips and MTM Möbius strips resonators on a 12 mil thick substrate with ε_r = 2.2.[9] As shown in the figure, metamaterial

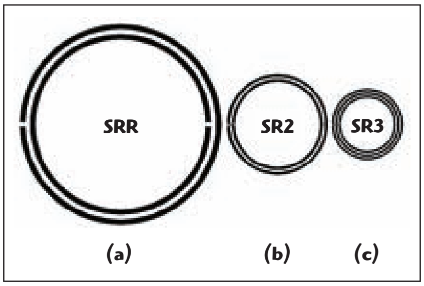

▲ *Fig. 6 Comparison of the sizes of the SRR (a) SR2 (b) and SR3 (c) at the same resonant frequency. The SR2 and SR3 are promising topologies for implementing a Möbius loop.*[18]

Möbius strips (MMS) exhibit superior S_{21} characteristics, with higher Q-factor and suppression of the spurious resonance modes. This enables stable broadband operation compared to MTM split rings and Möbius strips resonators, which exhibit undesired second-order modes.

Mode jumping is analyzed by solving the boundary conditions of the printed MTM resonator. The Möbius metamaterial resonator (MMR) shown in Figure 8 conserves the quantity that gives invariance of solutions under a 2π rotation with a definite handedness (discussed in the first article of this series, published in the November 2014 issue). The MMS has the unique characteristic of self phase-injection properties along the mutually-coupled surface of the strips, which enables a higher quality factor for a given cou-

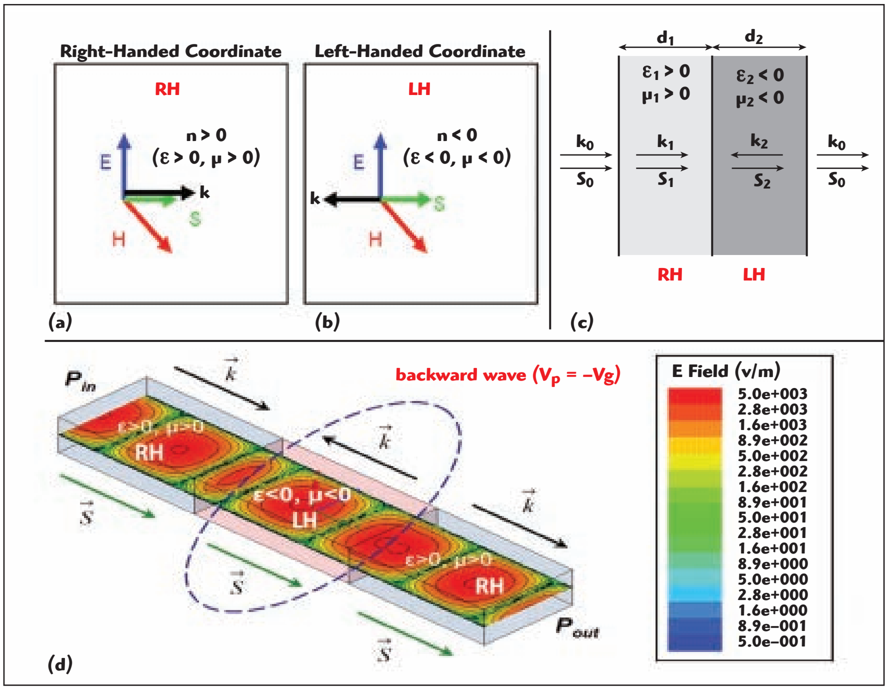

▲ *Fig. 7 RH propagation properties for materials with ε and μ > 0 (a) LH propagation properties for materials with ε and μ < 0 (b) two-layer structure with the left a RH material and the right a LH material (c) HFSS simulation of the plane wave propagation using LH and RH materials (d).*[1]

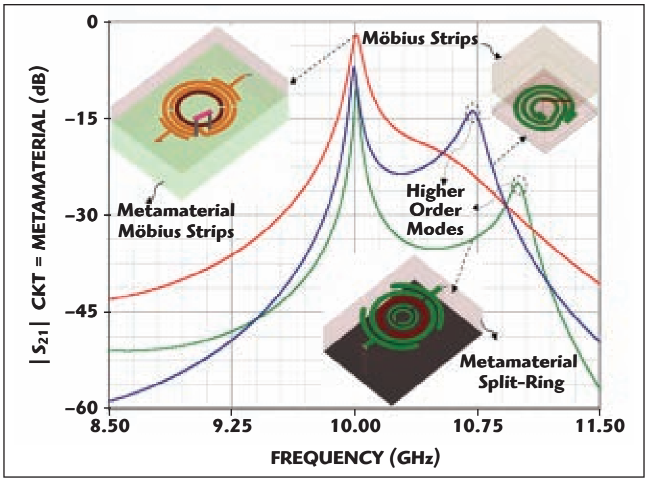

▲ *Fig. 8 Simulated S_{21} of metamaterial split rings (a) Möbius strips (b) and metamaterial Möbius strips resonator networks (c).*[9]

pling coefficient β_j. The coupling coefficient β_j depends on the geometry of the perturbation, given by[9,22]

$$\beta_j = \left(\frac{\int \varepsilon E_a . E_b \, dv}{\sqrt{\int \varepsilon E_a^2 \, dv \int \varepsilon E_{bd}^2 \, dv}}\right)_{electrical-coupling} + \left(\frac{\int \mu H_a . H_b \, dv}{\sqrt{\int \mu H_a^2 \, dv \int \mu H_b^2 \, dv}}\right)_{magnetic-coupling} \quad (24)$$

where E_a and H_a are the respective E and H fields produced by the MMS and E_b and H_b are the corresponding fields due to the perturbation ($d \neq 0$) or nearby adjacent resonator.[9]

In equation 24, the first term represents the coupling due to the interaction between the E fields of the resonators, and the second term represents the H coupling between the resonators.

Depending on the strength of interaction, multi-mode dynamics exist related to E, H, and hybrid coupling. ***Figure 9*** shows the unloaded Q of MTM and multi-coupled planar resonators over a range of operating frequencies from 2 to 16 GHz. The Q is estimated by experimental measurement of S-parameters using a vector network analyzer.[22]

CONCLUSION

Artificial negative index materials (metamaterials) have been newsworthy for a number of years. This article investigates how the implementation of MTM microwave resonators can achieve advantageous properties, showing that the metamaterial Möbius resonator can achieve high Q-factors.

The third article, which will be published in the January 2015 issue, will discuss several metamaterial Möbius resonator tunable oscillator circuits,[22] showing that oscillators using these resonators offer promising performance. ■

References

1. C. Caloz and T. Itoh, “Metamaterials for High-Frequency Electronics”, *IEEE Proceedings*, Vol. 93, No. 10, pp. 1745–1752, October 2005.
2. V. Veselago, “The Electrodynamics of Substances with Simultaneously Negative Values of ε and μ, *Soviet Physics-Solid State*, Vol. 8, No. 12, pp. 2854–2856, 1967.
3. J.B. Pendry et al., “Extremely Low Frequency Plasmons in Metallic Mesostructure,” *Physical Review Letters*, Vol. 76, No. 25, pp. 4773–4776, June 1996.
4. J.B. Pendry et al., “Magnetism from Conductors and Enhanced Nonlinear Phenomena,” *IEEE MTT Transactions*, Vol. 47, pp. 2075–2084, November 1999.
5. D.R. Smith et al., “Composite Medium with Simultaneously Negative Permeability and Permittivity,” *Physical Review Letters*, Vol. 84, No. 18, pp. 4184–4187, May 2000.
6. A. Iyer and G. Eleftheriades, “Negative Refractive Index Metamaterials Supporting 2-D Waves,” *MTT-S Digest*, pp. 412–415, 2002.
7. C. Caloz and T. Itoh, “Application of the Transmission Line Theory of Left-Handed (LH) Materials to the Realization of a Microstrip LH Transmission Line,” in *Proceedings IEEE-AP-S USNC/URSI NRS-Meeting*, Vol. 2, pp. 412–415, 2002.
8. C. Caloz and T. Itoh, “Novel Microwave Devices and Structures Based on the Transmission Line Approach of Meta-Materials,” *MTT-S Digest*, pp. 195–198, 2003.
9. A.K. Poddar, “Slow-Wave Resonator Based Tunable Multi-Band Multi-Mode Injection-Locked Oscillators,” *Research Report*, “RF and Microwave Techniques Brandenburg University of Technology Cottbus-Senftenberg 2012”, https://www-docs.tu-cottbus.de/mikrowellentechnik/public/poddar_report_long_ebook.pdf.
10. U. Hasar et al., “Differential Uncertainty Analysis for Evaluating the Accuracy of S-Parameter Retrieval Methods for Electromagnetic Properties of Metamaterial Slabs,” *Optics Express*, Vol. 20, No. 27, 2012.
11. J. Manuel and T. Alves, Metamaterials

Procedure for how to use the N, TNC and 7/16 Push-On male. Push-On Connectors mate with any standard female connector of the same connector style.

1. Convert your standard Assembly into a Push-On Assembly using the Nf to Nm Push-On Adapter.

2. Put your fingers firmly onto the knurls of the “Lock Nut”.

3. Push “Lock Nut” forward and engage the Push-On end of the Adapter with the mating female. Back nut must be released.

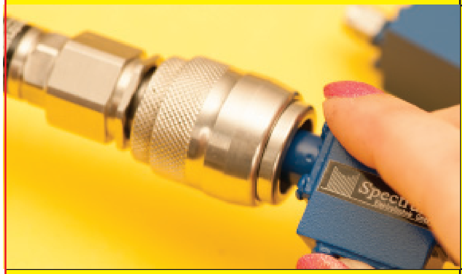

4. The Connection has been completed, easy and fast. The connector has been locked on safely.

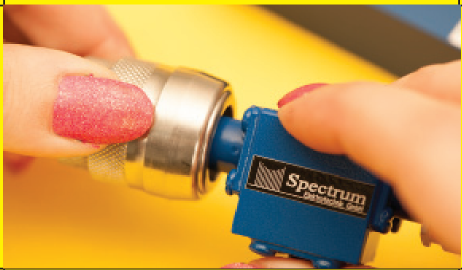

5 . To unlock (when “Back Nut” is in unlocked mode) push the “Lock Nut” forward and stop reverse movement by setting your fingers onto the “Back Nut”.

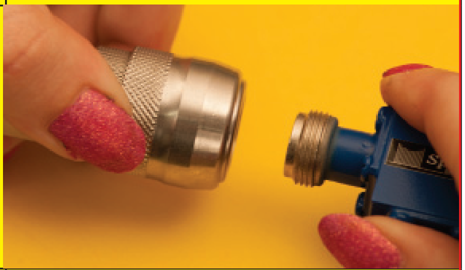

6. Keep fingers on “Back Nut” to ensure that “Lock Nut” cannot slide back and pull the connector off.

Procedure for how to use the SMA male and SMA female Push-On connectors. SMA Push-On Connectors mate with any standard connector of the same but opposite connector style.

1. Convert your standard cable assembly into a Push-On Assembly by threading the standard female side of the adapter onto the male connector of the assembly.

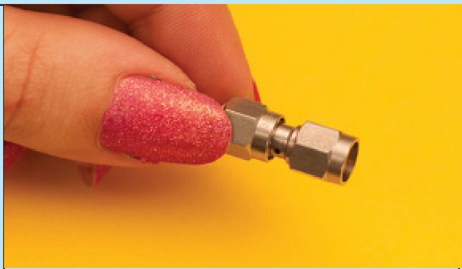

2. Your standard SMA male cable assembly is converted into an SMA male Push-On Assembly.

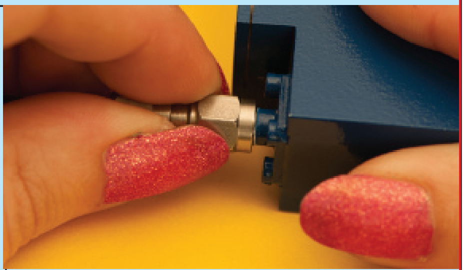

3. Just slide the Push-On SMA male Connector onto any standard SMA female. The connection is securely completed in seconds.

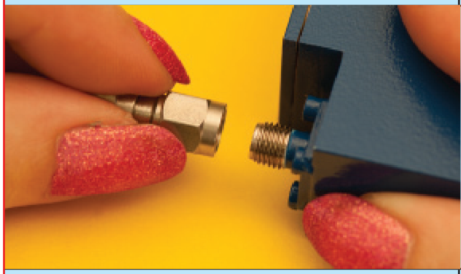

4. To disconnect, just pull the connector off.

Spectrum Elektrotechnik GmbH

Please contact us at:
www.spectrum-et.com
Email: sales@spectrum-et.com
Phone: +49-89-3548-040
Fax: +49-89-3548-0490

Spectrum Elektrotechnik GmbH

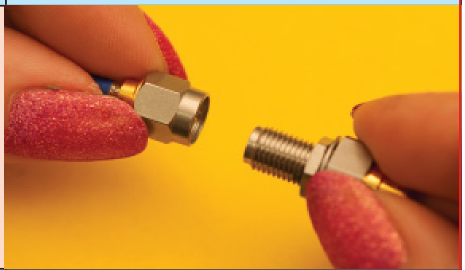

1. Convert your standard cable assembly into a Push-On Assembly by threading the standard female side of the adapter onto the male connector of the assembly.

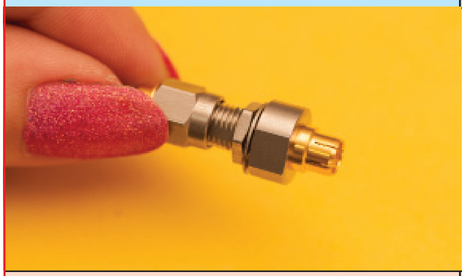

2. Your standard SMA male cable assembly is converted to a Push-On SMA female Cable Assembly.

3. Just slide the Push-On SMA female Connector onto any standard SMA male. The connection is securely done in seconds.

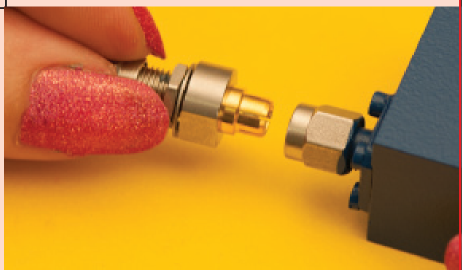

4. To disconnect, just pull the connector off.

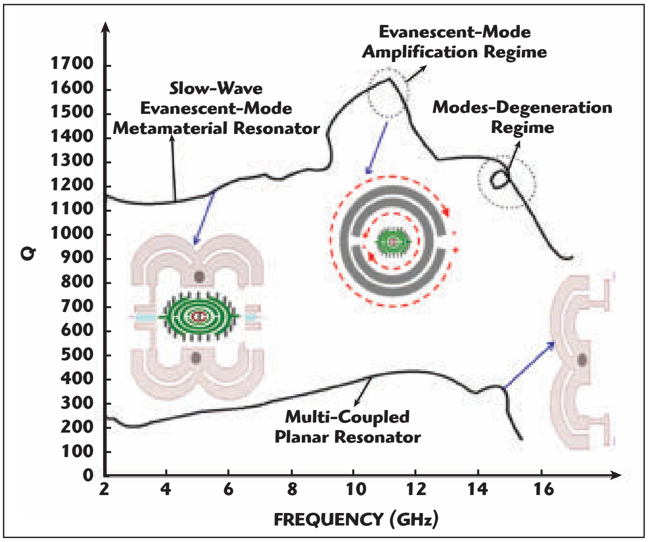

▲ *Fig. 9 Unloaded Q-factor of multi-coupled resonator, slow-wave evanescent-mode metamaterial resonator and evanescent mode amplified resonance regime.*[9]

with Negative Permeability and Permittivity: Analysis and Application," *MS-Thesis*, Univ. Tecnica de Lisboa Instituto Superior Tecnico, 2010.

12. R.A. Shelby et al., "Experimental Verification of a Negative Index of Refraction," *Science 2001*, pp. 292, 77–79.
13. Y. Shang et al., "Design of High-Q Millimeter-Wave Oscillator by Differential Transmission Line Loaded with Metamaterial Resonator in 65-nm CMOS," *MTT-Transactions*, Vol. 61, No. 5, pp. 1892–1902, May 2013.
14. N. Engheta, "An Idea for Thin Subwavelength Cavity Resonators using Metamaterials with Negative Permitivity and Permeability," *IEEE Antenna and Wireless Propagation Letters*, Vol. 1, pp. 10–13, 2002.
15. R. Marqués et al., "Comparative Analysis of Edge- and Broadside-Coupled Split Ring Resonators for Metamaterial Design–Theory and Experiment" *IEEE Transactions on Antennas Propagation*, Vol. 51, No. 10, pp. 2572–2581, October 2003.
16. J.D. Baena et al., "Equivalent-Circuit Models for Split-Ring Resonators and Complementary Split-Ring Resonators Coupled to Planar Transmission Lines", *MTT-Transactions*, Vol. 33, pp. 1451–1460, April 2005.
17. J.D. Baena et al., "Artificial Magnetic Metamaterial Design by Using Spiral Resonators," *Physical Review-B69*, 2004.
18. G. Sisó et al," Miniaturization of Planar Microwave Devices by Means of Complementary Spiral Resonators (CSRs): Design of Quadrature Phase Shifters," *Radio-Engineering*, Vol. 18, No. 2, pp. 145–148, June 2009.
19. U.L. Rohde, A.K. Poddar and D. Sundararjan "Printed Resonators: Möbius Strips Theory and Applications," *Microwave Journal*, November 2013.
20. M. Gokkavas et al., "Experimental Demonstration of a Left-Handed Metamaterial Operating at 100 GHz," *Physical Review Letter*, The American Physical Society, pp. 193103-1 to193103-4, 2006.
21. N. Engheta, "An Idea for Thin Subwavelength Cavity Resonators using Metamaterials with Negative Permitivity and Permeability," *IEEE Antenna and Wireless Propagation Letters*, Vol. 1, pp. 10–13, 2002.
22. A.K. Poddar, "Slow-Wave Resonator Based Tunable Multi-Band Multi-Mode Injection-Locked Oscillators," *Dr. Ing. habil Thesis*, Brandenburg University of Technology Cottbus-Senftenberg, Germany, 2014.

EMC Simulation in the Design Flow of Modern Electronics

Andreas Barchanski
CST AG, Germany
Jens Krämer, Pietro Luzzi
Festo AG[1], Germany

EMC compliance is a necessary condition for releasing products to market. National and international standards bodies such as the IEC[2] and the FCC[3] define limits on the emissions a device is allowed to produce, and automotive and aerospace manufacturers can set even stricter standards for their OEM suppliers. If these standards are not met, the product cannot be sold.

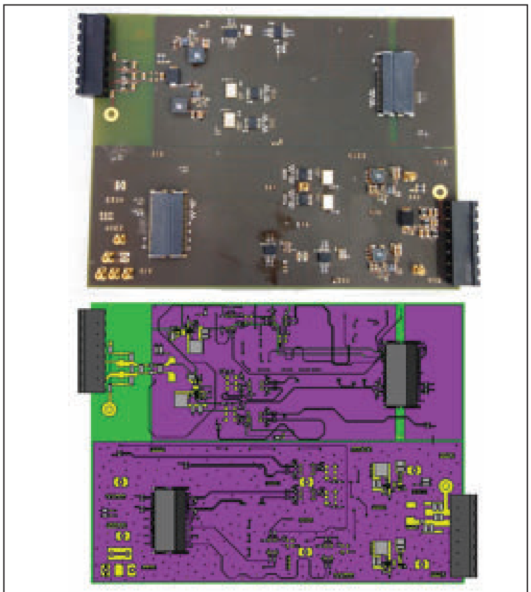

Fig. 1 Manufactured demonstrator board (top) and the equivalent simulation model (bottom).

EMC engineering has traditionally been the domain of measurement alone, with the result that EMC compliance was only considered late in the design process, since it required a working prototype. Correcting EMC problems at this late stage can be cost-intensive, especially if multiple prototype iterations are required.

In addition, although measurement can help identify the symptoms of EMC issues, it is only of limited use for identifying the root causes of the problems. This means EMC troubleshooting using measurement is often limited to applying countermeasures such as filters and additional shielding, which can increase the size and the cost of the product, instead of tackling the problem at its source.

Simulation allows EMC compliance to be analyzed earlier in the design process, and in greater depth than is possible with measurement alone. Because simulation doesn't require a physical prototype, it can be used to investigate many different configurations and

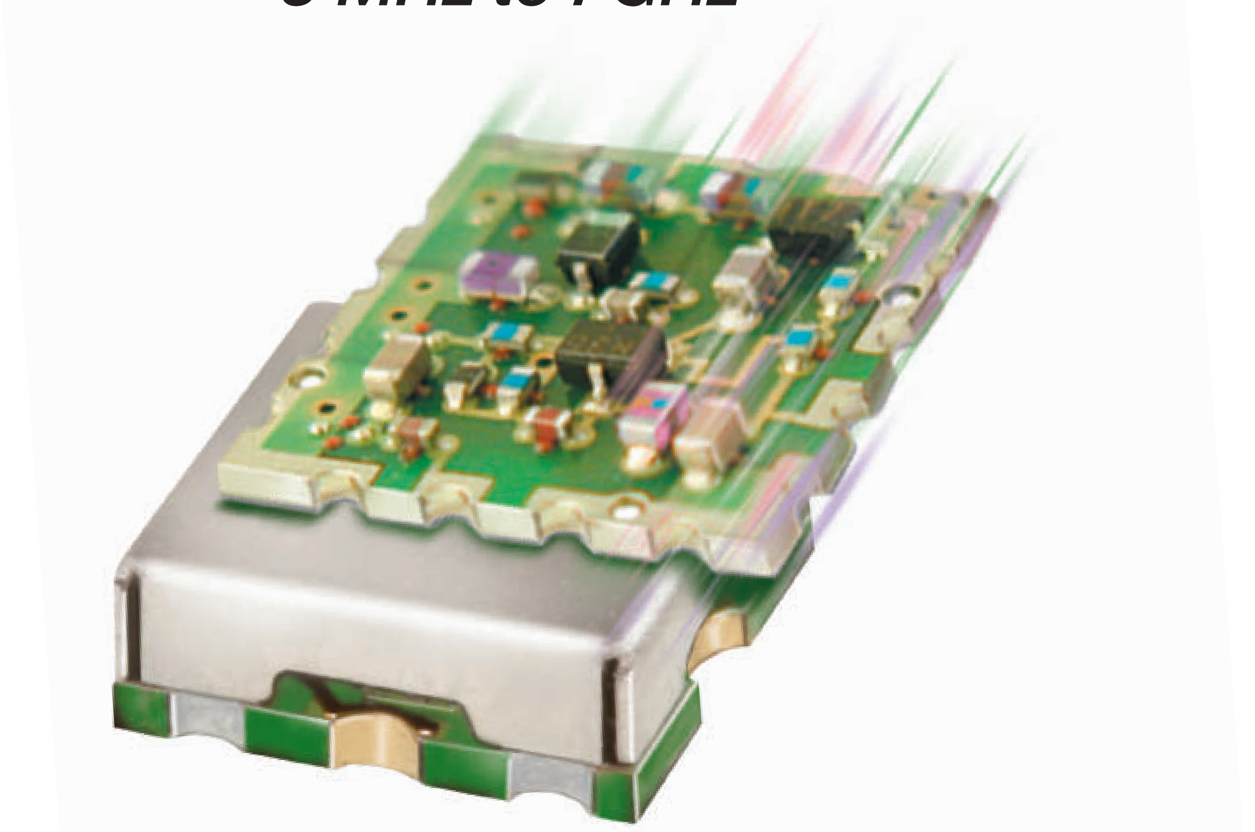

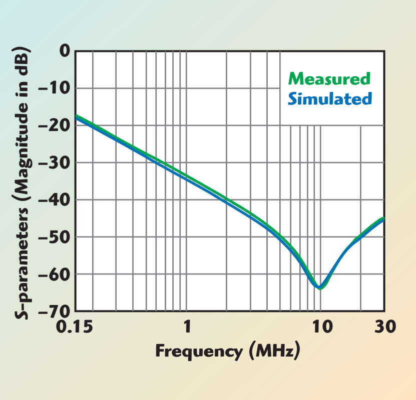

▲ *Fig. 2 Measured and simulated S-parameters for the input filter, used to extract the parasitic values of the filter.*

answer fundamental "what if?" questions about the design. Decisions that are made early in the design process – for example, the arrangement of the components within the device – are usually difficult to change later on and can be crucial for the EMC compliance of a device.

Simulation is also helpful at the troubleshooting stage, where it is a complementary tool to measurement. Current and field visualization can serve to highlight the locations of EMC problems. They offer more insight into the behavior of the device than a blip on a spectrum analyzer graph can provide, although the measurement is still critical for the final decision as to whether the device passes or fails the test.

This article considers how to test and develop the EMC workflow for modern electronic devices. The demonstrator board (see ***Figure 1***) is based on modern electronic designs, and the principles outlined here are applicable to a wide range of devices. On this board, the power is routed through an input filter to a voltage regulator module (VRM) that drives a power delivery network (PDN) on the PCB. A number of single ended and differential drivers are placed on the board. Some of them are routed over a connector and all of them are finally terminated on the board.

The demonstrator board contains two versions of the same system on a common substrate – one designed to offer good EMC performance (the upper half of the board in Figure 1, called the "good" layout), and one designed to offer poorer performance (the lower half, called the "bad" layout).

The components were selected so the board has noise sources in various frequency bands: the VRM is typically driven at a few hundred kHz up to low MHz, the single ended nets typically emit from a few tens of MHz up to 1 GHz, while the frequencies on the differential nets can go as high as 6 GHz.

SIMULATION WORKFLOW

The first step of electronic layout is to define the logic of the board by sketching out a circuit schematic. However, it is not always possible to estimate the EMC performance just from the schematic, especially when considering radiated emissions instead of conducted emissions. The EMC performance of a device depends not only on its circuit-level representation, but also on the distribution of the capacitors, the routing of the nets and the interactions between signal lines and components. Only a 3D simulation can reveal these effects.

This means that circuit-level simulation methods coupled to full-wave 3D EM simulation can complement each other. These can be combined in a number of different ways: for example, a 'Combine Results' task, based on the superposition principle, can be used to calculate the field distribution when a circuit is attached to a 3D model without having to resimulate the entire 3D model, while true transient/EM co-simulation can be used to integrate circuits, including nonlinear components, into a full-wave 3D simulation.

The first step is to define the model geometry and import CAD and EDA data for PCBs and enclosures. Lumped elements, ports, probes and field monitors are also defined at this stage. The ports are what will later provide the link between the full-wave simulation and the circuit simulation. Once these are set up, the simulation can begin.

Full wave solvers can be broadly divided into time domain and frequency domain methods. For conducted emissions, where the frequency range is narrow and the fields are confined to the electrically small board, the frequency domain solver is usually the best choice. A frequency domain direct solver only requires one pass to simulate all the ports, which is useful for densely populated boards.

For radiated emissions, a time domain method is a better fit. The time domain solver needs to simulate each port separately, but it can simulate a broad band of frequencies at once, and is more efficient than the frequency domain technique for electrically large simulations.

Regardless of which simulation method is used, the results are the same: the S-parameters of the model and the field distribution inside it. These S-parameters can be used to produce a circuit-level model of the component, which can be incorporated into the schematic of the device.

Circuit solvers are much faster than 3D solvers and, for a simple circuit, a spectrum can be calculated within seconds. This means that the circuit elements can be adjusted interactively, and optimization of the circuit can be carried out in a reasonable length of time. This is especially useful for extracting equivalent circuits for elements and for helping simulation and measurement agree more closely.

In order to match the simulation and measurement, the parasitic values of the mounted elements must be known. To allow the input filter to be simulated accurately, an equivalent circuit is added to the simulation model representing the parasitics inherent in the test fixtures. By using the ‘Tune’ function, the values of the parasitics are varied until the simulation’s behavior matches the measurement. These values are then applied across multiple simulations, while maintaining good agreement between measurement and results (see ***Figure 2***).

CONDUCTED EMISSIONS

Two parts of the system are involved in conducted emissions: the input filter and the voltage regulator. For the analysis presented here, a constant load of 2.5 Ω is placed on the board. This load leads to a high current, so the emission is also quite high. This is, therefore, a worst case set-up.

The conducted emission will be measured using ports at the connector that are connected on the other side to an electric boundary, acting as a virtual reference. This electric boundary creates a low-impedance path for the return current. It is not an ideal external ground, as this cannot exist in a 3D model.

As already discussed, the frequency domain solver is a good choice for most conducted emissions simulations due to the narrow band nature of the signals. In this case the finite element method (FEM) based solver in CST STUDIO SUITE®[4] is used to generate the S-parameters. Once the 3D simulation has been run and a schematic block produced, the rest of the circuit can be added (see ***Figure 3***). This means a source representing the LT8610 VRM[5], derived from a functional simulation using the manufacturer’s LTSpice tool, and a line impedance stabilization network (LISN) as specified in the CISPR 16 test standard[6].

The circuit can then be simulated in either the time domain or the frequency domain. Both methods are available regardless of which solver was used for the 3D simulation. Here, an input signal is used which represents the switching effect of the VRM. In this case, a frequency domain method is used, which takes three seconds – extremely fast compared to full-wave simulation.

The results of this frequency domain simulation are shown in ***Figure 4***, calculated between the 0 V input and the protective earth (PE). One capacitor is used in the filter for the first simulation (shown on the top), while in the second simulation (shown on the bottom), a capacitor is inserted into the 24 V branch. The second capacitor improves the emission for the 24 V connection (not shown) but worsens the emission level for the 0 V branch (shown on the bottom). Even where there are discrepancies between simulation and measurement due to the noise-floor of the measurements, simulation offers an excellent prediction of the trends within the data. The increase in the maximum value and the position of the peak are both calculated by the simulation.

Replacing the switching noise with a broadband excitation also makes it possible to assess the performance of the filters and optimize their construction. Since each additional component carries a small cost in terms of money and production time, identifying components which do not contribute to the EMC performance of a device is beneficial. In the simulation in ***Figure 5***, one set of capacitors at the input is found to have virtually no effect on the emissions from the PCB and can be safely removed. Because of the speed of the circuit simulation, dozens

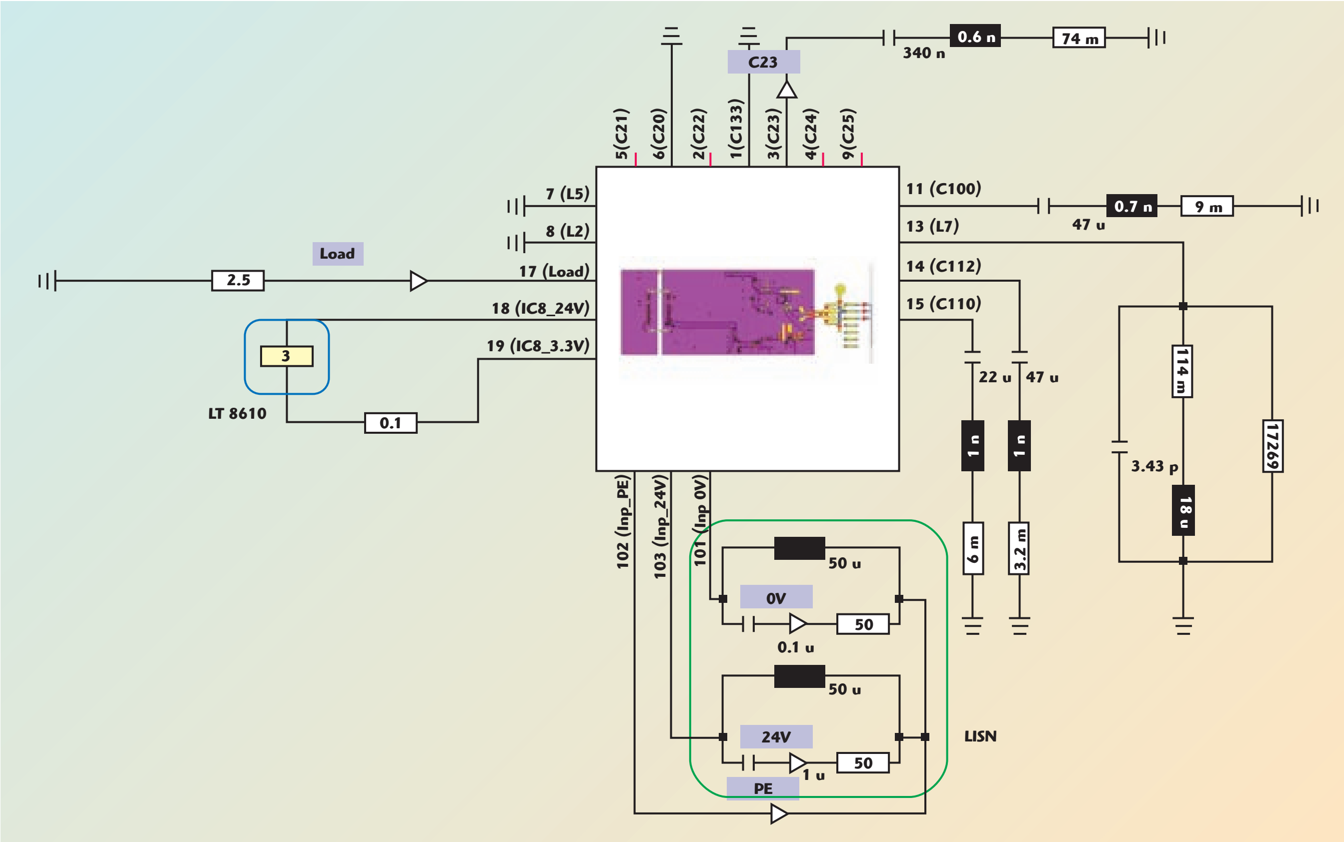

▲ *Fig. 3 Circuit for a conducted emissions test setup. The simulation block is the large square in the center.*

of components can be investigated within a few minutes.

RADIATED EMISSIONS

For radiated emissions simulations, a different approach is needed. Here, it is usually the field values within the 3D model that are of interest, rather than the voltages at the ports, so field monitors and probes should be defined in areas of interest. A time domain solver is a good choice here, given the broadband nature of the radiated emissions (in this case, 30 MHz to 1 GHz). In this example, the emissions from a trace on the 'good' PCB were analyzed using the finite integration technique (FIT) transient solver. The trace runs close to the edge of the reference plane, which means it is a likely candidate for producing radiated emissions.

Again, only one full-wave simulation needs to be carried out. After the field values have been calculated once, the 'Combine Results' task can calculate the change in the fields for arbitrary changes to the excitation and termination.

The ability to visualize fields allows engineers to identify the structures and modes which are responsible for the emissions. ***Figure 6*** shows the emissions from the trace at three different frequencies. At the lowest frequency, the field is confined to the trace and the radiation is very low. At 350 MHz, however, there is a resonance in the power-ground system of the PCB, and this mode radiates a significant amount of energy. There is a second peak in the emissions at 700 MHz corresponding to a higher order mode, with the bottom layers oscillating in antiphase.

Once the sources of radiated emissions have been identified, the layout can be modified to attempt to mitigate them. In this case, we move the trace a few millimeters away from the edge of the reference plane. As shown in ***Figure 7***, this successfully reduces the emissions in the vertical direction, but has less impact on emissions in the horizontal direction. This suggests that additional countermeasures may be needed, such as shielding.

In many EMC test chambers, the floor acts as a ground plane and can reflect signals. This can have a significant effect on the measured emissions,

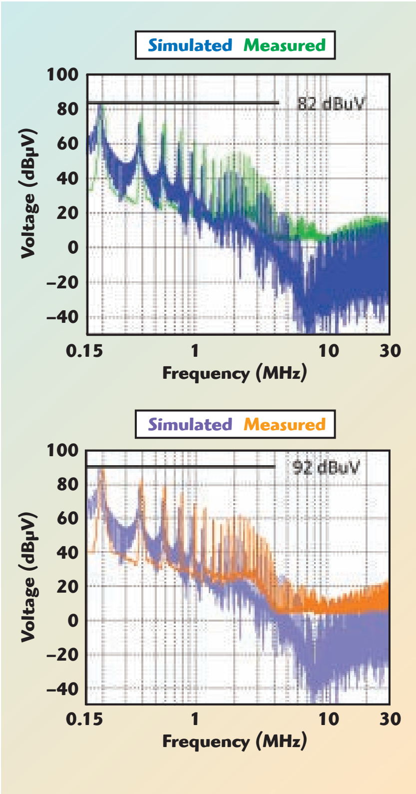

▲ *Fig. 4 Comparison of simulation and measurement for conducted emissions for a one-capacitor filter (top) and a two-capacitor filter (bottom).*

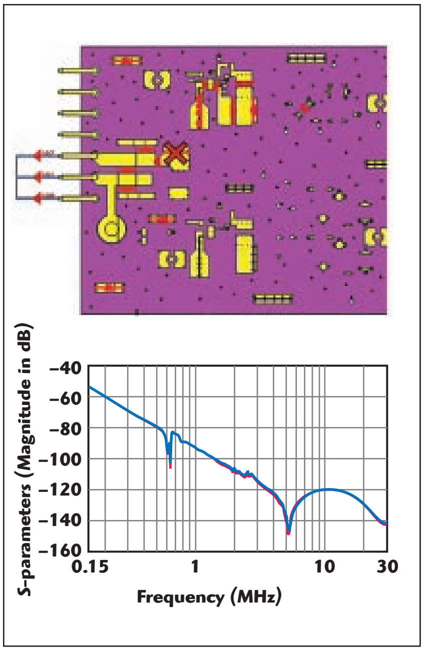

▲ *Fig. 5 The location of the capacitors under investigation (top). The conducted emissions from the 'good' PCB (bottom), with (red) and without (blue) the highlighted capacitors.*

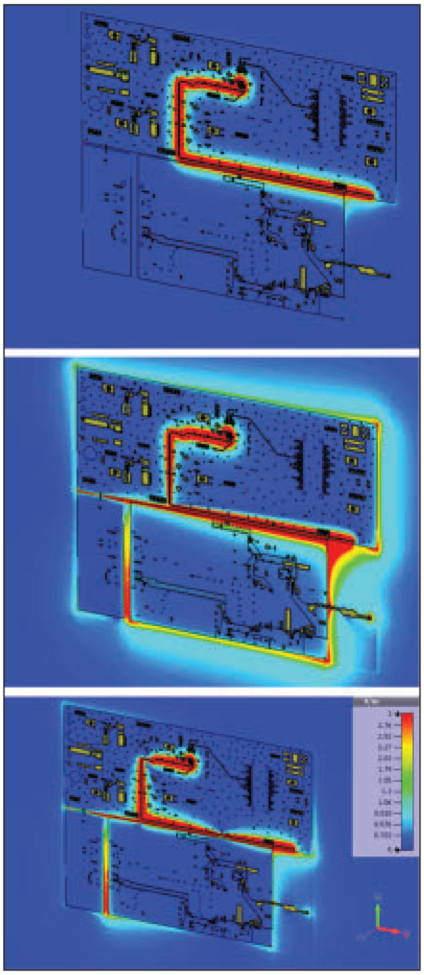

▲ *Fig. 6 Electric field around the PCB at 100 (top), 350 (center) and 700 MHz (bottom).*

as shown in ***Figure 8***, and should be taken into account by the simulation. Including the PCB, with all its fine details, directly in a full-scale model of an anechoic chamber would result in a large simulation domain with an extremely dense mesh. The simulation can be much more efficient if it is a two-step process.

The first step is to simulate the PCB in a small simulation domain with a "field source monitor" surrounding it. The field source monitor records the tangential E and H fields around the PCB and outputs them as a near-field source file. This near-field source is then imported into a second simulation of the anechoic chamber, using a much coarser mesh. According to Huygens' Principle, the second simulation will create the same radiated emissions as the full 3D model, and it only requires a few minutes. The same approach can be used for modeling other structures

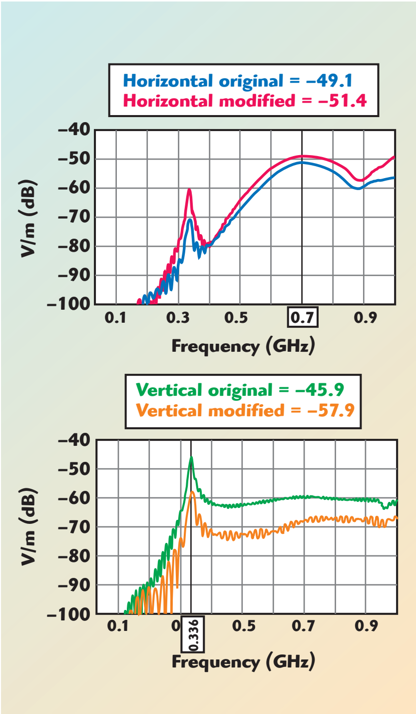

▲ *Fig. 7 Electric field values 3 m from the PCB showing the reduction in emissions in the horizontal (top) and vertical (bottom) directions when the trace is moved.*

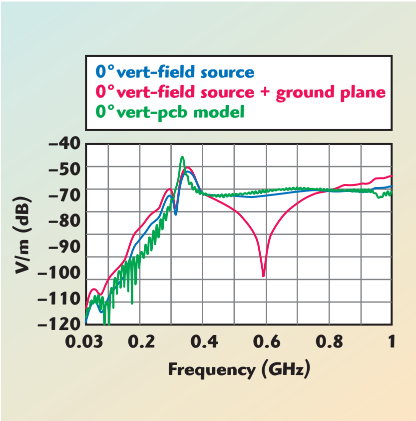

▲ *Fig. 8 The E field values at 3 m from the PCB. The red line shows the impact of the floor on the detected emissions.*

which can affect emissions, such as the housing of a PCB.

CONCLUSION

Simulation is a useful tool for the EMC analysis of complex electronics and allows engineers to identify possible EMC problems early in the design process. Simulation can identify trends which are subsequently confirmed by the measurements. Broadband simulations, in particular, are fast and straightforward and can provide useful data even in cases where the complexity of the measurements makes a direct comparison between simulation and measurement difficult. ■

References

1. Festo, www.festo.com
2. IEC/TR EN 61000, Electromagnetic Compatibility (EMC)
3. Code of Federal Regulations, Title 47, Part 15 (47 CFR 15), *Federal Communications Commission (FCC)*
4. CST STUDIO SUITE, https://www.cst.com
5. LT8610: 42 V, 2.5 A Synchronous Step-Down Regulator with 2.5 μA Quiescent Current, http://www.linear.com/product/LT8610
6. CISPR 16, Specification for radio disturbance and immunity measuring apparatus and methods

Andreas Barchanski *is the EMC market development manager at CST. He holds an M.Sc. degree in physics and a Ph.D. in numerical electromagnetics from the Technical University Darmstadt. He joined CST as an application engineer in 2007. Besides EMC, his main interest lies in the simulation of various electronic systems ranging from high speed digital to power electronics.*

Jens Krämer *is the EMC simulation and testing manager at Festo, a leading world-wide supplier of automation technology and a leader in industrial training and education programs. He holds a diploma in electronics from the University Stuttgart. His main interest lies in energy propagation on PCBs and through connectors – both intentional and unintentional.*

Pietro Luzzi *is an EMC consultant at Festo. He holds a bachelor's degree in electrical engineering. In 2012 he joined the EMC Simulation & Testing department, where he plans circuit boards and simulates a variety of interactions between EMC and the PCB.*

HPXO series

High Performance Crystal Oscillators

Model	Frequency (MHz)	DC Bias VDC [Typ.]	Minimum Output Power (dBm)	Frequency Stability Over Temp. (ppm) [Typ.]	Phase Noise (dBc/Hz) [Typ.]			
					@ 100 Hz	@ 1 kHz	@ 10 kHz	@ 100 kHz
HPXO100	100	+12 @ 120 mA	+10	<+/-0.2	-140	-162	-174	-183
KHPXO100	100	+12 @ 120 mA	+10	<+/-0.2	-140	-162	-174	-183
HPXO125	125	+12 @ 120 mA	+10	<+/-0.2	-140	-162	-174	-183
HPXO128	128	+12 @ 120 mA	+10	<+/-0.2	-138	-160	-172	-180

RoHS

FEATURES:

- *Excellent Performance*
- *Oven / Voltage Controlled*
- *Ultra Low Phase Noise*
- *High Stability*
- *Standard Compact Package*
- *Low-G Sensitivity*

Talk To Us About Your Custom Requirements.

SYNERGY®
MICROWAVE CORPORATION

Phone: (973) 881-8800 | Fax: (973) 881-8361
E-mail: sales@synergymwave.com
Web: WWW.SYNERGYMWAVE.COM
Mail: 201 McLean Boulevard, Paterson, NJ 07504

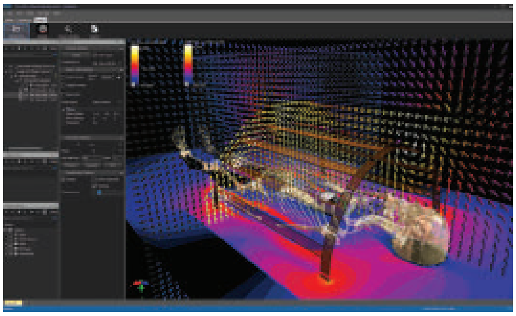

Simulation Platform Offering Multiphysics, Multiscale Simulation

Schmid & Partner Engineering AG (SPEAG)/
Zurich MedTech AG (ZMT)
Zürich, Switzerland

SEMCAD X Matterhorn has been released following a complete overhaul of the previous version of SEMCAD X. The Matterhorn version is a cutting-edge and versatile electromagnetic simulation platform, claimed to represent the first leap into multiphysics, multiscale simulation realism in complex environments. A major improvement is the SEMCAD X Matterhorn platform upgrade to Sim4Life, making it the only multiphysics platform in life sciences.

SEMCAD X MATTERHORN

Powerful solvers allow for simulations from DC to light via finite difference time domain (FDTD), conformal and finite element method (FEM) solvers. The graphical user interface (GUI) offers the capability for setting up and maintaining simulation projects with context dependence, filtering/scoping, ribbons, simultaneous multiple trees and a high level of interactivity. It is fully optimized for Microsoft Windows 8 with visual enhancements and support for external input devices (e.g., gestures, 3D mouse).

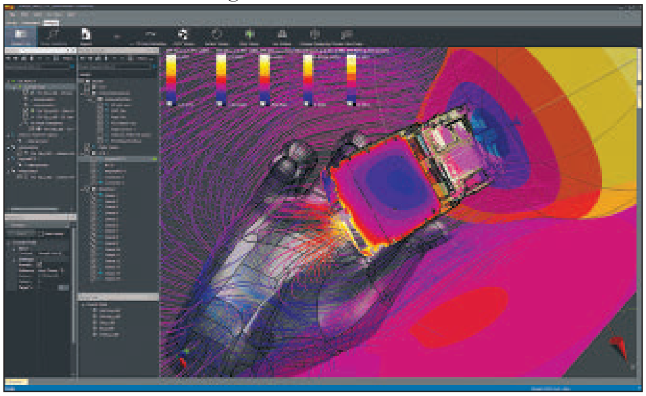

▲ *Fig. 1 An example of the visually appealing handling and rendering of complex setups by SEMCAD X Matterhorn, which shows mobile phone simulations in real usage conditions.*

SEMCAD X Matterhorn functions as a single harmonic entity, providing ease of use and clarity when used with computational instruments. It enables drag/drop between different solvers/setups/results and offers a comprehensive materials database.

A Python scripting framework is embedded into the GUI (supported by a new editor and the Enthought engine), allowing for automation, customization and the integration of user tools without requiring extensive coding experience.

With a fast graphics processing unit (GPU) based solver, all solvers (FDTD, conformal, FEM) and meshers/voxelers are now message passing interface (MPI) parallelized, offering efficient computation. A novel task manager ensures effective utilization of high performance computing (HPC) resources. The system also supports cloud computing.

SEMCAD X Matterhorn provides fast and visually appealing handling and rendering of

HIGH POWER

100 MHz to 20 GHz

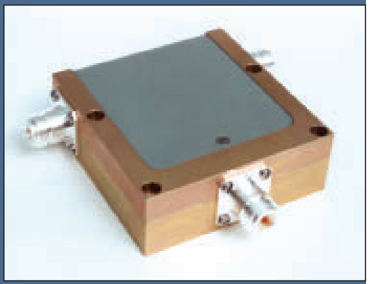

For Military/Radar Applications.

Isolators/Circulators

As one of the leading suppliers of ferrite components in the industry, UTE Microwave has pioneered innovative designs, quality craftsmanship and exceptionally high quality products. Custom designs, standards...many of them off-the-shelf, are the result of over 35 years of experience in the industry. UTE Microwave continues this tradition with new products for ever changing applications. Our broad line of HIGH POWER, low loss circulators and isolators spans the spectrum from below 100 MHz in coax/stripline units to waveguide devices at 18 GHz for both peak and average powers.

100 MHz HIGH POWER Circulator for Medical, Scientific and Industrial applications

A new HIGH POWER Circulator suitable for FM Broadcast, Scientific and Medical applications is now available. The unit provides 10 MHz bandwidth in the 85–110 MHz spectrum.

Specifications are 20 dB min. isolation, 0.3 dB max. loss and 1.25 max. VSWR. Operating power is 1 kW average and 25 kW peak. The 8-1/2" hex x 2" thick unit operates over a 15°–50° C temperature range. DIN 7/16 connectors are standard. Other units are available at higher frequencies.

HIGH POWER Drop-in Series

A broad line of low loss HIGH POWER Drop-in circulators are available from VHF to Ku band including Kilowatt average power levels at VHF thru S band. L and S band radar are a specialty. A few of these are shown here.

A) 2.7–3.1 GHZ 1 kW pk, 100 W av

B) 1.2–1.4 GHZ 3 kW pk, 300 W av

C) UHF TV Band 5 kW pk, 500 W av

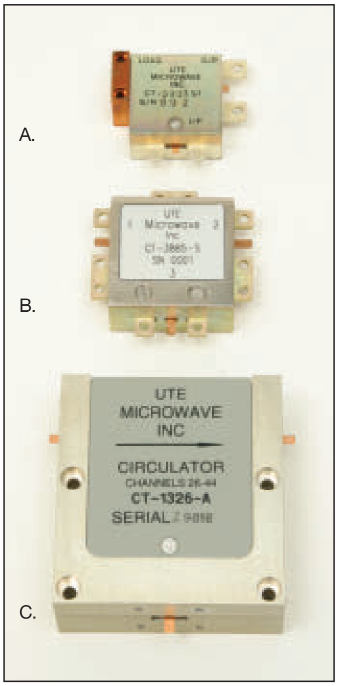

Our "POWER-LINE" serves the COMMUNICATIONS, TELECOM, MEDICAL, SCIENTIFIC, TV, PCS and INDUSTRIAL markets.

The following models are examples of our High Power units

Model No.	Power	Connectors	Freq. Range
CT-1542-D	10 Kw Pk 1 Kw Av	DIN 7/16	420–470 MHz
CT-2608-S	3 Kw Pk 300 W Av	"Drop-in"	1.2–1.4 GHz
CT-3877-S	2.5 Kw Pk 250 W Av	"Drop-in"	2.7–3.1 GHz
CT-3838-N	5 Kw Pk 500 W Av	N Conn.	2.7–3.1 GHz
CT-1645-N	250 W Satcom	N Conn.	240–320 MHz
CT-1739-D	20 Kw Pk 1 Kw Av	DIN 7/16	128 MHz Medical

FEATURES:

- Power levels to 5 KW CW, 75 KW Pk.
- Low Intermod Units
- Low Loss Options
- Extended Octave Bandwidths
- Power Monitors and DC Blocks
- Iso Filter-Monitor Assemblies

Broadband Units • Common Band Devices • High Isolation Units • Multiport Devices • Drop-In Devices • Wireless/PCN Devices • High-Power Industrial/Medical Iso Adaptors Waveguide Junctions • High-Power TV Units • VHF and UHF Devices

sales@utemicrowave.com

UTE MICROWAVE INC.
3500 Sunset Ave., Asbury Park, NJ 07712
Tel: 732-922-1009 Fax: 732-922-1848
E-mail: info@utemicrowave.com

Contact us for more information on our extensive product line and current catalog. We accept Visa, MC, Amex

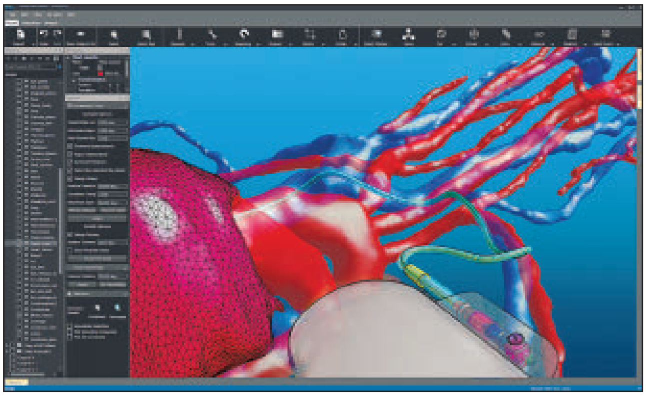

▲ *Fig. 2 Sim4Life provides powerful physics solvers and advanced tissue models for directly analyzing real world biological phenomena and complex technical devices. Here it is being used to assess the safety of pacemakers.*

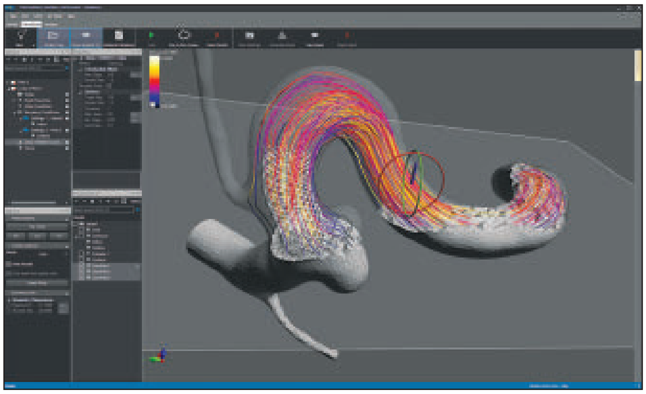

▲ *Fig. 3 Sim4Life solvers are specifically developed for highly complex problems in computational life sciences. The illustration shows vascular flow in a blood vessel with an aneurysm.*

the most complex setups, image data and results (see ***Figure 1***) using a combination of the company's own 3D OpenGL rendering engine QTech and the VTK package.

SIM4LIFE

Sim4Life is a powerful multiphysics simulation platform for constructing and simulating complex and predictive computational models of real-world phenomena in life sciences, medicine and medical technology. The platform provides industry and academia with all the in silico tools necessary for designing and optimizing medical devices and treatments, assessing safety and efficacy, enriching personalized medicine strategies and conducting biomedical research.

It combines computable high-resolution human phantoms with powerful physics solvers and advanced tissue models to directly analyze biological real world phenomena and complex technical devices in a validated biological and anatomical environment (see ***Figure 2***). The Sim4Life platform also offers leading performance with all the features expected from a multiphysics CAE/TCAD platform.

The platform natively supports the Virtual Population ViP 3.0 models that include integrated posing and morphing tools. Other publicly available animal and human anatomical models are also supported, and all tissues are linked to a continually updated physical properties database.

The powerful Sim4Life solvers are specifically developed for complex computational problems, as shown in ***Figure 3***. Most kernels are HPC accelerated, running on the latest computer clusters and are smoothly integrated into an advanced coupling framework. The current platform includes different solvers for EM, thermal and flow, with acoustics coming soon.

The integrated tissue models offer the unique ability to model and analyze physiological processes, with perfusion, tissue damage and neuronal models.

The Sim4Life Framework efficiently facilitates all steps in complex multiphysics modeling, from defining the problem, discretizing, simulating and analyzing, to visualizing the results with clarity and flexibility.

Schmid & Partner Engineering AG (SPEAG)/Zurich MedTech AG (ZMT), Zürich, Switzerland
www.speag.com
www.zurichmedtech.com

Development System for 60 GHz Radio Links

Pasternack Enterprises
Irvine, Calif.

Terry Jarnigan, CEO of Pasternack
Visit mwjournal.com/pasternackinterview
to read his in-depth interview.

ExecutiveInterview

After decades of remaining dormant for want of suitable applications, millimeter wave systems operating at 60 GHz are finally appearing. Short range, very high data rate wireless links for cellular backhaul, multi-building hops, video surveillance and airport security screening are now joining the few services already in operation. To aid in the development of systems for the unlicensed 57 to 64 GHz band, Pasternack Enterprises in collaboration with Vubiq Inc., has developed the PEM003-KIT Transmit/Receive Development System, which lets designers create transmit – receive paths at varying distances and change key parameters to verify and optimize the performance of their designs.

The PEM003-KIT consists of four primary hardware components: transmitter and receiver PC boards (see ***Figure 1***) and WR15 waveguide antenna modules that together allow a transmission – reception path to be created. The developer can experiment with the characteristics of the path using supplied Windows-based software that acts as a control panel and enables system monitoring, configuration and experimentation (see ***Figure 2***).

Two WR15 antenna modules are available. The first covers a board-to-board communication distance of 30 to 50 m, with 20 dBi of gain; the second covers distances between 200 and 300 m, with 34 dBi gain.

The control processors on the development system boards communicate with the software on the PC via a USB connection, which also powers the boards (AC adapters are provided for both boards as well). Baseband signals are routed via a high speed connector on the rear of each board. Optional expansion boards provide a transition to a set of MCX coaxial connectors for the baseband and external reference clock signals.

In a typical scenario, the transmitter's baseband source, such as an arbitrary waveform generator (AWG), creates two channels of vector (I and Q) or standard modulation formats such as BPSK or QPSK. The AWG can generate error correction coding, equalization and other characteristics, enabling a range of commonly-used modulation techniques to be used. The system provides frequency presets for 802.11ad and other standards. System designers can also create unique baseband signals using MATLAB or other tools.

The transmitter and receiver software graphical interfaces show the respective block diagrams and the control parameters that can be adjusted (see Figure 2). The screen also shows board and module voltages and temperatures as well as synthesizer lock and band tuning status. System settings are saved to non-volatile memory, and the last parameter set saved to memory configures the transmitter or receiver on start-up.

International Microwave Symposium
IEEE 17-22 May 2015 · Phoenix, Arizona, USA MTT-S

IMS

2015 PLENARY SPEAKER

SOFT ASSEMBLIES OF RADIOS, SENSORS AND CIRCUITS FOR THE SKIN

- Dr. John Rogers

Swanlund Chair, Professor of Materials Science and Engineering, Professor of Chemistry
University of Illinois, Urbana-Champaign

Professor John A. Rogers obtained BA and BS degrees in chemistry and in physics from the University of Texas, Austin, in 1989. From MIT, he received SM degrees in physics and in chemistry in 1992 and the PhD degree in physical chemistry in 1995. From 1995 to 1997, Rogers was a Junior Fellow in the Harvard University Society of Fellows. He joined Bell Laboratories as a Member of Technical Staff in the Condensed Matter Physics Research Department in 1997, and served as Director of this department from the end of 2000 to 2002.

He is currently Swanlund Chair Professor at the University of Illinois at Urbana/Champaign, with a primary appointment in the Department of Materials Science and Engineering, and joint appointments in several other departments, including Chemistry. He is Director of the Seitz Materials Research Laboratory.

Rogers' research includes fundamental and applied aspects of materials for unusual electronic and photonic devices, with an emphasis on bio-integrated and bio-inspired systems. He has published more than 450 papers and is inventor on over 80 patents, more than 50 of which are licensed or in active use. Rogers is a Fellow of the IEEE, APS, MRS and the AAAS, and he is a member of the National Academy of Engineering and the American Academy of Arts and Sciences. His research has been recognized with many awards, including a MacArthur Fellowship in 2009, the Lemelson-MIT Prize in 2011, the MRS Mid-Career Researcher Award and the Robert Henry Thurston Award (American Society of Mechanical Engineers) in 2013, and the 2013 Smithsonian Award for Ingenuity in the Physical Sciences.

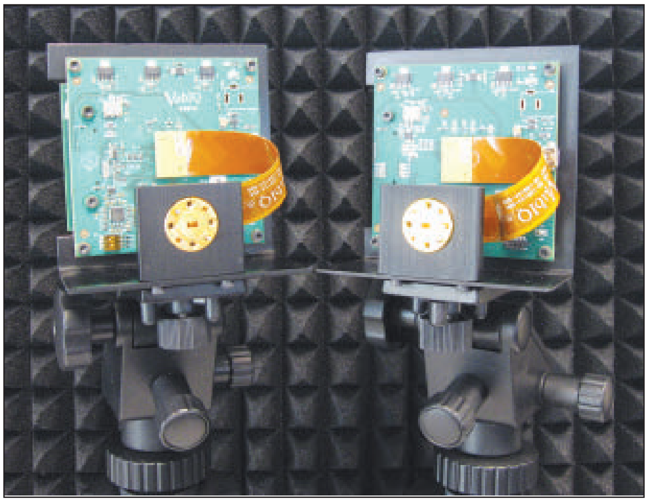

Fig. 1 The PEM003-KIT's primary components are the transmitter and receiver PC boards, shown mounted on their tripods, and WR15 waveguide antenna modules.

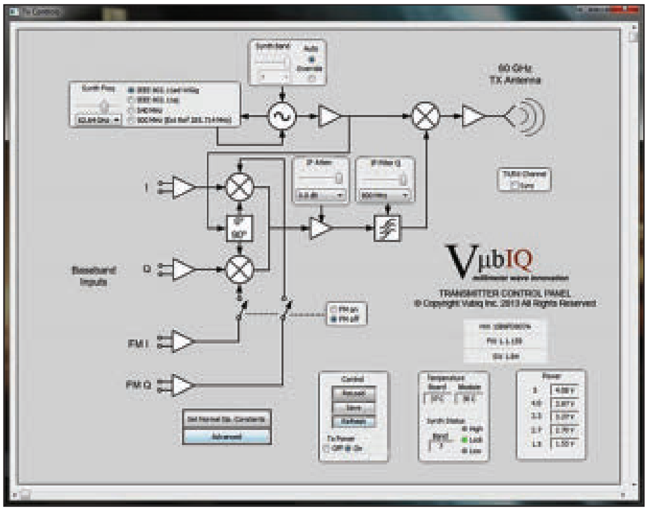

Fig. 2 The control panel for the transmit board shows the block diagram, configuration and adjustable parameters.

The frequency can be set from 57.24 to 64.80 GHz in 540 MHz steps or from 57 to 64 MHz in 500 MHz steps when using an external reference oscillator. IF attenuation can be adjusted for either board, with lower attenuation values resulting in higher gain and vice versa. IF bandwidth control provides the highest Q (narrowest bandwidth) at 800 MHz and lowest Q (widest bandwidth) at 1.2 GHz, with five settings in between.

High frequency roll-off can be set with a virtual slider or by selecting 200, 300, 500 MHz and 1.4 GHz presets. Low frequency roll-off presets are 30 and 300 kHz and 1.5 MHz. The baseband signals can be removed from the output stages for use during testing, if no signals are desired at the baseband outputs.

The system includes board/waveguide module mounting brackets, two bench top tripods, two USB cables, control and configuration software, two power supplies and eight MCX-to-SMA coax cables. The expansion board option contains two daughter cards and eight coaxial cables. The daughter cards fit into header connectors on the transmit and receive boards and are configured to allow the phase-matched MCX-to-SMA cables to connect baseband data from test equipment into the development system. Other options include a baseband modulation plug-in and 500 MHz single sideband I/Q oscillator.

The PEM003-KIT 60 GHz development system makes designing, optimizing and verifying a candidate system far easier than constructing one from "scratch." It includes all hardware and software needed to construct a complete transmit – receive path. Through its simple yet comprehensive interface, system characteristics can be modified and verified using signal or spectrum analyzers, oscilloscopes or other instruments. It is a versatile platform capable of using a broad array of baseband signals that represent the higher-order modulation employed in common data systems. It also allows custom waveforms to be defined with software tools such as MATLAB.

VENDORVIEW

Pasternack Enterprises
Irvine, Calif.
www.pasternack.com

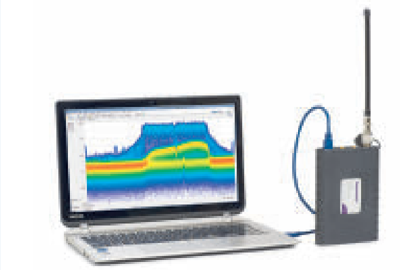

Affordable, Full-Featured Highly Portable Spectrum Analyzer

The Tektronix RSA306 portable spectrum analyzer sets a new price – performance threshold. Priced at $3,490, the handheld unit covers 9 kHz to 6.2 GHz with 40 MHz of real time bandwidth, measures signals from -160 to +20 dBm, weighs just 1.2 lbs and is powered by a USB 3.0 connection to a laptop or desktop PC that performs the signal analysis.

The PC hosts Tektronix SignalVu-PC software that provides a complete suite of spectrum analyzer features, including 17 different measurements. The basic SignalVu-PC package is included at no additional charge; add-on options include mapping and various signal analyzers: vector, WLAN, P25, pulse and audio. An open API allows custom development of Windows-based interfaces using MATLAB or Python, to manipulate the raw data coming from the instrument. To ensure 100 percent probability of intercepting signals, the PC must have a fourth generation Intel i7 processor with at least 8 GB of RAM and running 64 bit Windows 7 or 8.

The size of the RSA306 is 5" × 7.5" × 1.2". A Type N connector for the RF input is located at one end, adjacent to inputs for a 10 MHz reference signal and external trigger as well as the USB 3.0 connection. The unit is ruggedized and meets Mil-Std 28800 Class 2 specifications.

Tektronix states the RSA306 offers comparable to superior sensitivity, accuracy and dynamic range at a fraction of the cost of a conventional spectrum analyzer. The company designed the RSA306 for budget-conscious and portable applications, including interference hunting, mobile radio network installation and maintenance, university lab classes and research and development.

Tektronix Inc.
Beaverton, Ore.
www.tek.com/spectrum-analyzer/rsa306.

SP6T Coaxial Switch

RF and wireless devices are equipped with many signal paths between input and output ports that undergo rigorous and complex testing. Therefore the use of coaxial switches is essential, allowing the user to easily switch between I/O ports and avoid the cumbersome task of having to disconnect and reconnect RF cables. The quality and reliability of an RF switch are critical to ensure repeatability of port-to-port testing and multiple devices being tested.

Dow-Key® Microwave has designed the Reliant Switch™ for the ATE market to be used in testing devices such as Systems on Chip (SoC) or 4G/LTE wireless signals during characterization, validation and production testing. It is a one-by-six bi-directional coaxial switch with a wide operating frequency range from DC to 26.5 GHz and a guaranteed insertion loss repeatability of 0.03 dB. Isolation ranges from 65 dB at the higher frequencies to 100 dB at the lower. Its third order intermodulation is typically -120 dBc (2 carriers at 20 W). Operating temperature is -25° to +75°C with power handling of 30 W at 4 GHz and 25°C.

The switch can operate in both break-before-make or make-before-break applications, has a fast switching speed of 15 ms and an extended life cycle where each position can switch a minimum of 5 million cycles. The Reliant Switch™ offers a variety of control options including +24 VDC coil voltage, TTL discrete logic and CAN bus.

VENDORVIEW

Dow-Key Microwave
Ventura, Calif.
(800) 266-3695
askDK@dowkey.com

Discover the Next Generation

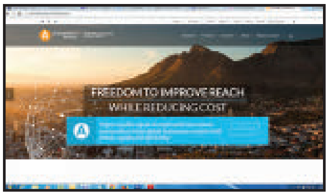

Advantech Wireless is ushering in a new generation of innovative solutions with the launch of their rebranded website, www.advantechwireless.com. Advantech Wireless aims to lead the global charge in making secure, wireless broadband total solutions available to those who need it most. Now more than ever, innovative satellite solutions can enable faster Internet, smarter applications for military and homeland security, and wider broadcast audiences in remote locations. Browse through the company's solutions to learn how they can help you make satellite communications smarter, more efficient and get the results you deserve.

Advantech Wireless
www.advantechwireless.com

Website Optimization

VENDORVIEW

American Microwave Corp. (AMC) has completely revamped their marketing materials with a new brochure and website. AMC has optimized their site by making it more applications oriented, adding more technical information and making it easier to navigate. AMC is an industry leader for pin diode based switches (SPST to SP65T), attenuators (digital, analog or current-controlled), detector log video amplifiers (50 and 70 dB dynamic range) and integrated microwave assemblies such as switch matrices, direction finding networks and other complex assemblies.

American Microwave Corp.
www.americanmic.com

Online Design Tool

API Technologies Corp. launched a new product configuration tool that helps engineers modify the company's standard RF/microwave products to meet their unique design parameters. The web accessible and mobile-friendly tool is available http://micro.apitech.com/configure. Current customization options include frequency range, noise figure, gain, output intercept points, power supply voltage and preferred package style. API's new design tool enables users to create a performance-based model of their chosen design in real-time. Users can print out a configuration summary, share their design via e-mail and social media and make modifications to performance criteria at any time.

API Technologies Corp.
www.apitech.com

Connect With AR

VENDORVIEW

Did you know AR RF/Microwave Instrumentation is active on Facebook, Twitter, LinkedIn and YouTube? Follow the company on these social media sites to find out important company news and which industry event they will be exhibiting at next. You will also find updated product news, links to industry resources and links to AR's press coverage. Visit AR's homepage at www.arww-rfmicro.com/html/00000.asp to link to these pages and more.

AR RF/Microwave Instrumentation
www.arworld.us

RF Inductor Finder

Coilcraft's new RF Inductor Finder web tool allows users to search and compare inductors based on their exact operating frequency, rather than just datasheet test frequencies. Users can optimize search results for Q factor, footprint, SRF, impedance, price or inductance. Users can also search for a range of inductances, specify a minimum Q at their operating frequency and select a particular body size. The new tool provides a better user experience with the ability to move and delete columns, view only selected products, see actual size photos, export results to excel or PDF and request free evaluation samples.

Coilcraft
www.coilcraft.com

Mission Critical Needs

VENDORVIEW

Crane Aerospace & Electronics Microwave Solutions has added more information to their website. Items include the new Ku-Band Iso Divider product line datasheets, an updated product finder and part number index, a new Microwave Solution overview and a new space products tab that highlights products for space applications. Crane's Microwave Solutions offers a wide range of product solutions from component level devices to complex, advanced integrated microwave assemblies.

Crane Aerospace & Electronics
www.craneae.com/mw

Radio Wireless Week

25 - 28 JANUARY 2015, SAN DIEGO, CA, USA

IEEE MTT-S APS EMB

http://www.radiowirelessweek.org/

Join Us for a Week Long Wireless Event
"Next Wireless Innovation"
At the Omni San Diego Hotel, California

Join us for the 10th annual IEEE Radio Wireless Week (RWW) in San Diego, California from 25-28 January 2015. This exciting week includes the IEEE Radio and Wireless Symposium (RWS) and the IEEE Topical Meeting on Silicon Monolithic Integrated Circuits in RF Systems (SiRF). Join us to learn about the latest in the wireless technologies and networks with colleagues while enjoying the beautiful southern California.

RWW: ***IEEE Radio Wireless Week***
RWS: ***IEEE Radio and Wireless Symposium***
PAWR: ***IEEE Topical Meeting on Power Amplifiers for Wireless and Radio Applications***
SiRF: ***IEEE Topical Meeting on Silicon Monolithic Integrated Circuits on RF Systems***
BioWireleSS: ***IEEE Topical Conference on Biomedical Wireless Technologies, Networks, and Sensing Systems***
WiSNet: ***IEEE Topical Meeting on Wireless Sensors and Sensor Networks***

Keynote Speaker - Chris Van-Hoof

Wearable Wireless Sensor Technologies for Truly Personalized Medicine and Wellness

Chris Van Hoof is Director of Wearable Healthcare at imec in Leuven, Belgium and Eindhoven, the Netherlands and imec Fellow. In the Wearable Healthcare program, imec and its industrial partners from across the value chain create and validate solutions at technology, component and application level. Chris Van Hoof has a track record of 20 years of initiating, executing and leading national and international contract R&D at imec. His work resulted in 3 startups (2 in the healthcare domain) and he delivered space qualified flight hardware to two cornerstone European Space Agency missions. After a PhD in Electrical Engineering (University of Leuven, 1992), Chris Van Hoof has held positions at imec at manager and director level in diverse technical fields (sensors and imagers, MEMS and autonomous microsystems, wireless sensors, body-area networks). He has published over 500 papers in journals and conference proceedings and given over 50 invited talks. Chris Van Hoof is also full professor at the University of Leuven (KULeuven).

Exhibits and Sponsorship Opportunity

This year's Exhibit will offer tabletops and full 10×10 exhibits. The exhibition will operate on two days. WicroApps talks and Demo Sessions will also be held in the Exhibition area. Rental fees for 2015 are $1500 per 10×10 booth space. Sponsors at the $3000 level and above will be offered one free 10×10 booth space. In the past few years the exhibition was SOLD OUT so please book early in order to insure premium exhibit space. For more about exhibits and sponsorship, visit

http://www.radiowirelessweek.org/exhibits/

HTTP://WWW.RADIOWIRELESSWEEK.ORG/

WebUpdate

RF and Microwave eCommerce

Fairview Microwave Inc. has launched its all new RF/microwave eCommerce website featuring powerful specification-based navigation, enhanced site search capabilities, live chat, detailed product pages and a newly designed user interface. Users can steer through more than 30 RF product categories with the site's unique specification-rich parametric navigation. Customers can search for their desired components via text-based site search, left-hand parametric search or the more traditional "drill-down" navigation. All of Fairview Microwave's more than 1,000,000 RF parts are quickly and easily located in just a few clicks.

Fairview Microwave Inc.
www.fairviewmicrowave.com

RF Calculators and Conversion Tools

VENDORVIEW

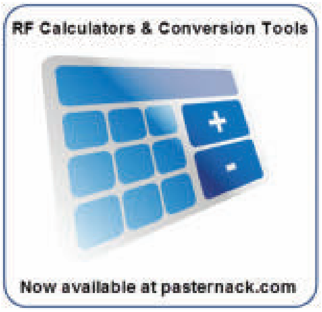

A total of 27 RF calculators developed by Pasternack provides users and buyers of RF components a valuable and easy-to-use resource. The new RF calculators and converters include link budget, coax impedance, RF power conversion (such as dBm to W), attenuation, frequency, wavelength, VSWR/return loss, torque, noise, Free Space Path Loss (FSPL), unit conversion, microstrip and more. Each calculator page includes a diagram or illustration of what the calculator is used for as well as the relevant mathematical formula. The calculator will also produce a "Find Related Products" button that directs users to Pasternack products that meet specific criteria.

Pasternack Enterprises
www.pasternack.com

Enhanced Search Functionality

Z-Communications Inc. announced the launch of their new mobile responsive website. The new www.zcomm.com features an updated look and feel with enhanced search functionality that allows users to view by product type or series name, sort results by any specification, display number of parts per page, filter results to search for specific values and download product data in Excel spreadsheet format. Users can also request custom VCOs, custom programmable PLLs and custom fixed frequency PLLs from their computer, smartphone or tablet devices.

Z-Communications Inc.
www.zcomm.com

Components

100 W Fixed Attenuator

Model series 351-338-XXX is a 100 W RF power (average) rated fixed attenuator. This 50 ohm device has an operating frequency range of DC to 3 GHz and is available in 3, 6 and 10 dB (attenuation accuracy ±0.75 dB), 20 and 30 dB (attenuation accuracy ±1 dB) as well as 40 dB (attenuation accuracy ±1.5 dB). Maximum VSWR is 1.20:1 (DC to 1 GHz) and 1.40:1 (1 to 3 GHz). The RF connectors are SMA female.

Broadwave Technologies
www.broadwavetechnologies.com

Filter Sample Kits

CTS Corp. announced the release of two new sample kits of electromagnetic interference (EMI) and radio frequency interference (RFI) filters specifically suited for microwave applications. CTS compiled two "C" type kits, 4300-900 and 4306-900, that are ideal for use in applications where board space and high performance are critical. The 4300-900 kit is an assortment of 10 parts from CTS' solder mount EMI/RFI 4300 series. The 4306-900 kit consists of 10 parts from CTS' press-in filter 4306 series.

CTS Corp.
www.ctscorp.com

SPDT Terminated Coaxial Switch

The D2 Series SPDT coaxial switches come in a variety of connectors, such as BNC, TNC, N and SMA. Models operate from DC to 12.4 GHz. Actuator options come in latching and failsafe modes, as well as units with TTL circuitry and integrated indicator circuits. Ducommun's design engineers can create custom versions for your specific applications.

Ducommun Inc.
www.ducommun.com

RF Rotary Joints

Fairview Microwave Inc. announced the company's new line of single-channel/single-axis and single-channel/multi-axis RF rotary joints. These joints are needed wherever RF signals are transmitted between stationary and moving parts of a system, including commercial and military radar, land-mobile-radio communications and anti-missile defense applications. Fairview's joints boast a compact design, excellent VSWR, low insertion loss, and minimal variation of RF performance during rotation. The operating frequency ranges from 0 to 18 GHz depending on the model.

Fairview Microwave
www.fairviewmicrowave.com

SP3T Absorptive PIN Diode Switch

Model S3L-69-2 is a SP3T absorptive PIN diode switch that operates from 2 to 18 GHz with

an isolation of 30 dB. This unit features an insertion loss of 2.45 dB with 2.0:1 VSWR in 50 ohms with a handling power of +20 dBm CW, 1 W max. The supply voltage accommodates up to ± 5 VDC @ +100/-60 mA. It offers 3 bits of TTL compatible logic and the switching speed is less than 100 nsec max. The package size is 2.00" × 1.25" × 0.50".

G.T. Microwave Inc.
www.gtmicrowave.com

2-Way Wilkinson Power Divider/Combiner

Marki Microwave's Wilkinson power divider/combiner splits one signal or combines two signals with a nominal loss of 3 dB and isolation between ports. Features include a unique CAD optimized design for industry leading bandwidth, isolation and balance. Surface mount options are available for some models.

Marki Microwave Inc.
www.markimicrowave.com

Compact 100 W Low PIM Terminations

VENDORVIEW

MECA's new compact 100 W low PIM terminations feature industry leading PIM performance of -165 dBc typical while handling full rated power to +85°C. All of the terminations cover 698 to 2700 MHz in a compact package measuring 8.5" × 3" and with 7/16 DIN, Type N or 4.1/9.5 (mini-DIN) connectors. VSWR is 1.10:1 typical, 1.20:1 max. Made in the U.S. with 36-month warranty.

MECA Electronics Inc.
www.e-MECA.com

Circulator

McManus Microwave introduced the Model 287 circulator. Operating in a frequency range from 225 to 400 MHz and offering power of 100 W (internal load is rated at 50 W CW), the M287 has a max. VSWR of 1.40:1. Min. isolation is 16 dB and max. insertion loss is 0.8 dB. Operating temperature range is -20° to +70°C. The M287 is only 1.5" × 1.5" × 0.63". McManus has produced custom ferrite components for industry leaders since 1990.

McManus Microwave
www.mcmanusmicrowave.com

High Speed Threshold Detector

VENDORVIEW

PMI model no. TD-1G12G-RL-CD-SFF is a high speed threshold detector designed to operate over 1 to 12 GHz. It has an adjustable

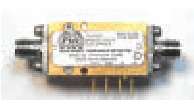

threshold level of -30 to -10 dBm and a VSWR of 3.0:1 max. This unit is a very small size with field removable SMA connectors on the input and output and has active low output.

Planar Monolithics Industries Inc.
www.pmi-rf.com

Terminated SPDT Switch

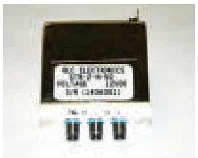

RLC Electronics' DC to 50 GHz terminated single pole, two position coaxial switches have proven reliability and excellent electrical performance. This series features extremely low insertion loss and VSWR over the entire range (1.1 dB max and 2:1 max, respectively, at 50 GHz) while maintaining high isolation (50 dB min). The switch has internal 2 W terminations that can be replaced by connectors for special applications.

RLC Electronics Inc.
www.rlcelectronics.com

Coax Switch Series

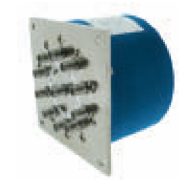

The CCT-38 is a broadband multi-throw, electromechanical coaxial switch designed to switch a microwave signal from a common input to any of 10 outputs. The CCT-38 normally open switch covers DC to 12 GHz and is available with 12, 15, 24 and 28 coil voltages. Internal 50 ohm terminations make the CCT-38 switches suitable for applications where unused ports must be terminated to eliminate noise.

Teledyne Coax Switches
www.teledynecoax.com

Full Band WR28 Waveguide Circulator

Model F3838-3325 is a full band WR28 waveguide circulator covering 26.5 to 40 GHz

with 0.6 dB maximum insertion loss, 16 dB minimum reverse isolations and 1.4:1 VSWR at input and output. It can handle 5 W of CW power. The RF ports are designed to match to UG-599/U waveguide flanges.

Wenteq Microwave
www.wenteq.com

50 dB Dual Directional Coupler

Werlatone Inc. introduced its full line of 700 to 4200 MHz directional couplers ranging from 100 to 2,000 W CW, and coupling values of 20 to 50 dB. Werlatone offers solutions ideal for military or commercial high power amplifiers, multi-

NOW USB & ETHERNET

RF SWITCH MATRIX

Efficiency for your test setup. Economy for your budget.

New Feature!
Switch Cycle Counting

DC to 18 GHz *from $385 ea.*

We're adding more models and more functionality to our line of RF switch matrices. All models now feature switch cycle counting with automatic calibration interval alerts based on actual usage, an industry first! This function improves test reliability and saves you money. Our new RC-series models feature both USB and Ethernet control, so you can run your test setup from anywhere in the world! Rugged aluminum cases on all models house our patented mechanical switches with extra-long life of 10 years/100 million cycles of guaranteed performance!*

Our easy-to-install, easy-to-use GUI will have you up and running in minutes for step-by-step control, full automation, or remote operation. They're fully compatible with most third-party lab software,† adding capabilities and efficiency to existing setups with ease! Visit minicircuits.com today for technical specifications, performance data, quantity pricing, and real time availability – or call us to discuss your custom programming needs – and think how much time and money you can save!

USB Control Switch Matrices

Model	# Switches (SPDT)	IL (dB)	VSWR (:1)	Isolation (dB)	RF P_{MAX} (W)	Price $ (Qty. 1-9)
NEW USB-1SP4T-A18	1 (SP4T)	0.25	1.2	85	2	795.00
USB-1SPDT-A18	1	0.25	1.2	85	10	385.00
USB-2SPDT-A18	2	0.25	1.2	85	10	685.00
USB-3SPDT-A18	3	0.25	1.2	85	10	980.00
USB-4SPDT-A18	4	0.25	1.2	85	10	1180.00
USB-8SPDT-A18	8	0.25	1.2	85	10	2495.00

NEW USB and Ethernet Control Switch Matrices

Model	# Switches (SPDT)	IL (dB)	VSWR (:1)	Isolation (dB)	RF P_{MAX} (W)	Price $ (Qty. 1-9)
RC-1SP4T-A18	1 (SP4T)	0.25	1.2	85	2	895.00
NEW RC-2SP4T-A18	2 (SP4T)	0.25	1.2	85	2	2195.00
RC-1SPDT-A18	1	0.25	1.2	85	10	485.00
RC-2SPDT-A18	2	0.25	1.2	85	10	785.00
RC-3SPDT-A18	3	0.25	1.2	85	10	1080.00
RC-4SPDT-A18	4	0.25	1.2	85	10	1280.00
RC-8SPDT-A18	8	0.25	1.2	85	10	2595.00

*The mechanical switches within each model are offered with an optional 10 year extended warranty. Agreement required. See data sheets on our website for terms and conditions. Switches protected by US patents 5,272,458; 6,650,210; 6,414,577; 7,633,361; 7,843,289; and additional patents pending.

†See data sheet for a full list of compatible software.

Mini-Circuits®

www.minicircuits.com P.O. Box 350166, Brooklyn, NY 11235-0003 (718) 934-4500 sales@minicircuits.com

521 rev F

octave platforms and test and measurement applications.
Werlatone Inc.
www.werlatone.com

Cables and Connectors

Phase Adjustable Connectors

Coaxial Components Corp. announced its next generation of the phase adjustable connector for RG405, the 3993-3. There has never been a faster or easier way to phase match a set of cables. Coaxicom has enhanced the direct solder versions of the phase adjustable connector for superior electrical performance. Just trim the cable, plug it in and solder to the connector body. Coaxicom specializes in the manufacture of RF connectors, attenuators, terminations, adapters, torque wrenches, phase adjusters and cable assemblies.
Coaxial Components Corp.
www.coaxicom.com

Coaxial Cable

VENDORVIEW

141 SMNM+ series Hand-Flex coaxial cables are ideal for integrating coaxial components and subsystems in tight spaces and dense system configurations. SMA to N-Type connection avoids the need for an adapter between components with SMA-F and N-F connection ports, reducing system cost and improving reliability. Sturdy, hand-formable cable construction maintains shape after bending with bend-radius as small as 8 mm. 141 SMNM+ coaxial cables have the advantages of wide frequency range and excellent return loss and insertion loss. Available in 12", 18" and 24".

Mini-Circuits
www.minicircuits.com

High Performance Test Cables

Response Microwave Inc., a global specialist in providing RF/microwave customer solutions for the defense and telecommunications market, announced the availability of its new TESTCABLZ family of robust test cables for use in production test applications. The new family offers BLU402 (0.163"od) or BLU405 (0.104"od) high performance flexible cable with choice of male or female SMA, N, and N18 connectors in straight configurations with a robust clamp attachment method.
Response Microwave Inc.
www.responsemicrowave.com

High Frequency 1.0 mm (W) Connector Line

Southwest Microwave Inc. introduced a new line of 1.0 mm (W) DC to 110 GHz connectors. Products in this high-frequency connector series include field-replaceable two and four-hole flange mount and thread-in connectors, direct solder cable connectors, and clamp-on end launch connectors, including low profile and reduced-size low-profile versions. Made in the U.S. and built to Southwest Microwave's rigorous performance and quality standards, 1.0 mm (W) connectors are rugged and durable.
Southwest Microwave Inc.
www.southwestmicrowave.com

Floating SMPM Coaxial Contacts

SV Microwave's new lightweight VITA 67 product line drops 70% of the mass from VITA 67 connections. SV's newest line, made from aluminum, utilizes the high density, high performance benefits of VITA 67, but at a fraction of the weight. SV's floating SMPM coaxial contacts ensure excellent RF performance in any mating condition. These are designed for side-by-side implementation with VITA 46 hardware and can be cabled to 0.086 and smaller coaxial cable.
SV Microwave
www.svmicrowave.com

Amplifiers

DLVA

VENDORVIEW

American Microwave Corp. announced its model CVR-120-50-CW DLVA, a form, fit, function replacement for the 2277635-4 Teledyne detector logarithmic video amplifier. It covers 1 to 20 GHz with 45 dB logging range, CW immunity, 40 nS rise time, -42 dBm TSS and 6 uSec, maximum recovery time. The DVLA is utilized in the ALQ-119 jamming system and is applicable (with minor modifications) to the ALQ-184 jamming system and other related platforms.
American Microwave Corp.
www.americanmic.com

Reverse Amplifier

ANADIGICS Inc. introduced a new reverse path amplifier optimized for data over cable service interface specification (DOCSIS) system standard version 3.1. The ARA2032 provides industry-leading linearity, output power and noise performance over a wide 5 to 300 MHz frequency range to enable advanced CATV services, including higher upstream data speeds. ANADIGICS continues to aggressively expand its world-class CATV infrastructure products to support anticipated network buildouts and upgrades, including the adoption of DOCSIS 3.1.
ANADIGICS Inc.
www.anadigics.com

TWT Amplifier

The Model 200 CW TWT amplifier has been designed to operate 200/250 W traveling wave tubes up to 18 GHz. All power supplies are regulated, phase shifted resonant mode DC to DC converter designs operating at 50 kHz.

The TWT power supplies feature full load efficiency greater than 90%, and fast regulation loop response which provides minimal output variations at any PRF including non-periodic and burst. Power supply and power line related spurious signals are below -50 dBc.
Applied Systems Engineering Inc.
www.applsys.com

Power Amplifier

VENDORVIEW

Custom MMIC announced the addition of the CMD217, a new 28 to 32 GHz GaN power amplifier in die form, to its growing product line. The CMD217 features greater than 20 dB of gain across its operating frequency range, with a corresponding output 1 dB compression point of +36.7 dBm and saturated output power of +39.3 dBm (8.5 W). Power added efficiency for the CMD217 is 28 to 35% across the band.
Custom MMIC
www.custommmic.com

Microwave Power Module

The dB-3758 is an integrated pulsed microwave power module (MPM) operating in X-Band providing 1000 W peak output power at a duty cycle of 6 percent. The RF signal path consists of a solid PIN diode modulator, solid state driver amplifier and a mini-TWT. The high-voltage power supply (HVPS) section uses a modular architecture and low-noise power supply topology with high efficiency solid-state power conversion circuits. A highly stable, solid-state modulator is used for TWT grid modulation.
dB Control
www.dBControl.com

Driver Amplifier

The MMG38151B is a broadband general purpose class A driver amplifier designed to meet the requirements of all 3G and 4G UMTS BTS amplifiers and general wireless applications operating from DC to 6000 MHz. At 3800 MHz, its P1dB is 13 dBm with an OIP3 of 25 dBm. The MMG38151B is biased with a single 5 V supply and a supply current of 47 mA. Its RF input and output are internally matched.

Freescale Semiconductor
www.freescale.com

Differential Amplifier

VENDORVIEW

The LTC6430-20, a 20 MHz to 2 GHz differential input and output 20 dB gain amplifier from Linear Technology, offers outstanding linearity of +51 dBm OIP3 and 2.9 dB noise figure at 240 MHz. It has a best-in-class output 1 dB compression point of +23.9 dBm. The LTC6430-20 is offered in an A-grade version, which is 100% tested and guaranteed to a minimum OIP3 of +44.8 dBm, +48.3 dBm typical at 380 MHz. Gain is also guaranteed to be a minimum of

IDGA
Institute for Defense and Government Advancement **Presents:**

MILITARY RADAR SUMMIT 2015

February 23rd-25th, 2015 | Washington D.C

Meeting Radar Requirements for Today's Military Operations

HIGH LEVEL SPEAKERS INCLUDE:

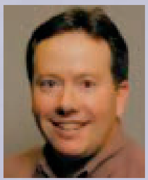

Kurt Sorensen
Manager SAR Sensor Technologies
Sandia National Laboratories

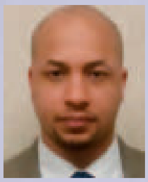

Courtney Liggins
ISR Lead
Customs and Border Protection/
Office of Geospatial Intelligence

Stuart Timerman
Director
Army Spectrum
Management Office

Peter Moo
Group Leader, Multifunction Radar
DRDC Defence Research and
Development Canada

Pertinent and Focused Discussion will Include:

- Modular upgrades to military radar infrastructure
- Combating foreign capabilities in electronic warfare and detection
- Developments in Over the Horizon Radar and MIMO
- The latest advancements in electronic warfare capabilities

REGISTER EARLY TO SAVE UP TO $700

www.MilitaryRadarSummit.com | 1-800-882-8684

NewProducts

19.6 dB and maximum of 22.1 dB.
Linear Technology Corp.
www.linear.com

26 to 40 Low Noise Amplifier

MITEQ's new Model JS5-26004000-30-15P is a state-of-the-art 26 to 40 GHz low noise amplifier with a 3 dB maximum noise figure. This model has a gain of 32 dB minimum in a small hermetically sealed package with field replaceable K-connectors. Available as RoHS compliant. MIL-883 screening is also available.

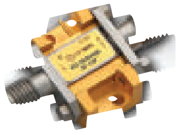

MITEQ Inc.
www.miteq.com

High Power Amplifier

VENDORVIEW

PE15A5008 is a broadband 6 W GaAs PHEMT MMIC-based coaxial power amplifier module designed to be used in a wide range of commercial and defense applications in the 3.5 to 7 GHz frequency range. The amplifier offers 19 dB small signal gain with the gain flatness of ±2 dB. This performance is achieved through the use of advanced GaAs PHEMT MMIC circuitry. The amplifier operates between -55° and 85°C, and is characterized by its light weight (45 g) and small size (1.5" × 1.2" × 0.56").

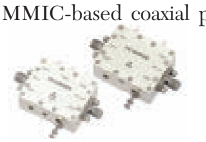

Pasternack Enterprises Inc.
www.pasternack.com

E-Band Full Band Low Noise Amplifier

VENDORVIEW

Model SBL-6039033050-1212-S1 is a full band, 60 to 90 GHz, low noise amplifier. The amplifier exhibits a typical small-signal gain of 30 dB and 5 dB noise figure throughout the entire E-Band, making it ideal for many applications ranging from test equipment to fully integrated communication systems. The amplifier requires single positive DC bias between +5 and +12 VDC at 30 mA. The standard model's input and output ports are in right angle configuration.

SAGE Millimeter Inc.
www.sagemillimeter.com

Systems

Digital Receiver

The K701 digital receiver supports one or two plug-in FMC modules, each providing up to eight independent channels of DDC and one spectrum analyzer embedded in a Xilinx Kintex-7 FPGA. It allows users to monitor the wide-band or narrow-band spectrum and record the data directly from the ADCs or down-convert the channels modulated on the IF band. The receiver can do contiguous recording at 1600 MByte until running out of disk space.

Innovative Integration
www.innovative-dsp.com

Sources

Ultra Low Noise Phase Locked Oscillator

The DCO2000-5 is a fixed frequency VCO that meets market demand for a cost effective, low noise frequency source. Center frequency is 2000 MHz and phase noise is -110 dBc/Hz at 10 kHz offset and -130 dBc/Hz at 100 kHz offset. Tuning sensitivity is 15 to 20 MHz/V, as a building block for phase locking to external stable references. Bias requirements are 4.5 V at 35 milliamps, maximum. Package size is a small 0.3" square surface mount configuration with a 0.080" maximum z-height.

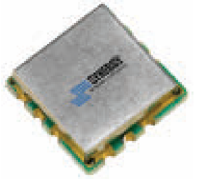

Synergy Microwave Corp.
www.synergymwave.com

Voltage Controlled Oscillator

Z-Communications Inc. announced a new RoHS compliant VCO model V590ME09-LF. It operates over the frequency range of 850 to 1050 MHz with 0.5 to 5 V tuning range. This VCO features a spectrally clean signal of -100 dBc/Hz @ 10 kHz offset while operating from a 5 VDC supply and drawing only 15 mA of current. The low cost V590ME09-LF is designed to deliver +5.5 dBm of output power into a 50 Ω load and covers the frequency band with an average tuning gain of 63 MHz/V.

Z-Communications Inc.
www.zcomm.com

Antennas

Horn Antenna

VENDORVIEW

The model ATH200M1G-1 high-gain horn antenna exhibits increasing gain with increasing frequency (up to 18 dB at 1000 MHz). With this useful performance characteristic, the antenna helps compensate for losses that occur elsewhere in an RF test system that generally increase with frequency. The model ATH200M1G-1 is well suited for either shielded room or free space testing. Optimum performance is achieved when used with model 3000W1000 and 4000W1000 broadband amplifiers for RF susceptibility testing.

AR RF/Microwave Instrumentation
www.arworld.us

GPS Helix Antennas

VENDORVIEW

Richardson RFPD Inc. announced the availability and full design support capabilities for two new GPS helix antennas from Maxtena Inc. Both of the new devices are built on Maxtena's proprietary Helicore® technology, which provides exceptional pattern control, polarization purity and high efficiency in a compact form factor. The M1575HCT-22P-SMA and M1575HCT-22P-MR are rugged high-performance passive antennas designed for the GPS L1 band and feature integrated SMA connectors. The ultra-light designs are rated IP-67/68, mounted and unmounted for added protection.

Richardson RFPD
www.richardsonrfpd.com

Multi-Octave 1 to 18 GHz Spiral Antenna

The QSP-RC-1-18-S-SG-R is an ultra small multi-octave wideband 1 to 18 GHz left and right hand circularly polarized spiral antenna suitable for applications where space and gain requirements are at a premium. At a diameter of 78 mm, with an SMA connector, the antenna provides excellent return loss, gain and axial ratio over the full 1 to 18 GHz operational band. Applications include ELINT and COMINT systems, radar warning receivers systems and spectrum management antenna arrays.

Steatite Q-par Antennas
www.steatiteqpar-antennas.co.uk

Test Equipment

Time Domain Analyzers

HYPERLABS has announced a major hardware and software update to its line of Time Domain Analyzers. Instruments such as the HL5208 and the HL2202 now feature fully differential channel pairs, edge stabilization, and faster, more accurate calibration. These products include a copy of the new XTDR™ software, with TDR, TDT, crosstalk and controlled impedance measurement capabilities.

HYPERLABS INC.
www.hyperlabsinc.com

100 HR Burn In

VENDORVIEW

Passive Plus Inc. now performs a 100 hour burn in on all leaded 1111, 2225, 3838, 6040 and 7676 series capacitors and assemblies. Typical electrical tests may not detect internal flaws such as voids, cracks, de-laminations and electrode discontinuities, which can lead to latent and/or catastrophic failures in high power applications. The PPI 100 hour burn in, is done at extended voltage and 125°C, with capacitance, dissipation factor (inverse of Q), and insulation resistance measurements taken before and after burn in.

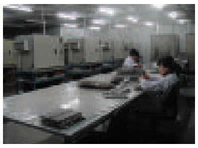

Passive Plus Inc.
www.passiveplus.com

MICRO-ADS

Near Field Communication
From Theory to Practice

Vedat Coskun, Kerem Ok, Busra Ozdenizci

The continuing theft of consumer data, such as the well-publicized breaches at Target and Home Depot, has prompted the financial industry and consumers to seek a more secure system for payments. Near field communication (NFC) has been marketed as providing a solution, yet adoption has been slow, due to the development of a financial ecosystem and the NFC technology. The recent introduction of Apple Pay will surely accelerate the development of retail-banking infrastructure and spur adoption of contactless payments, which could ultimately result in the demise of credit cards.

This significant societal shift warrants an understanding of NFC technology. The book "Near Field Communication" satisfies that goal by providing a comprehensive overview. The authors cover all aspects of NFC, from standards and operating modes, to security and privacy, to applications and business models. More than a survey, the book provides the technical depth needed to analyze the requirements of a new NFC based system, design an NFC project and program an application using Java.

While "Near Field Communication" was written before Apple Pay was introduced, it describes several contactless payment and ticketing trials as well as application prototypes tested in several cities. Oulu, Finland, for example, evaluated NFC for recording school attendance, paying for parking, selecting food at restaurants and simplifying the process for the elderly to order meals from a community services agency.

The book was written to inform a broad audience with varying interests in NFC: business and ecosystem analysts, mobile commerce consultants, project managers, system and application developers, mobile developers, software engineers and students.

The authors are with the NFC Lab in Istanbul, Turkey, which conducts multidisciplinary research on NFC technology and tracks global trials and adoption.

In addition to the print-on-demand hardcover edition, an e-book version is available from Amazon and Google Play.

To order this book, contact:

John Wiley & Sons Ltd.
The Atrium
Southern Gate, Chichester
West Sussex, United Kingdom
www.wiley.com

390 pages, $120
ISBN: 978-1-119-97109-2

BE SEEN IN '15!

2015 MICROWAVE JOURNAL EDITORIAL CALENDAR

Microwave Journal
Frequency Matters.

	EDITORIAL THEME	BONUS DISTRIBUTION
JAN	Radar and Antennas	GOMACTech DesignCon IDGA Military Radar Summit
FEB	High Frequency Components, Boards and Systems	Mobile World Congress SATELLITE 2015 IEEE EMC & SI
MAR & SUPPLEMENT	Test and Measurement	EDI CON (Electronic Design Innovation Conference) Microwave & RF WAMICON
	Cables and Connectors	IEEE MTT-S IMS
APR	IEEE MTT-S IMS Show Issue	IEEE MTT-S IMS *IMS Show Daily Sponsorship Opportunities* CS Mantech AUVSI
MAY & SUPPLEMENT	Amplifiers and Oscillators	Space Tech Expo Sensors Expo & Conference *IMS Show Daily Sponsorship Opportunities*
	Aerospace & Defense Electronics	EW Europe European Microwave Week
JUN	Semiconductors/MMICs/RFICs	
JUL	RF & Microwave Software and Design	IEEE EMC/EMC Europe
AUG	European Microwave Week Show Issue	European Microwave Week *EuMW Show Daily Sponsorship Opportunities* CTIA Super Mobility Week
SEP & SUPPLEMENT	Satellite and Radio Communications	AMTA 2015
	Military Microwaves	MILCOM *EuMW Show Daily Sponsorship Opportunities*
OCT	Passive and Control Components	Asia Pacific Microwave Conference IEEE AutoTest
NOV & SUPPLEMENT	Government and Military Electronics	GOMACTech 2016
	High Speed Design	Mobile World Congress 2016
DEC	Industrial, Scientific and Medical Applications	IEEE MTT-S Radio and Wireless Symposium

For more information, visit mwjournal.com/advertising

AdvertisingIndex

Advertisers in blue are enabled with the layar app

Sales Representatives

Microwave Journal
Frequency Matters.

Eastern and Central Time Zones
Chuck Boyd
Northeast Reg. Sales Mgr.
(New England, New York, Eastern Canada)
685 Canton Street
Norwood, MA 02062
Tel: (781) 619-1942
FAX: (781) 769-5037
cboyd@mwjournal.com

Michael Hallman
Eastern Reg. Sales Mgr.
(Mid-Atlantic, Southeast, Midwest)
4 Valley View Court
Middletown, MD 21769
Tel: (301) 371-8830
FAX: (301) 371-8832
mhallman@mwjournal.com

Pacific and Mountain Time Zones
Brian Landy
Western Reg. Sales Mgr.
(CA, AZ, OR, WA, ID, NV, UT, NM, CO, WY, MT, ND, SD, NE & Western Canada)
144 Segre Place
Santa Cruz, CA 95060
Tel: (831) 426-4143
FAX: (831) 515-5444
blandy@mwjournal.com

International Sales
Richard Vaughan
International Sales Manager
16 Sussex Street
London SW1V 4RW, England
Tel: +44 207 596 8742
FAX: +44 207 596 8749
rvaughan@horizonhouse.co.uk

Germany, Austria, and Switzerland (German-speaking)
WMS.Werbe- und Media Service
Brigitte Beranek
Gerhart-Hauptmann-Street 33,
D-72574 Bad Urach
Germany
Tel: +49 7125 407 31 18
FAX: +49 7125 407 31 08
bberanek@horizonhouse.com

Israel
Liat Heiblum
Oreet International Media
15 Kineret Street
51201 Bene-Berak, Israel
Tel: +972 3 570 6527
FAX: +972 3 570 6526
liat@oreet-marcom.com

Korea
Young-Seoh Chinn
JES Media International
2nd Floor, ANA Bldg.
257-1, Myungil-Dong
Kangdong-Gu
Seoul, 134-070 Korea
Tel: +82 2 481-3411
FAX: +82 2 481-3414
yschinn@horizonhouse.com

Japan
Katsuhiro Ishii
Ace Media Service Inc.
12-6, 4-Chome,
Nishiiko, Adachi-Ku
Tokyo 121-0824, Japan
Tel: +81 3 5691 3335
FAX: +81 3 5691 3336
amskatsu@dream.com

China
Michael Tsui
ACT International
Tel: 86-755-25988571
Tel: 86-21-62511200
FAX: 86-10-58607751
michaelT@actintl.com.hk

Hong Kong
Mark Mak
ACT International
Tel: 852-28386298
markm@actintl.com.hk

Ed Kiessling
Traffic Manager/Inside Sales
685 Canton Street
Norwood, MA 02062
Tel: (781) 619-1963
FAX: (781) 769-6178
ekiessling@mwjournal.com

MicrowaveJournal's

STEM Works

IoT [In•ter•net of Things]

The linking together of ubiquitous intelligent objects on a global scale. The Internet was originally developed to enable large, institutional computer systems to communicate remotely. Through Moore's Law, computing power continues to increase exponentially with a corresponding reduction in size and cost. This is accompanied by an ever expanding capacity for data transmission and storage. Along with the development of sophisticated sensors, this has enabled inanimate objects around us to become more and more intelligent and able to interact both individually and collectively in complex ways, through the Internet, with human beings, other objects and the environment around them.

October 29, **1969**, the first message is sent over the ARPANET, predecessor of the Internet.

Early **1980s**, one of the first Internet-enabled appliances is a Coke machine at Carnegie Mellon University instrumented to communicate its status to programmers located several floors above, saving them a wasted trip should it be empty.

January **1983**, the Internet protocol suite (TCP/IP) is introduced as the standard networking protocol on the ARPANET, marking the start of the modern Internet.

September **1991**, an article in "*Scientific American*" by Mark Weiser of Xerox PARC, describes the future of computing where "specialized elements of hardware and software, connected by wires, radio waves and infrared, will be so ubiquitous that no one will notice their presence."

1999 Bill Joy (co-founder of Sun Microsystems) describes an Internet of sensors and device-to-device communication that embeds machine intelligence in everyday life. Kevin Ashton of Procter & Gamble first uses the term "Internet of Things" to link the Internet with RFID technology in P&G's supply chain concept.

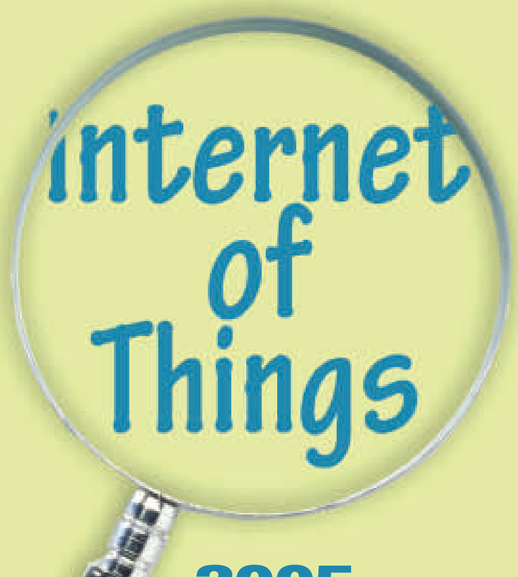

2005 The Interaction Design Institute Ivrea (IDII) in Ivrea, Italy, introduces Arduino, an inexpensive and easy-to-use single-board microcontroller enabling experimenters to connect and control everyday objects through the Internet.

October **2011**, an example of home automation, Nest Labs introduces a cloud-connected thermostat that learns occupant behaviors and preferences, and adjusts temperature automatically.

April **2012**, Google begins testing Google Glass, a wearable technology in the form of an optical head-mounted device that displays information collected wirelessly through the Internet as directed by the user.

December **2013**, Qualcomm and others form the AllSeen Alliance to develop an open framework for enabling the IoT. The following year, Intel establishes a competing group called the Open Interconnect Consortium.

Scan page using layar app

WERLATONE®

Truly Custom Designs

Couplers | Combiners/Dividers | Hybrids | Filters

Multi-Port Couplers
Model C7067

How Many Ports?

Custom Connectors !
Model C9219

What's your Interface?

Radial Combiners
Model D9706

How Many Inputs?

Big Stuff !
Model D8421

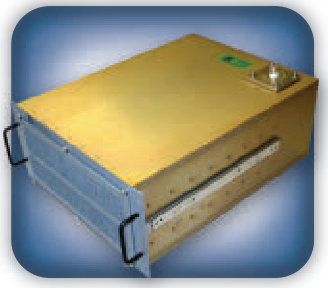

How Much Power?

Isolated N-Ways
Model D9714

Radial With Isolation?

Absorptive Filters
Model AF9350

Low Pass, High Pass?

Send Us Your Specs!!

Some of our Customer Driven Designs

Model	Type	Frequency (MHz)	Power (W CW)	Insertion Loss (dB)	VSWR
C7067	Directional Coupler, 4 Coupled Ports	123-133	2,250	0.15	1.20:1
C9219	Directional Coupler, Unflanged	640-660	3,500	0.1	1.15:1
D9706	16-Way Combiner / Divider	2,700-3,500	6,000	0.35	1.35:1
D8421	8-Way Combiner / Divider	1.5-30	12,000	0.3	1.30:1
D9714	5-Way Combiner / Divider	1,175-1,375	1,500	0.4	1.35:1
AF9350	Absorptive UHF Low Pass Filter	10-500	400	0.5	1.25:1

* Specifications are for reference only and subject to change without notice.

Werlatone, Inc. 17 Jon Barrett Road Patterson, NY 12563 (845) 278-2220 www.werlatone.com sales@werlatone.com